
Rational design of allosteric modulators: challenges and successes

Alexios Chatzigoulas^{1,2} and Zoe Cournia^{1,*}

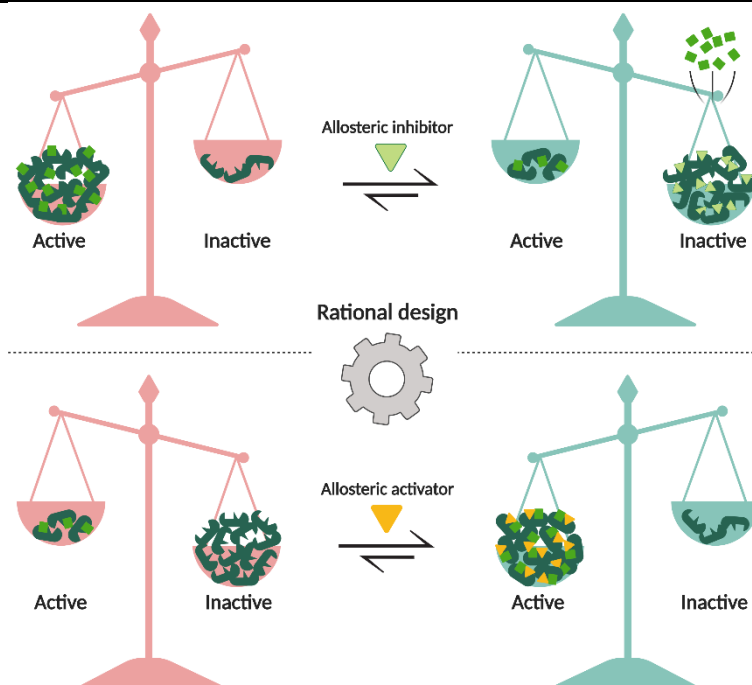
¹ Biomedical Research Foundation, Academy of Athens, 4 Soranou Ephessiou, 11527 Athens, Greece

² Department of Informatics and Telecommunications, National and Kapodistrian University of Athens, 15784 Athens, Greece

Abstract

Recent advances in structural biology and computational techniques have revealed allosteric mechanisms for an abundance of targets leading to the establishment of rational design of allosteric modulators as a new avenue for drug discovery. Considering that allostery is an intrinsic property of the protein conformational ensemble, allosteric drug design has the potential to develop into an innovative approach to modulate the dysregulation of therapeutic targets that are considered to be undruggable at their orthosteric site, explore strategic design opportunities to tackle new chemical space, or develop mutant-specific therapies to target mutations occurring far from the enzyme active site. Traditionally, allosteric drug discovery has been performed through high-throughput screening or through serendipitous discoveries; however, recent developments in structure-based and ligand-based methods have led to exciting advancements of designing bioactive allosteric ligands rationally. In this review article, we highlight the advantages and disadvantages of allosteric modulators and present structure-based and ligand-based drug design methodologies for the identification of allosteric binding sites and allosteric modulators. We also illustrate representative studies for allosteric modulators design for proteins belonging to a wide range of protein families, also considering irreversible binding with covalent allosteric modulators. Additionally, we analyze challenges and successes in the rational design of allosteric inhibitors and activators. Finally, we present the future of rational allosteric ligand design with newly built computational tools that we expect to be applied in future studies, concluding to theoretical and practical guidelines for allosteric ligand design strategies and identify knowledge gaps that need to be addressed to improve efficiency in allosteric drug design.

Contact: zcournia@bioacademy.gr



Allostery is an intrinsic property of the conformational ensemble. Rational allosteric drug design can lead to the development of modulators that shift the conformational equilibrium towards a specific state. Allosteric inhibitors shift the equilibrium towards the inactive state, where the orthosteric ligand cannot bind, while allosteric activators shift the equilibrium towards the active state, where the orthosteric ligand binds with high affinity.

1 Introduction

Allostery can be defined as a functional change of the orthosteric site generated by a perturbation produced from the binding of an effector to a distant site (allosteric site). The effect at the allosteric site is linked to the active site by conformational changes and dynamics that transmit the allosteric effect in a wave-like manner along pathways of amino acids (allosteric pathways) within the protein regulating its activity.¹ This biological phenomenon was first introduced by Cristian Bohr over a century ago, who observed positive cooperativity of oxygen binding to the hemoglobin protein.² Initially, numerous formalisms emerged to explain

this phenomenon³⁻⁶ until the derivation of the Monod-Wyman-Changeux (MWC) concerned model,⁷ which used for the first time the term “allosterism” to describe this cooperativity, along with the Koshland-Némethy-Filmer (KNF) sequential model⁸; these remained for years the two leading allosteric models. The current approach to describe allostery is that a perturbation at an allosteric site of a protein structure leads to a shift in equilibrium populations, suggesting that allostery is a property of the conformational ensemble.⁹⁻¹¹ Based on this redistribution of the conformational ensemble, it is surmised that allostery is not only associated with the cooperativity between enzyme subunits, but it is an intrinsic property of all dynamic

proteins.^{12, 13} Therefore, in the protein conformational ensemble different allosteric mechanisms pre-exist; thus, the binding of an allosteric modulator stabilizes the active form of the allosteric domain, which through the preexisting allosteric pathways modulates the activity (positively or negatively) of the functional domain, remodeling the free energy landscape.^{11, 14} However, this notion has been challenged by other studies showing that allostery can be observed in the absence of a structural pathway,¹⁵ suggesting the conformational ensemble as a framework to explain allostery through the statistical nature of the interactions responsible for the transmission of information.^{10, 16}

Since the first discovery of allosteric modulators, it has been shown that most protein receptors can accommodate allosteric sites in addition to their orthosteric (active) sites.^{13, 17, 18} Due to the various diverse possible allosteric effects allosteric modulators can be classified into different subtypes. Positive allosteric modulators (PAMs) enhance the potency of the endogenous agonist inducing relaxed states for both the allosteric and orthosteric sites, while negative allosteric modulators (NAMs) reduce the effect of the orthosteric ligand/substrate inducing a tense state for the orthosteric site (Figure 1).¹⁹ Allosteric modulators, which have a high affinity for an allosteric binding site, yet with no effect on protein activity are termed neutral or silent allosteric modulators (SAMs). SAMs may also act antagonistically to other allosteric ligands that bind in the same allosteric site (Figure 1).²⁰ In addition to PAMs, NAMs, and SAMs, allosteric partial or full agonists, antagonists, and inverse agonists also exist, capable of modulating the protein activity by bind-

ing to the allosteric site, irrespective of the absence or presence of an orthosteric ligand.²¹ Furthermore, allosteric modulators may act simultaneously as modulators for endogenous ligands and as allosteric agonists, which are called ago-allosteric modulators, increasing the efficacy and modulating (positively, negatively, or neutrally) the potency of the endogenous ligand.^{22, 23} In kinases and phospholipases, allosteric ligands bind to remote cavities, distant from the orthosteric site, and stabilize unique, inactive conformations.^{24, 25}

Over the past years, rational drug design has been mainly facilitated in orthosteric sites as allosteric sites and the effect induced by allosteric ligands on protein function are often unknown. Additionally, structural information of allosteric modulators bound to proteins is limited compared to active site ligand – protein complexes. At the same time, many protein therapeutic targets have been considered undruggable or difficult to target in the orthosteric site for a variety of reasons, for example, extremely tight binding of the substrate, absence of a known orthosteric site, or selectivity issues arising from a highly conserved active site across proteins of the same family, such as kinases or G-protein-coupled receptors (GPCRs). Targeting undruggable protein targets in combination with the recent patent cliff has generated an increased interest in allosteric drug design over the past few years. This growing interest has motivated the creation of structural databases of allosteric ligands bound to proteins and raised interest in rational, experimental, and computational methods predicting allosteric sites and allosteric pathways, enabling the rational design of bioactive allosteric lig-

ands.²⁶⁻³³ Despite these efforts, most allosteric bioactive ligands hitherto have been discovered by high-throughput screening (HTS)³⁴⁻³⁷ often followed by structure-activity relationship (SAR) optimizations³⁸⁻⁴² with limited applications of computer-aided drug design. Going forward, new structural information coming to light^{42, 43} in combination with novel methodologies and approaches can bolster allosteric rational drug design.

In this review, we focus on rational, computer-aided allosteric drug design methods and applications and less in medicinal chemistry optimizations, which are countless (for a recent review see Ref.⁴⁴). First, we discuss the advantages and challenges in allosteric ligand dis-

covery and proceed with summarizing methods for discovering allosteric pathways and predicting allosteric sites and cryptic pockets. We present structure-based and ligand-based studies that have been employed to successfully design allosteric modulators for several protein families, and address the obstacles that must be overcome such as the identification of cryptic allosteric pockets not detectable in crystal structures and the need for conformational ensemble generation to account for protein flexibility. The variety of different structural and computational approaches that are presented herein may offer key principles and strategies for the design of allosteric modulators and serve as practical considerations for computer-aided allosteric drug discovery.

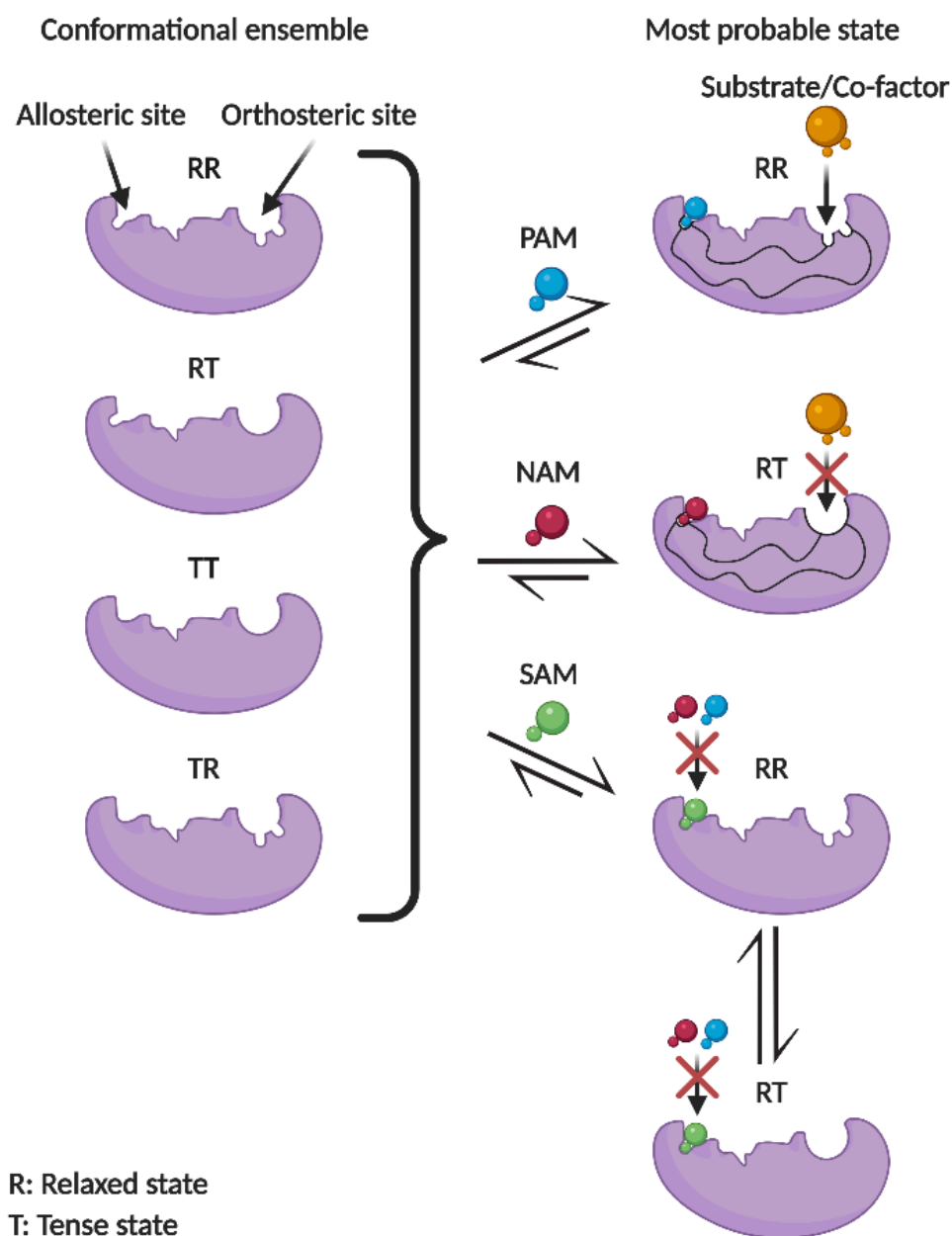


Figure 1. Schematic representation of positive allosteric modulator (PAM), negative allosteric modulator (NAM), or silent allosteric modulator (SAM) binding on allosteric sites on a receptor and the effect on the protein orthosteric site. All binding sites can adopt two states, the relaxed (R), where the substrate/co-factor can bind with high affinity, and the tense (T), where the substrate/co-factor cannot bind or binds with low affinity. All possible combinations are expressed in a two letter code, e.g., RT, where each letter denotes the state of the allosteric and the orthosteric sites, respectively. In the unbound conformational ensemble there are four possible combinations of protein states with different probabilities based on the free energy landscape. Binding of an allosteric modulator shifts the conformational ensemble towards the relaxed form (in case of a PAM) or the tense form (in case of a NAM) for the orthosteric site through preexisting allosteric pathways. Binding of a SAM in the allosteric site does not affect the orthosteric site, which can exist in either of the relaxed or the tense states. However a SAM binds with high affinity acting as an antagonist to other allosteric modulators, blocking the allosteric regulation.

2 ALLOSTERIC MODULATORS: PROS & CONS

Allosteric modulators may demonstrate improved properties in terms of subtype selectivity and specificity, reducing side effects⁴⁵⁻⁴⁸ compared to orthosteric ligands because allosteric sites are less evolutionary conserved than orthosteric sites.^{49, 50} Thus, they may target proteins that have been considered undruggable in the absence of an orthosteric site or very tight binding of the substrate/native ligand, and they may also selectively target and inhibit mutant proteins in cancer, while displaying limited binding to the wild type (WT).^{19, 51, 52} The importance of selectively targeting mutant proteins is demonstrated by the fact that treatment with allosteric inhibitors in cancer may overcome drug resistant mutations as demonstrated in a recent study of co-administering nilotinib and the allosteric inhibitor ABL001 to the oncogene BCR-ABL1, which showed that this combination can completely overcome drug resistance without recurrence after the end of the treatment, verifying the hypothesis that the dual inhibition of oncogenes using distinct targeting mechanisms might improve treatment outcomes by providing enhanced target coverage.⁵³ Moreover, allosteric modulators stabilize a unique conformation of the protein ensemble, providing a new pharmacology for the receptor (e.g. ligand-biased signaling).⁵⁴⁻⁵⁶ Another effect of allosteric modulators is that they bind noncompetitively, allowing the endogenous ligand to bind to the orthosteric site, enabling modulation of the receptor rather than switching the activity on or off entirely such as orthosteric ligands.⁴⁵ Additionally, PAMs act synergistically with orthosteric ligands, in-

creasing their affinity, thus decreasing the orthosteric ligand dosage.²¹ Moreover, allosteric effectors are saturable, meaning that once allosteric sites are occupied, no additional effects can be observed.²⁴ Finally, probe dependence is one of the unique features of allostery, which allows a protein to respond differently to the same allosteric modulator when different orthosteric or endogenous ligands are bound.⁵⁷⁻⁵⁹ Intriguingly, this feature reflects the bidirectional regulation between allosteric and orthosteric sites.⁶⁰ Therefore, signaling bias and probe dependence are allosteric features that have the potential to lead to unambiguous and precise allosteric ligand design.⁶¹

On the other hand, the discovery of allosteric bioactive ligands presents challenges beyond those encountered in orthosteric drug discovery. Allosteric sites are often shallower and narrower than orthosteric sites hampering the discovery of allosteric drugs with sufficient binding affinity.^{46, 62} Additionally, because of the variety of different mechanisms of modulation that were mentioned before, along with the binding affinity the allosteric efficacy must also be taken into consideration,^{29, 63} because minor differences in allosteric modulators can lead to opposite effects in the protein function.^{24, 64, 65} Furthermore, although orthosteric sites are straightforward to discover due to the known location of substrate binding, allosteric sites are often unknown or difficult to discover, as they are only accessible in specific protein conformations that may not have an associated resolved 3D structure.^{31, 66} It turns out that is also difficult to predict allosteric sites using classical molecular dynamics (MD) simulations

as allosteric effects often occur through conformational changes in the microsecond,⁶⁷⁻⁶⁹ or millisecond time scale.⁷⁰⁻⁷³ Finally, allosteric sites are less evolutionarily conserved across protein families compared to orthosteric sites, but there are also less evolutionarily conserved among subspecies complicating testing in different species homologs, that is, human versus rodent receptors.^{29, 74, 75}

Despite the above-mentioned disadvantages, the advantages outweigh the challenges, and the design of allosteric modulators holds a significant promise for drugging proteins considered to be undruggable, but also for modulating the activity of orthosteric ligands providing better selectivity with fewer side effects, smaller dosage, reduced toxicity, modulating the protein activity instead of switching it on or off, inducing signaling bias, and overcoming drug resistance.

3 METHODS

Structure-based allosteric drug design has proven challenging owing to the limited resolved 3D protein structures bound to allosteric modulators. Allosteric sites are often cryptic remaining undiscovered in protein conformations. Cryptic pockets are most often absent in the unbound structure, and only in the presence of the ligand the cryptic site relaxed state becomes dominant in the conformational ensemble.³¹ Thus, in order to unveil these cryptic sites, the conformational space of the apo and/or holo protein structures must be examined; molecular simulations can be an efficient way to generate an ensemble of conformations and explore these sites. Molecular simulation techniques for this

purpose are molecular mechanics calculations such as MD or Monte Carlo (MC) simulations complemented by techniques that produce conformational ensembles such as Markov state models (MSMs), or enhanced sampling techniques such as weighted ensemble MD, metadynamics, coarse-grained simulations or combinations of methods.⁷⁶⁻⁸¹ Site detection algorithms may then be utilized on protein conformers to discover new putative allosteric sites.⁸²⁻⁸⁷ An important consideration after identifying new cavities is whether these sites can communicate with functional domains of the protein such as the active site, thus being able to act allosterically and modulate protein function upon ligand binding. Several techniques have been developed for this purpose, which we describe below.

Allosteric sites can be targeted with small molecules aiming to shift the conformational landscape towards a specific state (active, inactive or intermediate). The subsequent step is structure-based design with various methodologies such as virtual screening or de novo design in a variety of protein conformers of the conformational ensemble to implicitly consider protein flexibility.^{88, 89} In many cases presented herein, homology modeling was facilitated in the absence of a crystal structure. When homology modeling is necessary, an efficient practice is to produce different homology models and screen known allosteric and orthosteric inhibitors along with inactive compounds and decoy molecules. The homology model, which ranks known allosteric and orthosteric inhibitors on top, can be considered the best structural conformation to be employed in further studies.^{90, 91}

In cases where the 3D protein structure or the required conformational state is not available, structure-based design might not be feasible. Allosteric ligand-based drug design does not rely on the 3D structure of the protein but on known active and inactive ligands that bind to the desired binding site. Typically, when only a few known allosteric binders are available, similarity search methods are applied,⁹¹⁻⁹³ while in the case that several active ligands exist, pharmacophore models that describe binding interactions and ligand physicochemical and structural properties can be generated.^{92, 94} Pharmacophore models are routinely subjected to virtual screening, filtering chemical libraries in search for compounds that encompass the same pharmacophore features, or for designing *de novo* allosteric ligands. Allosteric pharmacophore modeling is not solely a ligand-based approach, but could also involve information about the binding site and residues that are important for binding.⁹⁵⁻⁹⁸

In the last decade, numerous methodologies and applications have been developed to explore allostery in proteins and predict putative allosteric sites or allosteric pathways. These can be broadly categorized in sequence-based and structure-based techniques. Sequence-based methods are based on the principle that allosteric pathways are evolutionarily conserved and that protein residues co-evolve in a correlated manner.^{99, 100} To quantify how residues co-evolve and identify patterns of correlated mutations, the statistical coupling analysis (SCA) method is performed to measure covariation between pairs of amino acids in a protein multiple sequence alignment (MSA) of an ensemble of homologous sequences, revealing allosteric

pathways and decomposing the protein into sectors.^{101, 102} This methodology has been facilitated in the pySCA Python package¹⁰³ for the REACH evolution-based strategy that rationally engineers allosteric control in proteins.¹⁰⁴ The drawbacks of the evolution-based approach are two-fold. First, its success is dependent on the number of available homologous sequences and the need of a 3D structure, which is not always available. Second, and most important, residue coevolution might not be necessarily related to allostery as it is discussed in refs.^{30, 105}

Structure-based methods are predominantly based on residue movement cross-correlation within the protein.¹⁰⁶⁻¹¹⁰ Motional correlations can be obtained from MD simulations or from conformational ensembles produced from MD,¹¹¹⁻¹¹⁶ MC simulations,^{117, 118} using principal component analysis (PCA) or from normal mode analysis (NMA), elastic network models (ENMs) such as the Gaussian network model (GNM),^{118, 119} the anisotropic network model,¹²⁰ or the torsional network model (TNM),^{121, 122} which uses torsion angles as degrees of freedom. Graph theory has been also employed, which provides a way of representing proteins in a reduced form, identifying allosteric pathways from the dynamic couplings between the residues of the orthosteric and the allosteric sites. In graph theory, proteins are represented by an atomistic graph network model, where nodes are atoms and weighted edges are the covalent and non-covalent bonds,¹²³ or by a coarse-grained network model, which is the most usual case, where nodes are residue C α atoms, or residue center of mass, connected with edges based on a distance cutoff maintained in the MD trajec-

tory at a certain percent (e.g., 75% of the MD trajectory)^{108, 124} or based on other inter-residue properties.^{125, 126} The edge weights are usually based on the covariance matrix of the displacement of C α atoms, or from mutual information analysis from MD simulations, and the allosteric hot spots and communities are identified using centrality measures, for example, betweenness centrality, eigenvector centrality and other metrics.^{124, 127-132} The allosteric pathway is then detected using the Dijkstra algorithm,¹³³ or the Bellman–Ford algorithm,¹³⁴ which finds the shortest path between two nodes in a graph. A plethora of tools integrating graph theory and network models for detecting protein dynamics and allosteric communications pathways have been recently reviewed in Ref. ¹³⁵. It must be noted that calculating cross-correlations using the covariance matrix may miss non-linear correlations and ignore orthogonal vibrations; for this purpose, approaches based on mutual information have been developed, which enable quantifying all correlations, including nonlinear and higher order correlations^{60, 111-113, 115, 116, 136, 137} or from the singular value decomposition.¹²⁰ Additionally, by using the covariance matrix, the time evolution information and dynamic properties of the system are lost.^{9, 30, 60} Another challenge in network-based methodologies using equilibrium sampling is that allosteric conformational changes may occur in time scales inaccessible to plain MD.³⁰ Enhanced sampling simulations may then be employed.^{30, 105} Available tools for the prediction of allosteric pathways are summarized in Table 1.

Path-based methods such as accelerated Molecular Dynamics (aMD),²⁴ and metadynamics²⁵

were developed to aid in sampling complex free energy states and landscapes. These calculations are used when systems are at equilibrium; when studying non-equilibrium properties, the Jarzynski method can describe the free energy between two states.²⁶ Non-equilibrium methods can be used to understand ligand unbinding pathways.²⁸ Early work was performed with metadynamics for docking ligands on flexible receptors in water, mimicking the real dynamics of a ligand binding/unbinding to a target. From these calculations it is possible to reconstruct the free energy surface and thereby compute a binding free energy. This approach was first applied to four protein-ligand pairs (β -trypsin/benzamidine, β -trypsin/chlorobenzamidine, immunoglobulin McPC-603/phosphocholine, and CDK2/staurosporine), whereby the docked geometry and the free energy of docking in all cases were correctly predicted.¹³⁸ More recently, a more generally applicable metadynamics scheme was developed for predicting free energy profiles and binding energies. For example, studies on GPCRs using a single collective variable (CV) together with well-tempered multiple-walker metadynamics with a funnel-like boundary were used predict binding free energies of 12 diverse ligands in five receptors to a root-mean-square error less than 1 kcal/mol.¹³⁹ In recent years, an application of metadynamics, binding pose metadynamics, has become increasingly popular as a method that allows for an efficient scoring of ligand poses in a protein binding pocket. Ligand poses can be evaluated in terms of their stability under the bias of the metadynamics simulation; the ones that are unstable are expected to be infrequently occupied in the free energy landscape, thus making

minimal contributions to the binding affinity. Recent results using crystal structures with ligands known to be incorrectly modeled, as well as 63 structurally diverse crystal structures with ligand fit to electron density from the Twilight database, show that binding pose metadynamics can successfully differentiate compounds whose binding pose is not supported by the electron density from those with well-defined electron density.¹⁴⁰ A novel protocol based on clustering of multiple walker metadynamics simulations allowed identifying the preferential binding mode from conformational ensembles for three GPCR structures and reproduced the correct allosteric binding mode known from the literature.¹⁴¹ In another study, MD and bias-exchange metadynamics simulations were utilized to elucidate the mechanism of how the natural substrate of κ -casein acts as an allosteric activator and to compute the free energy surface for the process.¹⁴² These examples illustrate the potential and exciting opportunities of enhanced sampling simulations for the investigation of allosteric ligands, yet these methods have not been fully exploited. An extensive review highlights recent advances and discusses challenges in predicting protein-ligand binding using metadynamics-based approaches, with an emphasis on structure-based design.¹⁴³

A plethora of computational methodologies and tools have recently utilized the wealth of available structural data and the predictive power of machine learning, often in combination with the aforementioned techniques, for predicting putative allosteric sites, allosteric signaling pathways, allosteric hotspots, and cryptic sites.¹⁴⁴⁻¹⁵⁶ The allosteric database ASD v3.0²⁸ and the allosteric benchmark ASBench¹⁵⁷ have

been extensively used for the training and testing of many developed tools for allosteric pocket detection. Tools such as Allosite¹⁴⁵ or Cryptosite¹⁴⁸ utilize pocket detection methods in conjunction with ASD to train machine learning algorithms *e.g.* SVD,^{145, 148} or Random Forests^{147, 155, 156} to predict allosteric sites. Moreover, to improve the predictive performance in identifying allosteric pockets in algorithms such as AlloPred,¹⁴⁶ machine learning can be combined with NMA (or ENMs),^{146, 149} node-weighted residue interaction networks,¹⁵¹ and MD simulations.¹⁵³⁻¹⁵⁵

Recently, methodologies combining allosteric communication and dynamics were introduced providing novel perturbation approaches to predict allosteric sites. Tee *et al.* exploited the bidirectional nature of allosteric communication to create a reverse perturbation approach, using a structure-based statistical mechanical model,¹⁵⁸ identifying allosteric sites by perturbing the orthosteric site.¹⁵⁹ Yao *et al.* introduced a method termed comparative perturbed-ensembles analysis¹⁶⁰ to study protein functional dynamics using conformational ensembles generated from MD simulations of the unperturbed (ligand free or WT) and perturbed (ligand-bound or point mutated) protein, instead of the conformational ensemble of a long MD simulation bound to a specific substrate.¹⁶⁰ The amino acid network approach called dCNA (difference contact network analysis)¹⁶¹ utilizes graph theory using two or more conformational ensembles as input (*i.e.*, ensemble of holo and ensemble of apo, or ensemble of WT and ensemble of mutant protein), and partitions the protein in communities. This novel correlation-based analysis is able to distinguish positive

versus negative allosteric responses during PAM and NAM binding.¹⁶⁰

Significant efforts towards the direction of discovery and investigation of cryptic or transient allosteric binding pockets have also appeared in the last decade. Most of the developed methodologies utilize mixed-solvent MD simulations using probes, which open and stabilize cryptic pockets,¹⁶²⁻¹⁶⁶ or enhanced sampling methods,^{66, 167-173} which effectively sample the opening of cryptic pockets. Other computational methodologies revealing cryptic binding pockets use MSMs,¹⁷⁴⁻¹⁷⁶ machine learning¹⁴⁸, and post-processing methods for MD trajectory and pocket flexibility analysis.^{177, 178} Many of the abovementioned cryptic site discovery methods have been implemented in software

programs and web-servers summarized in Table 1, and are discussed in detail in recent reviews.^{179, 180}

We will not extend further into the aforementioned computational techniques and tools, as they have been extensively described and discussed in numerous recent reviews, also listing the accessible available web-servers and stand-alone programs implementing the abovementioned methodologies.^{30, 32, 33, 60, 105, 110, 129, 135, 180-183} Here, we review several successful examples of rational design of allosteric modulators categorized by protein families. The protein targets, the methods and tools utilized, and the results are summarized in Table 2. A list of abbreviations can be found in Table 3.

Table 1. Computational tools and databases for the prediction of allosteric sites, allosteric pathways, and cryptic sites.

Allosteric pathway prediction tools and databases	Website URL	Description	License
Allo ¹⁵⁰	https://github.com/fibonaccirabbits/allo	Stand-alone python machine learning predictors that classify protein sites as allosteric or orthosteric and rank allosteric pockets	Free
AlloDriver ¹⁸⁴	http://mdl.shsmu.edu.cn/ALD/	Web-server tool analyzing high-throughput clinical data on allosteric mutations implicated in cancer, and mapping them to allosteric/orthosteric sites derived from 3D protein structures	Free
AlloFinder ¹⁸⁵	http://mdl.shsmu.edu.cn/ALF/	Web-server tool for automatic discovery of allosteric modulators, utilizing a combination of tools for allosteric drug design	Free
AlloMAPS ¹⁸⁶	http://allomaps.bii.a-star.edu.sg/	Web database providing data on energetics of allosteric signaling obtained with the structure-based statistical mechanical	Free

		model of allostery (SBSMMA) ^{158, 159}	
AlloPred ¹⁴⁶	http://www.sbg.bio.ic.ac.uk/allopred/home	Web-server tool combining NMA with machine learning for allosteric binding site identification	Free
Alloscore ¹⁸⁷	http://mdl.shsmu.edu.cn/alloscore/	Web-server tool using machine learning for predicting and scoring the affinity of allosteric ligand–protein interactions	Free
AlloSigMA ^{188, 189}	http://allosigma.bii.a-star.edu.sg/	Web-server tool calculating energetics of allosteric signaling resulting from ligand binding and mutations based on SBSMMA ^{158, 159} to predict allosteric sites and pathways	Free
AlloSite ^{145, 149}	http://mdl.shsmu.edu.cn/AST/	Web-server tool combining machine learning with a perturbation-based ENM model to predict allosteric sites	Free
AllosMod ¹⁹⁰	https://modbase.compbio.ucsf.edu/allosmod	Web-server tool sampling protein conformations based on a modeled energy landscape and sets up and runs MD simulations, identifying allosteric conformational changes	Free
AR-PRED ¹⁵⁶	https://github.com/samitmishra0628/AR-PRED_source	Stand-alone tool written in Perl and MatLab utilizing machine learning to predict allosteric and active site residues	Free
ASD ^{28, 191, 192}	http://mdl.shsmu.edu.cn/ASD/	Web database providing data on experimentally determined allosteric proteins, modulators, cavities, and pathways	Free
ASBench ¹⁵⁷	http://mdl.shsmu.edu.cn/asbench/	Web database providing a benchmark set of unique allosteric sites and a benchmark set of structurally diverse allosteric sites	Free
COMMA2 ¹⁹³	http://www.lcqb.upmc.fr/COMMA2/	Stand-alone software identifying allosteric communication pathways and predicting deleterious mutations	Free
CovCys ^{119, 194}	http://www.pkumdl.cn/cavityplus	Web-server tool using machine learning to predict whether cysteine residues within a pocket are druggable and suitable for covalent allosteric drug design	Free
CorrSite ^{109, 119}	http://www.pkumdl.cn/cavityplus	Web-server tool predicting allosteric binding sites utilizing GNM to calculate residue fluctuation cross-correlations between putative allosteric sites and the	Free

		orthosteric site	
DynOmics ¹⁹⁵	http://dyn.life.nthu.edu.tw/oENM	Web-server tool predicting allosteric communications and functional residues utilizing ENMs to calculate residue fluctuation cross-correlations	Free
Enspara ¹⁹⁶	https://github.com/bowman-lab/enspara	A Python stand-alone tool predicting allosteric communication via correlation measurement of rotameric and dynamical states with CARDS ¹¹⁵	Free
ExProSE ¹⁹⁷	https://github.com/jgreener64/ProteinEnsembles.jl	A Julia stand-alone distance geometry-based tool generating protein ensembles from two or more structures and predicting allosteric sites	Free
GRALL ¹⁹⁸	https://ifm.chimie.unistra.fr/grall	Web database providing information on all allosteric ligands of Glycine receptors	Free
MCPath ¹¹⁷	http://safir.prc.boun.edu.tr/clbet_server/	Web-server tool predicting allosteric pathways and functional residues utilizing MC to generate paths based on the weighted inter-residue interactions	Free
MutInf ¹¹¹	https://simtk.org/projects/mutinf	A python package analyzing data from MD simulations to identify statistically significant correlated motions	Free
NACEN ¹⁵¹	http://sysbio.suda.edu.cn/NACEN/	An R package applying machine learning on node-weighted amino acid networks to predict allosteric residues and sites	Free
PARS ¹⁹⁹	http://bioinf.uab.cat/cgi-bin/pars-cgi/pars.pl	Web-server tool combining pocket structural conservation measures with NMA and detecting changes on protein dynamics upon ligand binding to a putative allosteric site	Free
ProSNEx ¹²⁶	http://prosnextool.com/	Web-server tool constructing and analyzing protein structure networks predicting allosteric communication between parts of protein utilizing NMA or interaction energies and various residue-based local or global network metrics	Free
pySCA ¹⁰¹⁻¹⁰³	https://github.com/ranganathanlab/pySCA	Python package for applying the SCA method in an MSA of an ensemble of homologous sequences to predict allosteric pathways	Free

SPACER ²⁰⁰	http://allostery.bii.a-star.edu.sg/	Web-server tool combining ENM and coarse-grained docking to detect conformational changes and predict allosteric communication and allosteric sites	Free
STRESS ¹¹⁸	https://github.com/gersteinlab/STRESS	Stand-alone tool predicting allosteric hotspot residues, which result in large protein conformational changes generated by MC simulations when bound by a probe, and by utilizing a dynamical network analysis methodology	Free
TNM ^{121, 122}	https://github.com/ugobas/tnm	Stand-alone tool predicting allosteric binding sites using NMA with TNM, using torsion angles as degrees of freedom, and calculating dynamical couplings between C α atoms	Free
WebPSN ^{201, 202}	http://webpsn.hpc.unimore.it	Web-server tool combining protein structure networks and ENM to investigate allosteric communication in proteins and nucleic acids	Free
Cryptic binding site identification tools	Website URL	Description	License
CAT ¹⁷⁸	https://github.com/ammvitor/CAT	Post-processing mixed-solvent MD simulations analysis toolkit for the prediction of allosteric and cryptic pockets	Free
CryptoSite ¹⁴⁸	https://modbase.compbio.ucsf.edu/cryptosite/	Web-server and stand-alone program utilizing machine learning	Free
JEDI ¹⁷³	https://github.com/michellab/jedi-utilities	A druggability score used as a collective variable, in order for proteins to adopt conformations that match the desired druggability scores in biased MD simulations	Free
MDmix ^{162, 163}	http://mdmix.sourceforge.net/	Mixed-solvent MD simulations method using probe molecules	Free
POVME ¹⁷⁷	https://github.com/POVME/POVME	Post-processing tool providing analysis of flexible pockets and other post-processing capabilities	Free
SILCS ¹⁶⁷⁻¹⁶⁹	https://silcsbio.com/software/	Fragment-based method utilizing MC for probe sampling and enhanced mixed	Commercial

		solvent MD simulations	
SWISH ^{66, 203}	https://github.com/OleinikovasV/CrypticSWISH	Hamiltonian replica exchange-based method using probe molecules	Free
TRAPP ¹⁷⁰⁻¹⁷²	https://trapp.h-its.org/	Druggability assessment of transient pockets utilizing rotamerically induced perturbation MD simulations methods	Free

4 RATIONAL ALLOSTERIC DRUG DESIGN

4.1 GPCRs

GPCRs are the largest family of integral membrane proteins comprising seven conserved transmembrane helices, three extracellular loops, and three intracellular loops. GPCRs are involved in many diseases and disorders²⁰⁴⁻²⁰⁸ and are sought-after drug targets. Approximately 34% of all US Food and Drug Administration (FDA) approved drugs target GPCRs.²⁰⁹ GPCRs are grouped in six classes (classes A-F) based on their sequence and functional similarity. Drug design in the orthosteric sites of GPCRs can be challenging because these sites are highly conserved across GPCR subfamilies causing side effects due to poor selectivity.²¹⁰⁻²¹² For this reason, allosteric drug design is frequently employed for GPCRs. Crystallization of GPCRs is complex due to their inherent flexibility and instability outside of the membrane, and thus most GPCR-targeting drugs were discovered by identifying lead compounds from HTS, followed by iterative trial and error optimizations. However, technological improvements have recently led to the high throughput X-ray determination of GPCR structures in complex with allosteric modulators, holding promise for the rational

allosteric drug design in these targets.^{42, 43, 213-215}

Below, we summarize examples of identifying allosteric mechanisms and allosteric ligand design on GPCRs using computational techniques.

M2 muscarinic acetylcholine receptor

Muscarinic acetylcholine receptors (mAChR) belong to class A GPCRs and consist of five subclasses (M1-5). M2 is important for modulating the cardiac function and the cognitive functions of learning and memory.²¹⁶ Dror et al. studied the structural basis of allosteric ligand binding in M2 elucidating its allosteric regulatory mechanism.⁶⁷ In their study, unbiased all-atom MD simulations of the human M2 receptor (PDB: 3UON)²¹⁷ was performed using the parallel supercomputer Anton²¹⁸ and the CHARMM force field.^{219, 220} In these simulations, the co-crystallized antagonist QNB was removed or replaced by NMS and known M2 allosteric modulators. Structurally diverse relevant drugs were also simulated independently with initial conformations more than 20 Å away from the extracellular vestibule center of M2. Results showed that all ligands bind to the same allosteric site at the extracellular vestibule, and that PAMs and NAMs act via two different allosteric mechanisms although they bind to the

same allosteric binding site. The computational binding modes were tested experimentally providing insights into the chemical modifications that can alter the effect of allosteric modulators from PAMs to NAMs and vice versa.

In another computer-aided drug design approach, aMD simulations²²¹ were applied to discover PAMs and NAMs for the M2 receptor.²²² In this study, simulations used the X-ray structures of the inactive QNB-bound (PDB: 3UON)²¹⁷ and active IXO-nanobody-bound M2 receptor (PDB: 4MQS)²¹² structures and trajectories were clustered to produce a conformational ensemble of M2. The extracellular vestibule allosteric site was then defined based on the binding location of the LY2119620 allosteric modulator (PDB: 4MQT, Figure 2).²¹² Subsequently, ensemble docking was performed using the National Cancer Institute (NCI) compound library,²²³ and high-throughput virtual screening (HTVS) followed by the induced-fit docking (IFD)²²⁴⁻²²⁷ method on the top 100 compounds docked and scored by Glide²²⁸⁻²³¹. A total of 38 compounds were tested experimentally to measure the binding affinity and the efficacy (PAMS or NAMs) resulting in 12 of them

being M2 allosteric modulators with binding affinity $\leq 30 \mu\text{M}$.

Using a different concept, several studies for the M2 receptor explored bitopic (or dualsteric) ligands as potential bioactive ligands that target both orthosteric and allosteric sites.²³² Valant et al. generated a homology model of M2 based on the crystal structure of the 2-adrenergic receptor and generated the lowest energy model using biased probability Monte Carlo (BPMC) simulations.²³³ Then, the mAChR known agonist McN-A-343 was docked onto the homology model; results showed that McN-A-343 is not an orthosteric ligand but rather a bitopic ligand consisting of an orthosteric and an allosteric moiety. Even more intriguing is the fact that the allosteric moiety of McN-A-343 is a PAM for orthosteric inhibitors, but a NAM for orthosteric agonists confirming the above-mentioned allosteric property termed probe dependence. Overall, these results can lead the way toward an alternative structure-based bitopic binding procedure targeting both allosteric and orthosteric sites, in the case where these sites are adjacent to each other, providing even better subtype and functional selectivity.^{234, 235}

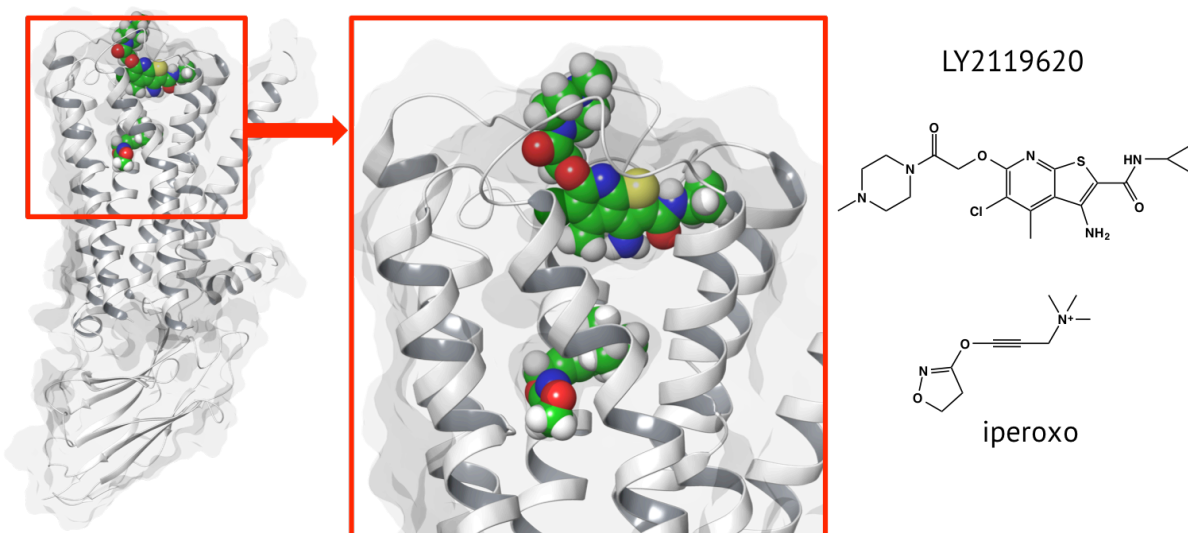


Figure 2. The crystal structure of M2 muscarinic acetylcholine receptor bound to the orthosteric agonist iperoxo and the PAM LY2119620 in an adjacent allosteric site above the orthosteric (PDB: 4MQT) is visualized on the left. On the right, the 2D representation of LY2119620 (top) and iperoxo (bottom) are shown.

Complement component 5a receptor

The complement component 5a receptor (C5aR) is a class A GPCR involved mainly in inflammatory responses, but also autoimmune, neuropathic pain, and neurological disorders.²³⁶⁻²³⁹ Based on a study of the neutral allosteric inhibitor reparixin binding to the minor pocket of the transmembrane region of CXCR1 and CXCR2,²⁴⁰ a hypothesis was made that this minor pocket is conserved across this GPCR family. Based on this assumption, a C5aR homology model was built using the crystal structure of C-C chemokine receptor type 5 (CCR5) bound to the HIV FDA-approved allosteric drug maraviroc (PDB: 4MBS)²⁴¹ as a template.²⁰⁵ Then, MD simulations were performed in the C5aR model for 1 ns using the Discovery Studio²⁴² software and the CHARMM force field,^{219, 220} and an average structure from the last 100 ps was built. Subsequently, a site-targeting library was designed based on struc-

tural characteristics of the minor pocket to identify new allosteric C5aR inhibitors. Molecule DF2593A was selected as the most promising lead and was docked using LiGenDock^{243, 244} to identify the binding poses with C5aR. In vitro and in vivo tests followed, identifying DF2593A as a potent and orally active C5a noncompetitive allosteric antagonist effective in rodent models for inflammatory and neuropathic pain. DF2593A is being developed by the Center for Research on Inflammatory Diseases in partnership with Dompé Pharma although currently there is no data on clinical development.²⁴⁵

Ovarian cancer G-protein coupled receptor 1

The ovarian cancer G-protein coupled receptor 1 (OGR1) is a class A GPCR encoded by the GPR68 gene, belonging to the proton-sensing GPCR family.²⁴⁶ Proton-sensing GPCRs are activated when the extracellular pH is below 7, and their expression is shown to be significant in acid-induced pain sensation.²⁴⁷ In a combined

experimental-computational study, first it was shown experimentally that the benzodiazepine drug lorazepam is a PAM of OGR1 and then the OGR1-lorazepam complex was modeled computationally.⁹⁰ To model the OGR1 structure, 407 OGR1 homology 3D models were created using MODELLER²⁴⁸ based on the CXCR4 structure (PDB: 3ODU),²⁴⁹ which were then expanded using ENM with the 3K-ENM program²⁵⁰ by additionally generating 2900 models. For each one of the total 3307 models, virtual screening of active benzodiazepines, inactive compounds from the National Clinical Collection library, and property-matched decoy molecules using the flexible ligand sampling algorithm in DOCK^{251, 252} was performed in five candidate allosteric sites. Iterative cycles of modeling and optimization resulted in the OGR1-lorazepam complex structure, where lorazepam was ranked first among the other decoy compounds, providing the correct binding pose of lorazepam and its allosteric binding site. Then, in order to discover more active PAMs than lorazepam, virtual screening of more than 3 million compounds against the lorazepam allosteric site of OGR1 was performed; this exercise resulted in the calculation and scoring of more than three trillion complexes. 17 compounds were selected for in vitro testing based on their ranking score, their interactions with OGR1, their chemical diversity, and also the score of their analogs. Four of them showed increased activity, but none of them was more active than lorazepam. Subsequently, hundreds of analogs of these early hits were docked and scored, and 25 of them were selected for testing; 13 of them were more active than lorazepam. The compound with the highest allosteric effect based on the standard allosteric operational model²⁵³ was named

ogerin. Optimization of ogerin continued by producing a virtual library of more than 600 ogerin analogs, docking into the OGR1 model, synthesis and assaying of 13 analogs, out of which three proved to be more active than ogerin. Additionally, ogerin showed high specificity as an OGR1 PAM over other proton-sensing GPCRs. Utilizing the Similarity Ensemble Approach²⁵⁴ program against a panel of 2,800 off-targets, ogerin and its analogs revealed association with adenosine receptors which was confirmed with physical profiling. Based on these results, again using SEA for computational screening, it was revealed that there is a cross-talk between OGR1, adenosine, and γ -Aminobutyric acid receptors allosteric modulators, which should be considered in future drug design in these receptors. The same procedure was followed for the psychosine receptor (GPR65), a receptor belonging to the same proton-sensing GPCR family, resulting in the discovery of allosteric agonists and NAMs, proving the general applicability of this approach.

Dopamine receptors

Dopamine receptors belong to Class A GPCRs and are neurologic drug targets as abnormal dopamine receptor function is implicated in many neuropsychiatric disorders, drug addiction, and Parkinson's disease.^{255, 256} Lane et al. studied computationally the dopamine receptor D₃ (D3R) by initially creating a benchmark set of 28 known D3R selective and potent antagonists from the ChEMBL database,²⁵⁷ then generating conformers based on the protein crystal structure (PDB: 3PBL)²⁵⁸ using NMA, followed by energy-based side chain sampling using an antagonist of the initial benchmark set.²⁵⁹ These protein conformers were then evaluated by virtual screening of the antagonist benchmark set and

decoy compounds, and were optimized using the iterative ligand-guided receptor optimization (LIBERO) algorithm.²⁶⁰ The best D3R (apo) model was selected, and the endogenous ligand dopamine was docked. For the identification of new potential allosteric bioactive ligands, a library of more than four million compounds was prepared using the Molsoft ScreenPub database, which was virtually screened in an allosteric pocket adjacent to the orthosteric site using the ICM-Pro^{261, 262} software. Subsequently, the top 300 compounds were selected and clustered (Tanimoto similarity), and the top 25 compounds were chosen for experimental tests to measure binding affinity, functional potency and selectivity, eventually identifying two potent NAMs.

The NAM with the highest potency in D3R was also selective for the dopamine receptor D₂ (D2R). Based on this finding, a recent study was conducted using SAR optimizations on this NAM. A library of analogs was constructed accounting not only for the binding affinity but also for their efficacy to restore dopamine function.²⁶³ The D3R NAM and its analogs were found to be also potent D2R NAMs, and three of the analogs were shown to be many-fold more selective for D2R over D3R. To model the allosteric binding of the above-mentioned NAMs, the co-crystallized structure of the antipsychotic drug risperidone bound to the D2R (PDB: 6CM4)²⁶⁴ was used. Risperidone was replaced with raclopride (which was used in the binding experiments) using docking with the ICM-Pro^{261, 262} software and the D2R/raclopride complex was optimized using BPMC. The D3R NAM along with its 33 analogs were docked in the D2R complex again using ICM-Pro, providing

insights into the interactions of these NAMs with the orthosteric ligand and the D2R. It is worth noting that given the structural morphology of the orthosteric and allosteric pockets, the rational design of bitopic drugs holds a promising alternative for the D2R and D3R proteins.²⁶⁵⁻²⁶⁸

Glucagon receptor

Rational allosteric drug design of class B GPCRs have been even more laborious than class A due to the very few structural models available. Glucagon receptor (GCGR or GLR) is a class B GPCR, which regulates blood glucose levels and glucose homeostasis.²⁶⁹ In a study performed before GCGR was crystallized,²⁷⁰ a GCGR homology model was designed based on the corticotropin-releasing factor type 1 receptor (CRFR1) template, which in turn was modeled as prototypical class B representative from non-competitive (allosteric) antagonists, extensive SAR and site-directed mutagenesis data available at that time.⁹¹ Subsequently, MD simulations of the CRFR1 model in a hydrated phospholipid bilayer environment were performed. Virtual screening of known CRFR1 antagonists along with chemically similar decoys using the Gold software²⁷¹ on the last snapshot of the MD trajectory, showed that the final model was accurate, distinguishing true actives from decoys. Then, the GCGR model was constructed based on a) the CRFR1 template, b) SAR data of known noncompetitive antagonists, and c) MD refinement, similar to the CRFR1 case. A second screening of an in-house database of ~2 million compounds with various physicochemical properties was carried out using Pipeline Pilot²⁷² against existing negatively ionizable (Set A) and neutral (Set B) noncompetitive GCGR antago-

nists. Results were further filtered with a ligand-based similarity search to one of the reference neutral noncompetitive GCGR antagonists using the ROCS software.^{273, 274} Selected compounds were then docked and scored in an allosteric hydrophobic pocket between transmembrane helices 3, 4, and 5 of the GCGR model using Gold.²⁷¹ Compounds with a high score were preprocessed and filtered based on protein-ligand interaction fingerprints (Tanimoto similarity) with the IFP²⁷⁵ program, yielding a total of 228 compounds for Set A and 125 for Set B, which were clustered giving a total of 23 compounds. These compounds were then assayed along with the reference allosteric antagonist L-168049 in a functional assay, and two inhibited glucagon activity; one showed the same potency as L-168049. Intriguingly, one of the inactive virtual hits of the GCGR was later identified to be a PAM of the glucagon-like peptide-1 receptor (GLP-1R).⁹¹

Purinergic receptors

Purinergic receptors are classified in two GPCR classes (P1 and P2Y receptors) and a ligand-gated ion channel class (P2X receptors). P1 receptors, also called adenosine receptors, consist of four types, A₁, A_{2A}, A_{2B} and A₃, which bind to adenosine and exert various biological effects in regulating normal cell physiology.²⁷⁶ The P2Y class consists of eight receptor types, P2Y₁, P2Y₂, P2Y₄, P2Y₆, P2Y₁₁, P2Y₁₂, P2Y₁₃, and P2Y₁₄, which bind to nucleotides and are expressed in almost all human cells; these are implicated in cardiovascular, central nervous system (CNS), and other diseases.²⁷⁷ Recent advances in X-ray crystallography have enabled the structure-based drug design of orthosteric, allosteric, and bitopic ligands in P1 and P2Y receptors,²¹³ predicting a putative allosteric site in the adeno-

sine A₃ receptor (A₃AR) using supervised MD simulations,²⁷⁸ and rationalizing SAR data of NAMs with docking studies in the P2Y₁R.²⁷⁹

4.2 Lipoxygenases

15-lipoxygenase

Lipoxygenases are iron-containing enzymes, which catalyze the deoxygenation of polyunsaturated fatty acids such as arachidonic and linoleic acids, and are involved in inflammatory response and cancer.^{280, 281} 15-lipoxygenase (ALOX15) is one of the six human lipoxygenases implicated in anti-inflammation as activation of ALOX15 may alleviate inflammatory responses.²⁸² In a study focusing on designing allosteric activators,²⁸³ the human ALOX15 was modeled based on the rabbit 15S-lipoxygenase crystal structure (PDB: 2POM)²⁸⁴ using PRIME.²⁸⁵⁻²⁸⁷ The modeled structure was minimized and equilibrated using Desmond^{288, 289} with the OPLS-AA/SPC force field²⁹⁰⁻²⁹² followed by six independent MD simulations of 10 ns each, which were then combined and clustered yielding 30 cluster representatives. The CAVITY^{86, 87} program was used for the prediction of binding pockets, and a mutual information approach with the MutInf¹¹¹ program was facilitated for the identification of clusters of residues with statistically significant correlations. Six highly populated protein cluster representatives with an open putative allosteric pocket conformation having the best CAVITY score, and which motions were correlated with the motions of the orthosteric site according to MutInf, were selected for virtual screening of the SPECS²⁹³ database initially with DOCK,^{294, 295} and then with AutoDock.^{296, 297} After manually evaluating the top 500 compounds for each of the six protein conformers, a total of 175 com-

pounds were selected for assaying resulting in one compound that increased the ALOX15 activity thereby improving the control of inflammation. Subsequently, the top 3000 generated from virtual screening were rescored using Glide^{26, 228-230} in order to discover binding modes similar to this activator. From this procedure, 54 compounds were selected for further in vitro testing resulting in the identification of another two allosteric activators, albeit not as effective and potent as the first one.

4.3 Viral Proteins

Human immunodeficiency virus type 1 (HIV-1) integrase

Human immunodeficiency virus type 1 (HIV-1) is one of the two HIV types that are responsible for the acquired immune deficiency syndrome (AIDS). Millions of people have passed away from this virus, and still, millions are currently infected highlighting the continuous need for drug development against this virus.²⁹⁸ HIV-1 integrase inserts the HIV genetic material in the DNA of the infected human cell. In a rational drug design study implemented 20 years ago, the co-crystallized structure of the 5CITEP inhibitor bound to HIV-1 integrase (PDB: 1QS4)²⁹⁹ was simulated with MD simulations for 2 ns.³⁰⁰ Flexible ligand docking of 5CITEP in protein conformations retrieved from the simulation using AutoDock^{296, 297} revealed that 5CITEP docked in a cryptic allosteric site adjacent to the orthosteric site that was not visible in the crystal structure.³⁰¹ Ten “butterfly” compounds able to bind in both sites were then designed based on the structure of 5CITEP and docked in ten of the protein conformers extracted from the MD simulations. It is important to note that the discovery of this allosteric site led to the develop-

ment of the FDA-approved drug raltegravir by Merck & Co.³⁰²

HIV-1 protease

The Carlson group has thoroughly investigated the HIV-1 protease (HIVp) computationally, an enzyme essential for the life-cycle of HIV,³⁰³ using a dynamic receptor-based pharmacophore model called multiple protein structures (MPS), which they created in an HIVp allosteric site named “eye site”.^{95, 304-306} They applied the MPS method on MD simulations of three unbound semi-open structures of HIVp (1HHP,³⁰⁷ 3HVP,³⁰⁸ and 3PHV)³⁰⁹ simulated for 3 ns each to generate a receptor-based pharmacophore model.⁹⁵ The MPS resulted in a seven-site pharmacophore model of the eye site, which was then virtually screened with the University of Michigan’s Center for Chemical Genomics compound database using MOE^{310, 311}. 11 compounds were identified as possible allosteric inhibitors, and a representative was chosen for simulations to test its binding stability. Five independent Langevin dynamics (LD) simulations for 5 ns each and ten MD simulations for 10 ns each revealed that this reference compound was relatively stable in the allosteric binding site. Follow-up experimental work showed that this compound exhibited HIVp inhibition of $IC_{50} = 18 \pm 3 \mu M$.

A Markush chemical-similarity search was performed on this reference compound using the UNITY^{312, 313} module of the SYBYL³¹⁴ program against four compound libraries matching 7230 compounds.⁹² These were scored and ranked based on shape and charge distribution similarity using ROCS^{163, 273} and EON,³¹⁵ and the first 200 compounds of each library were manually examined resulting in 48 compounds that were

subjected to experimental testing. These assays revealed that a compound is an allosteric inhibitor, equipotent in the WT and the multidrug-resistant HIV-1p proteins. Further examination with five independent MD simulations and five independent LD simulations of 20 ns ensued, where the compound was docked in the HIVp allosteric site using the Glide^{26, 228-230} module. MD simulations showed a stable binding of this compound, while LD simulations showed reversible binding and unbinding. An analysis of protein collective motions from the MD trajectories on the complex and apo HIVp structures showed that the compound induces significant localized changes in the protein structures.

HIV-1 reverse transcriptase

HIV-1 reverse transcriptase (HIV-RT) is the enzyme responsible for converting the HIV RNA genome into DNA, an essential step in retroviral replication.³¹⁶ HIV-RT possesses a unique and highly selective hydrophobic allosteric pocket in which many diverse allosteric inhibitors called non-nucleoside reverse transcriptase inhibitors (NNRTIs) have been designed, six of them now being FDA-approved.³¹⁷⁻³²⁰ In a computer-aided NNRTI design journey that nearly lasted 20 years,³²¹ lead generation using *de novo* design with the BOMB³²² software, virtual screening with Glide,^{26, 228-230} and lead optimization with free energy perturbation (FEP) calculations combined with MC with the MCPRO³²³ program led to the discovery of NNRTIs and their optimization from micromolar to picomolar concentrations, the most potent NNRTIs reported to date.³²⁴⁻³³⁰ This computational procedure of lead generation and optimization led to the discovery and crystallization of picomolar activity NNRTIs selective for the Y181C and Y181C/K103N HIV-RT mutant proteins.³³¹⁻³³³

Flavivirus NS2B-NS3 protease

Flavivirus is a genus composed of more than 70 viruses causing severe and deadly diseases. The *Flavivirus* NS2B-NS3 protease complex is critical for the *Flavivirus* replication and is emerging as an essential drug target.³³⁴ An inspection of the crystal structures of the holo (PDB: 3U1I)³³⁵ and apo (PDB: 2FOM)³³⁶ forms of the Dengue virus DENV protease complexes revealed an allosteric pocket opposite to the active site apparent only in the inactive apo state of the NS2B-NS3 protease complex.³³⁷ This allosteric site was virtually screened with the NCI diversity set II compound library using the AutoDock Vina³³⁸ suite; the top 29 compounds were then assayed as potential allosteric DENV protease inhibitors. Three of them inhibited the NS2B-NS3 protease complex activity, and one showed high potency and effective inhibition of the Dengue virus 2, Zika virus, West Nile virus, and Yellow fever virus. Moreover, MSA revealed that the NS3 residues forming this allosteric pocket are highly conserved among *flaviviruses*, indicating that this site can be a potential target for drug development for other *flaviviruses*, too.³³⁹

HCV Nonstructural protein 5B

Hepatitis C virus (HCV) is the cause of hepatitis C, which is an infectious disease leading to liver cirrhosis, failure, and cancer, with millions of affected people worldwide.³⁴⁰⁻³⁴² One of the non-structural protein of HCV, the RNA-dependent RNA polymerase (RdRp-NS5B), essential for replicating the HCV viral RNA, contains five allosteric sites.³⁴³ Pharmacophore-based studies followed by virtual screening and hit optimizations on these allosteric sites yielded potent ligands able to inhibit the function of RdRp-NS5B allosterically.^{344, 345} We refer the readers to a recent review that summarizes the

structure-based and ligand-based drug development against RdRp-NS5B along with other non-structural proteins of HCV.³⁴⁶

4.4 Heat shock proteins

Hsp90

Heat shock proteins (Hsps) are responsible for protecting cells when they are stressed by high temperatures but they can also act as chaperones assisting the folding of other proteins.³⁴⁷⁻³⁴⁹ Hsp90 is emerging as an important cancer target. MD simulations of 70 ns were performed in the ATP bound, the ADP bound, and the apo Hsp90 using the crystal structure (PDB: 2CG9)³⁵⁰, the GROMACS³⁵¹ software and the GROMOS³⁵² force field.³⁵³ Subsequently, correlation analysis on the MD trajectories, essential dynamics, and GNM were applied as a signal propagation analysis procedure showing the existence of a connection between the C-terminal domain (CTD) and the ATP site. The five most representative conformations of the CTD were extracted by clustering the MD trajectories, which along with the initial crystal structure were used for the identification of possible allosteric pockets using the pocketFinder module of the ICM^{261, 262} software. One of the predicted allosteric sites was visible in all conformers and was employed to build a six-feature pharmacophore model for virtual screening.³⁵⁴

The NCI compound database was filtered applying the allosteric pharmacophore model and 36 putative lead compounds were selected; 14 were assayed generating biased allosteric inhibitors disrupting the communication with various client proteins. The most potent compound was then rationally optimized^{355, 356} (summarized in detail in a recent review).³⁵⁷

Hsp70

Hsp70 plays a critical role in oncogenesis, and similarly to Hsp90 it is a key cancer target. Hsp70 was modeled using as templates the N-terminal crystal structure of the human Hsp70 protein (PDB: 1S3X),³⁵⁸ the Escherichia coli Hsp70 substrate binding domain structure (PDB ID: 2KHO),³⁵⁹ and the *Caenorhabditis elegans* Hsp70 C-terminus structure (PDB: 2P32)³⁶⁰ with the PRIME^{85, 285, 286} module.³⁶¹ After alignment and refinement of the modeled human Hsp70, the SiteMap³⁶²⁻³⁶⁴ module was utilized for the discovery of putative allosteric sites. Manual inspection of the resulting cavities showed that the most druggable site is located in the N-terminal domain, which was chosen for the design of allosteric inhibitors. Several scaffolds were designed and patented taking into advantage a cysteine residue in the allosteric site for covalent binding. The lead compound was then docked computationally to examine interactions in the allosteric site and was further assayed in vitro proving that this compound is an Hsp70 modulator. Subsequently, SAR studies were performed providing novel anticancer allosteric inhibitors with competent potencies that selectively interact with the novel allosteric pocket of Hsp70.^{357, 365-367}

4.5 Kinases

3-phosphoinositide-dependent protein kinase 1

Protein kinases regulate the activity of other proteins usually by phosphorylating certain amino acids or lipids using ATP. Dysregulation of protein kinases is involved in many diseases and cancer.³⁶⁸⁻³⁷⁰ The 3-phosphoinositide-dependent protein kinase 1 (PDK1 or PDPK1) is a member of the AGC kinase subfamily of protein kinases, which possesses a regulatory site

separate from the ATP and the substrate binding sites, termed PDK1-interacting fragment (PIF) pocket.³⁷¹ In a study targeting PDK1, the active structure of PKA (PDB: 1ATP),³⁷² which is a member of the same AGC kinase subfamily containing this allosteric site, was used to define a pharmacophore model,⁹⁸ instead of the available PDK1 crystal structure, which is in a semi-active state (PDB: 1H1W).³⁷³ A virtual screening exercise of the Maybridge compound database ensued, and a total of 220 visually evaluated hit compounds were tested in vitro. Two of the compounds showed increase of PDK1 activity, and revealed that targeting this allosteric site lead to the transition between the inactive and active states of PDK1.

In a more recent study targeting the same allosteric site of PDK1,³⁷⁴ a structural ensemble of six PDK1 conformations was produced: the first structure was derived from the co-crystallized structure of PDK1 bound to the allosteric activator PS48 (PDB: 3HRF),³⁷⁵ where the PIF site is found in a closed conformation, the second from the co-crystallized structure of PDK1 bound to the covalent allosteric modulator 1F8 (PDB: 3ORX),⁶⁴ where the PIF site is in an open

conformation, which was then replaced in the first model, the third by producing a semi-open PIF conformation using the MODELLER²⁴⁸ program, and the other three structures were produced by optimizing the position of the Arg131 side chain using PLOP^{85, 285, 286} in the first three PIF conformations. Next, a compound library was built from the ZINC^{376, 377} database using the DUD-E³⁷⁸ procedure containing 6.300 ligands that were structurally dissimilar from the 112 known binders of the PIF site, but having a similar physicochemical profile with them. These ligands were docked in all six conformers in the PIF site using the DOCK^{251, 252} program, and three compounds were selected for assaying based on docking score rankings, geometry filtering, and visual inspection. Two out of three compounds bound in the PIF pocket and modulated PDK1 activity. Based on these two compounds, 518 analogs were extracted from the ZINC^{376, 377} database, and were docked to the six conformers resulting in 15 compounds that scored equally or better than the two parent compounds. One displayed stronger inhibition than the parent compounds in in vitro assays, and was co-crystallized with ATP bound to PDK1 (PDB: 4XX9, Figure 3).

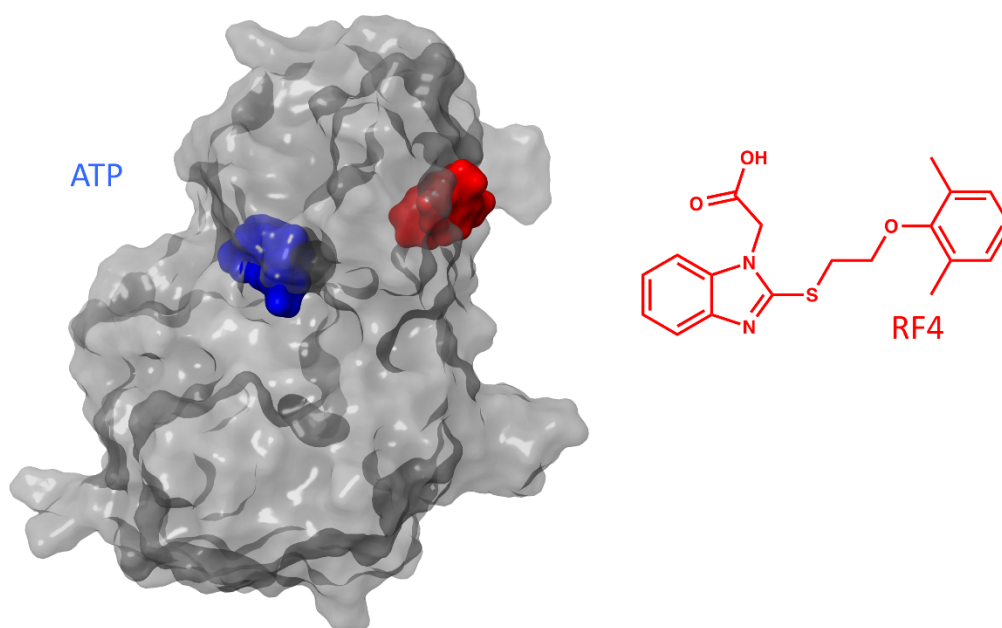


Figure 3. The crystal structure of PDK1 with the orthosteric (blue) and allosteric PIF-pocket (red) binding sites in surface representation is visualized on the left (PDB: 4XX9). On the right, the 2D representation of the allosteric compound RF4 is depicted in red.

Epidermal growth factor receptor

Epidermal growth factor receptor (EGFR) is a transmembrane kinase protein of the receptor tyrosine kinase (RTK) superfamily. Its mutations are implicated in lung cancer, and ligand design is pursued to selectively target mutant forms of EGFR but not the WT protein.³⁷⁹ HTS of 2.5 million compounds on the L858R/T790M EGFR mutant vs. the WT EGFR unveiled a noncompetitive inhibitor that is highly selective for the mutant protein.⁵² The X-ray co-crystal structure of the mutant protein with this inhibitor validated binding in an allosteric site adjacent to the active site of the inactive state (PDB: 5D41). Medicinal chemistry optimizations led to the rational discovery of an allosteric inhibitor being 1000-fold more selective for the L858R/T790M EGFR mutant as well as non-selective for 250 other kinases. Lastly, in vivo studies of the op-

timized allosteric inhibitor in combination with the dimer-disrupting antibody cetuximab resulted in an effective treatment for mutant-driven lung cancers in mice. Recently, the crystal structure of EGFR T790M/C797S/V948R in complex with this allosteric inhibitor was reported (PDB: 5ZWJ) showing a noncompetitive reversible binding with high specificity and potency for the T790M mutant EGFR.³⁸⁰

Tropomyosin receptor kinase A

Tropomyosin receptor kinase A (TrkA) is another member of the RTK family associated with inflammatory pain.³⁸¹ In an HTS study allosteric inhibitors of TrkA were discovered and patented.³⁸² The most selective allosteric inhibitor of TrkA over TrkB was crystallized (PDB: 6D1Y)³⁸³ validating its allosteric nature. This hit molecule was optimized to a lead molecule (PDB: 6D1Z),³⁸³ and a lead optimization vir-

tual chemical library of 11,000 compounds was created based on analysis of water molecule positions and energetics in the allosteric binding site using the WaterMap³⁸⁴⁻³⁸⁷ module.³⁸³ This compound library was prepared using Lig-Prep³⁸⁸ and was virtually docked using Glide^{26, 228-230} in the allosteric site of the crystal structure mentioned above; the top-scoring 100 compounds were examined in vitro. One of the screened compounds showed significant improvement in potency and selectivity over TrkB/C and was further optimized resulting in an orally non-toxic highly selective and potent allosteric inhibitor (PDB: 6D20)³⁸³. In the end, three different allosteric inhibitors were crystallized revealing similar binding patterns (Figure 4, PDB IDs: 6D1Y, 6D1Z, 6D20)³⁸³.

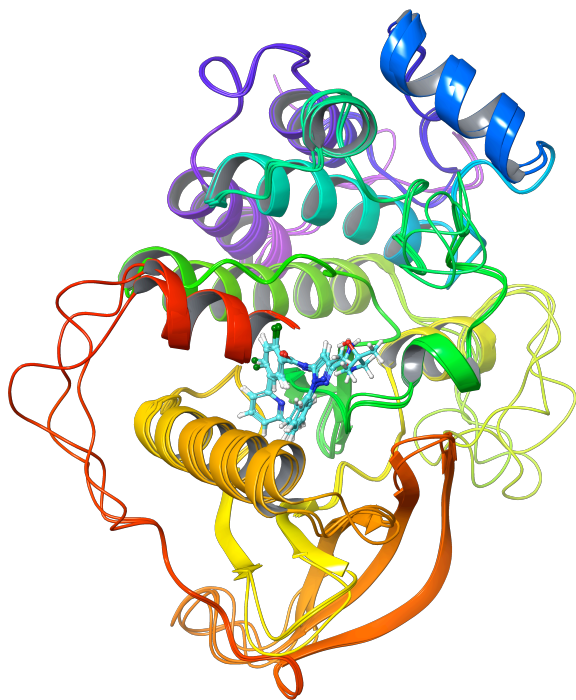


Figure 4. Superimposed crystal structures of Troponin receptor kinase A bound to three different allosteric inhibitors (PDBs: 6D1Y, 6D1Z, and 6D20). N-terminal residues 481-483 were truncated for clarity.

4.6 Phosphatases

Tyrosine-protein phosphatase non-receptor type 11

Phosphatases are enzymes that regulate the activity of proteins by removing phosphate groups through hydrolysis, usually with an opposite effect than kinases. Phosphatases together with kinases modulate protein activity in cells constituting significant components of the cell regulatory network. Protein tyrosine phosphatases (PTPs) regulate the dephosphorylation of tyrosine residues participating in cell proliferation, differentiation, and survival.^{389, 390} Tyrosine-protein phosphatase non-receptor type 11 (PTPN11 or SHP2) is a member of PTPs, which mutants are implicated in several pathophysiological diseases such as the Noonan syndrome and juvenile myelomonocytic leukemia.^{391, 392} In a scaffold-based drug design approach combining pharmacophore modeling, ligand docking, and MD simulations, the crystal structure of SHP2 in complex with the allosteric inhibitor SHP099 (PDB: 5EHR)^{393, 394} was used to produce 10 receptor-ligand pharmacophore models with the Discovery Studio.^{242,96} Using selectivity scores and receiver operating characteristic analysis, the best pharmacophore model was chosen and was further validated by redocking SHP099 in the crystal structure, which resulted in a similar binding conformation. Subsequently, the allosteric inhibitor SHP099 was divided into three scaffolds, each of which was replaced using the ZINC^{376, 377} database providing a library of nearly 5 million compounds. ADMET (absorption, distribution, metabolism, excretion, and toxicity) filtering reduced this library to 100,000 compounds, which was then subject to a two-way virtual screening. First, pharmacophore screening using Discovery Stu-

dio was performed; compounds scoring higher than SHP099 were then virtually docked using the CDOCKER utility of Discovery Studio, yielding eight compounds with better in vitro binding than SHP099. Subsequently, MD simulations were carried out on the apo structure of SHP2, the SHP2 in complex with SHP099, and the SHP2 in complex with the top-scoring compound for 20 ns each using GROMACS.³⁵¹ The top-scoring compound showed the same inhibitory activity as SHP099 albeit with a more favorable binding conformation.

In another study targeting the T253M/Q257L SHP2 double mutant, two additional putative allosteric sites different than the SHP099 allosteric binding site were predicted using SiteMap.^{219, 362, 363 395} After screening a library of approximately 1.5 million compounds experimentally, compounds that were inactive in the full conformation of SHP2, active in the phosphatase domain of SHP2 (active site), and inactive in the T253M/Q257L double mutant SHP2 were discarded. SHP099 is inactive in the T253M/Q257L double mutant of SHP2 and as a result compounds targeting the SHP099 allosteric binding site are also predicted to be inactive. Subsequently, one weak inhibitor with equipotent activity in the WT and the mutant SHP2 was co-crystallized with SHP2 (PDB: 6BMR³⁹⁵), revealing that this inhibitor binds in a new allosteric site. Structure-based design optimizations taking into account this new allosteric binding site led to the identification of another two inhibitors, which were also crystallized bound to SHP2 (PDBs: 6BMX, 6BMV).³⁹⁵ Visualization of these three crystal structures revealed that the SHP099 allosteric binding site remained unperturbed offering the possibility

of dual inhibition. Dual inhibition was later confirmed with biochemical and crystallographic studies for SHP099 and the three new allosteric inhibitors resulted in biochemical enhancement of IC₅₀ along with dual binding in both allosteric sites via crystal structures (PDBs: 6BMU, 6BMY, 6BMW). Further SAR optimization studies taking into account the crystal structures of SHP2 co-crystallized with the allosteric inhibitor SHP099 (PDB: 5EHR) and with two HTS allosteric hits (PDBs: 6MD9, 6MDA) produced a pharmacophore model accounting for the protein-ligand interactions of the SHP099 allosteric pocket.^{396, 397} Many new orally bioavailable allosteric inhibitors demonstrating high potency and selectivity were discovered with some of them being crystallized with SHP2 (PDBs: 6MDB, 6MDC, 6MDD, 6MD7) confirming that they bind to the same allosteric site that stabilizes an auto-inhibiting conformation.

4.7 Ligand-gated ion channels

γ-aminobutyric acid type A receptor

Ligand-gated ion channels are transmembrane proteins, which allow ions to pass the cell membrane after the binding of a neurotransmitter. The γ-aminobutyric acid type A receptor (GABA_AR) is a ligand-gated ion channel implicated in the CNS and is an essential target for antiseizure drug development.^{398, 399} In a study performed before GABA_AR crystallization, 37 homology models of GABA_AR were derived from cysteine-loop receptor family members, and the allosteric modulator diazepam along with other benzodiazepine ligands were docked using the FlexX⁴⁰⁰ and FlexE⁴⁰¹ software packages, in order to discard those with poor lipophilic interactions producing six final models.⁴⁰² Then,

energy minimization was performed generating thousands of poses, which were clustered to identify similar binding modes, leading to three clusters, in which homogenous subsets of poses were extracted (common binding modes). These were evaluated based on ligand interactions and experimental evidences, and validated by virtual screening of benzodiazepine-binding-site ligands and decoy molecules generated from the DUD³⁷⁸ database, using pharmacophore modeling with the LigandScout⁴⁰³ software. The pharmacophore model of the most promising binding mode was used for the discovery of new ligands by screening almost 100,000 compounds from the DUD³⁷⁸ database. In the top 0.5% ranked compounds, ligands showing anti-convulsive activity were tracked in the literature, and commercially available representatives were assayed, leading to the discovery of two hits inhibiting the benzodiazepine-binding site of GABA_ARs. Additionally, docking-based virtual screening was performed on the GABA_AR models using the same binding mode employed to generate the pharmacophore model. An in-house library of 1,010 chemically diverse fragment-like molecules was virtually screened using the PLANTS⁴⁰⁴ docking method with rigid and flexible docking. From the top 30 ranked compounds, 10 were selected for experimental validation, with two of them inhibiting the benzodiazepine-binding site.

In a similar structure-based allosteric ligand discovery study, targeting pLGICs, and specifically, *Gloeobacter violaceus* ligand-gated ion channel (GLIC), a close homolog of GABA_AR, led to the discovery of allosteric modulators.⁴⁰⁵ The crystal structure of GLIC bound to the general anesthetic propofol (PDB: 3P50),⁴⁰⁶ which acts as a

PAM in GABA_AR, was embedded in a dioleoylphosphatidylcholine lipid membrane and was equilibrated for 25 ns using MD simulations with the GROMACS³⁵¹ software. Propofol along with 100 decoy molecules selected according to the DUD-E³⁷⁸ procedure were docked in 302 structures retrieved from the simulation using the DOCK^{251, 252} program. The structure with the best ranking for propofol was virtually screened using the DOCK program and more than 150,000 molecules from the ZINC^{376, 377} database. Inspection and filtering of the 700 top-ranked compounds led to 22 compounds, which along with seven analogs were selected for assaying. More than half of them were identified as GLIC hits with three of them producing greater modulation than propofol. In the end, these hits were also tested on GABA_AR, with many of them modulating GABA_AR, although none of them having better potency than propofol.

In a ligand-based allosteric drug design study, a pharmacophore model was derived based on two different allosteric modulators, which putatively bind to the same GABA_AR allosteric site using the LigandScout⁴⁰³ software.⁹⁴ A conformational ensemble was generated for each ligand, and the best matching pose between them was calculated. A shared pharmacophore model was derived from this conformational pair, and it was used as a virtual screening filter of several compound libraries. Various modifications in the selected top hit compound led to the discovery of 39 structural analogs, which were tested in vitro. Two of them were tested in vivo displaying low-dose anticonvulsant activity and GABA_AR selectivity.

Glycine receptors

Glycine receptors (GlyRs) are pentameric glycine-gated chloride ion channels with a critical role in CNS that mediate inhibitory neurotransmission in the spinal cord and brain stem and retina.⁴⁰⁷ In an ensemble-based virtual screening study, MD simulations of the transmembrane domain (TMD) of the NMR structure of the human GlyR- α 1 (PDB: 2M6I)⁴⁰⁸ embedded in a pure 1-palmitoyl-2-oleoylphosphatidylcholine (POPC) and two POPC/cholesterol lipid bilayer systems were performed using the GROMACS³⁵¹ software and the Amber03⁴⁰⁹ force field.⁴¹⁰ For each system, three parallel 50 ns replicate simulations were performed followed by RMSD clustering, yielding 180 protein conformational representatives. Then, the DrugBank⁴¹¹ database of 1,549 FDA-approved compounds was virtually screened in the THC binding site of all GlyR- α 1 TMD representatives twice, with and without lipid molecules using the AutoDock Vina³³⁸ program. Virtual screening resulted in 14 compounds in the top 25 of both virtual screens, and 11 of them along with another two compounds with a better score than THC were further experimentally tested. 12 compounds were shown to potentiate GlyR- α 1, providing an overall hit rate of 92% with seven compounds being more potent than THC and also being selective GlyR- α 1 modulators with respect to other members of the Cys-loop receptor superfamily. Eventually, this led to identifying FDA-approved drugs with analgesic effect.

In a hit-to-lead optimization study performed by Amgen Inc., an HTS hit compound with modest potency was improved using SAR and medicinal chemistry optimizations. This study led

to a highly active potentiator (AM-3607),⁴¹² which was co-crystallized with human GlyR- α 3 revealing bound to a novel allosteric site adjacent to the orthosteric site where glycine binds.⁴¹³ Aiming in the discovery of new classes of GlyR potentiators, a virtual library of hundreds of commercially available sulfonamides was designed and evaluated based on the structure and property similarity with the HTS hit compound; this effort led to the property-guided parallel synthetic discovery of two compounds with improved properties.⁴¹⁴ Hit-to-lead and SAR optimizations in one of them resulted in a lead compound having retained potency for GlyRs and exhibiting improved lipophilic efficiency and selectivity against other Cys-loop receptors. Moreover, a pharmacophore model was built based on the presumed bioactive conformation of the HTS hit compound and an internal Amgen library of more than half a million compounds was virtually screened with MOE¹³⁹, resulting in 4,267 hit compounds. These compounds were screened with functional assays and 17 hit compounds were discovered, among which a novel and structurally different class of sulfone modulators.

Recently, a web database named GRALL was designed containing all allosteric ligands that modulate the GlyR- α 1 and GlyR- α 3 function, providing information on their putative binding sites, the direction of modulation, the potency and others.¹⁹⁸ This database is expected to be a significant asset in the structure-based allosteric drug discovery of GlyRs.

Acid-sensing ion channels

Acid-sensing ion channels are also expressed in CNS and are implicated in various neurological diseases such as multiple sclerosis, Parkinson's

disease, and many others.⁴¹⁵ In a recent study focusing on identifying novel acid-sensing ion channel 3 (ASIC3) modulators, a ligand-based *in silico* screening of the FDA-approved drug library eDrug3D⁴¹⁶ using the PAM 2-guanidine-4-methylquinazoline (GMQ) as a query structure was performed.⁴¹⁷ Using ROCS^{163, 273} in combination with manual inspection of the top 150 ranked hits identified five drugs as potential hits, which were validated experimentally; one drug, named GBZ, was confirmed as an ASIC3 activator. To assess whether GBZ acts allosterically, three homology models of ASIC3 based on the closed, open, and desensitized states of ASIC1 were used for five independent blind docking runs with GMQ and GBZ in the entire trimer structures using AutoDock.^{296, 297} Both drugs preferentially docked to a pocket located in the palm domain. Furthermore, a GBZ derivative, called sephin1, which was in clinical trials and was not included in the eDrug3D database, exhibited higher similarity with GMQ than the aforementioned drugs, bound to the same non-proton ligand-sensing domain site, and was shown experimentally to activate the ASIC3.

Nicotinic acetylcholine receptors

Nicotinic acetylcholine receptors are members of the Cys-loop family of ligand-gated ion channels and are implicated in neurological and neuromuscular disorders.⁴¹⁸ In a similar study of virtual screening already FDA-approved drugs on the $\alpha 7$ nicotinic acetylcholine receptor ($\alpha 7$ nAChR), 25 known $\alpha 7$ nicotinic acetylcholine receptor (nAChR) PAMs were docked in a transmembrane site of revised structural models of the $\alpha 7$ nAChR TMD⁴¹⁹ in the open and closed conformations.⁴²⁰ These PAMs were then clustered based on RMSD, and six pharmacophore models were created for the largest

clusters in the open and the closed conformations using ROCS.^{163, 273} A set of 42 known $\alpha 7$ nAChR PAMs along with decoy molecules generated using DecoyFinder⁴²¹ and the ZINC^{376, 377} database were virtually screened to validate the pharmacophore models. The best pharmacophore model for the open and the closed conformations were chosen for virtual screening of the FDA-approved drug DrugBank⁴¹¹ database. Filtering of the top 100 hits from each model resulted in 81 compounds, and four of the highest-ranked members of the four classes of compounds that were represented in the 25 top-ranked hits were experimentally tested, resulting in an inhibitor of Na-K-Cl cotransporter protein, called furosemide, acting as a PAM, and a Carbonic anhydrase II inhibitor, a Cyclin-dependent kinase 2 inhibitor, and a DNA gyrase antibiotic, acting as NAMs.

4.8 Caspases

Cysteine-aspartic proteases 3 and 7

Cysteine-aspartic proteases (caspases) are a family of enzymes implicated mainly in cell apoptosis. Caspase deficiency is connected with tumor development, while its upregulation increases cell death.^{422, 423} Caspase-3 is a significant target as it is a primary effector in the execution-phase of cell apoptosis.⁴²⁴ In a site-directed fragment-based ligand discovery study searching for chemical fragments that bound near existing surface cysteines, an allosteric site of caspase-3 was discovered, and then two allosteric inhibitors named DICA and FICA were identified and crystallized with caspase-7 (PDB: 1SHJ and 1SHL respectively),⁴²⁵ as caspase-3 and -7 display high sequence identity and structural similarity.^{426, 427} In a recent computational caspase-3/7 allosteric drug design study, the

caspase-7/DICA complex crystal structure was employed to virtually screen a library of FDA-approved drugs from the ZINC^{376, 377} database using DOCK,^{251, 252} after the breaking of the disulfide bond of Cys290/DICA, for the identification of reversible binding allosteric bioactive ligands.⁴²⁸ The exact same procedure was implemented for the orthosteric site to distinguish compound features depending on their preferred binding site. Comparing the top 25 allosteric hits with the top 25 orthosteric hits, differences were observed in their average net charge and polar/apolar desolvation. Taking into account these results, only five compounds that scored in the top 100 in the allosteric site and did not score in the top 100 in the orthosteric site were further tested experimentally. Four compounds showed significant inhibitory activity in caspase-3, concluding that these already FDA-approved drugs can inhibit the caspase-3 and -7 allosterically.

4.9 Oxidoreductases

D-3-phosphoglycerate dehydrogenase

D-3-phosphoglycerate dehydrogenase (PHGDH) is a tetramer enzyme that belongs to the family of oxidoreductases, which catalyzes chemical reactions utilizing NAD⁺ as a cofactor.⁴²⁹ It is the first enzyme in the pathway of serine biosynthesis and can also be allosterically inhibited by serine, thus regulating the serine production. In a computational study using PHGDH from *E. coli*, the coarse-grained two-state G \bar{O} model⁴³⁰ was used to identify novel allosteric sites by generating an ensemble of active and inactive states.⁴³¹ Using the unbound (PDB: 1YBA)⁴³² and the bound (PDB: 1PSD)⁴³³ crystal structures, Langevin dynamics simulations were performed

using the Cafemol⁴³⁴ software, parameterized so that the unbound state was dominant in the ensemble. Moreover, the CAVITY^{86, 87} program was implemented to predict new pockets, and subsequently, perturbations were induced in these pockets in another coarse-grained simulation. A site was considered as allosteric in the event of a population distribution change. Two novel allosteric sites were predicted in the PHGDH enzyme, and virtual screening was performed in one of them using DOCK^{294, 295} with the SPECS²⁹³ compound library and then using the AutoDock Vina³³⁸ program to screen the top 10,000 compounds. The top-ranked 1000 compounds were manually inspected and 178 were tested in vitro. Three novel allosteric inhibitors were discovered, revealing a low μ M inhibitor, validating the predicted site as allosteric.

The same virtual screening procedure was applied on the other predicted allosteric site, where 170 compounds were tested in vitro resulting in a significant inhibition of the PGDH activity from three compounds.⁴³⁵ Intriguingly, two of those exhibited a rise in the activity of PGDH in low concentrations and inhibition in high concentrations. SAR studies were conducted on these two compounds using the PHASE⁴³⁶ engine and compounds with high similarity to the parent compounds were virtual docked using the Glide^{26, 228-230} module. 25 compound analogs from each of the two parent compounds were selected for in vitro experiments resulting in seven allosteric inhibitors in total, with one of them having a better inhibitory activity than the parent compounds.

Glutathione peroxidase 4

Glutathione peroxidase 4 (GPX4) is one of eight members of the glutathione peroxidase family,

which is a subfamily of oxidoreductases that protect cells against oxidative damage. Down-regulation of GPX4 is associated with inflammation and cell ferroptosis.^{437, 438} In a recent study for rationally designing allosteric activators, the pocket detection CAVITY^{86, 87} program was utilized on the human U46C mutant GPX4 crystal structure (PDB: 2OBI),⁴³⁹ and the predicted sites were analyzed with the motion correlation CorrSite¹⁰⁹ program, identifying one of the predicted sites as allosteric.⁴⁴⁰ This site was also further validated as allosteric by analyzing its dynamic changes and the correlated motions with the substrate site using MD simulations. Subsequently, the SPECS²⁹³ library was screened using the Glide^{26, 228-230} module with the SP scoring function, and then the top 10.000 compounds were virtually screened with the more accurate XP scoring function. The top 2.000 compounds were inspected manually, and 251 of them were tested experimentally resulting that the top compound selectively increases the maximum GPX4 activity by 263%. SAR studies of the top compound identified eight new GPX4 activators with some being more potent in suppressing ferroptosis and inflammation than known activators.

4.10 Sirtuins

Sirtuin 6

Sirtuin 6 (SIRT6) is a protein with multiple functions including modulation of cellular senescence and apoptosis, DNA repair, Tumor necrosis factor protein production regulation, and others.⁴⁴¹⁻⁴⁴³ The Zhang group used their allosteric pocket detection tool, Allosite,^{145, 149} to identify putative allosteric sites on the SIRT6 protein (PDB: 3ZG6).^{444,445} Allosite predicted a previously-discovered deep hydrophobic allo-

steric site,⁴⁴⁶ and subsequently seven compound libraries consisting a total of more than five million compounds were virtually docked using GLIDE^{26, 228-230}. The top 20 ranked compounds were experimentally tested, with two demonstrating μ M activation. The common scaffold of these two compounds was used as a starting point for medicinal chemistry optimizations, leading to two compounds with an order of magnitude lower EC₅₀, and strong selectivity in the sirtuin protein family. Binding of these compounds in the allosteric site was verified experimentally with mutagenesis and crystallography (PDB: 5Y2F), delivering promising lead compounds for non-small cell lung cancer.⁴⁴⁷

4.11 High-temperature requirement A protein

Helicobacter pylori is a gram-negative bacterium found in the stomach linked with gastritis, ulceration and stomach cancer.⁴⁴⁸⁻⁴⁵⁰ The high-temperature requirement A protein (HtrA) is responsible for the migration of this bacterium across the epithelial barrier and is a new therapeutic target for the abovementioned diseases.⁴⁵¹ In a receptor-based virtual screening approach for the identification of allosteric inhibitors of HtrA,⁹³ a homology model from various HtrA protein sequences followed by sequence alignment using the BLAST⁴⁵² tool showed that the 3D structure with the highest sequence identity was the 3MH6⁴⁵³ PDB. Then, the 3MH6 sequence was aligned with the other sequence homologs using the ClustalW⁴⁵⁴ program, and the HtrA comparative model was built using Modeller²⁴⁸. A pocket distal to the orthosteric site was discovered using the PocketPicker⁴⁵⁵ tool. Subsequently, the PoLiMorph⁴⁵⁶⁻⁴⁵⁸ receptor-based screening

module, which evaluates complementarity of pockets and ligands, was used to calculate graph descriptions of the distal site and ligands collected from the SPECS²⁹³ Natural Products and Screening Collection libraries. From a chosen hit, two analogs were derived from a ligand-based similarity search experiment using PoLiMorph and one of them displayed in vitro allosteric inhibitory action on HtrA.

4.12 Beta-lactamases

TEM β -lactamase

TEM β -lactamases are enzymes produced by gram-negative bacteria responsible for drug resistance of β -lactam antibiotics.⁴⁵⁹ In the study of Bowman *et al.*, 1,000 MD simulations were performed in the apo TEM β -lactamase structure (PDB: 1JWP)⁴⁶⁰ as well as 400 MD simulations including a known allosteric inhibitor (PDB: 1PZO)⁴⁶¹ using GROMACS³⁵¹ and the Amber03 force field⁴⁰⁹ for a total aggregated simulation time of $\sim 100\mu\text{s}$ in order to explore the conformational space.¹⁷⁴ Then, MSMs were employed utilizing MSMBuilder⁴⁶² to capture the protein states in the energy landscape minima. Putative binding pockets were identified using LIGSITE⁴⁶³ in representative structures from each MSM. To distinguish which pockets were cryptic, pockets identified in the apo structure were discarded, and the rest were clustered, successfully identifying a known cryptic allosteric site along with another two novel cryptic pockets, which were verified experimentally.¹⁷⁵ Subsequently, virtual screening was applied to the known cryptic allosteric site against a library of 12,695 compounds with the Surflex-dock program⁴⁶⁴ using the 1PZO PDB. The top-40 scoring

compounds were tested experimentally, resulting in a hit compound acting as PAM.⁴⁶⁵ The same compound library was then docked in 15 structures of the most populated protein states of the MSM containing this cryptic site using a Boltzmann-weighted docking approach that takes into account the population information from the MSM.⁴⁶⁶ 71 top-scoring compounds were then assayed resulting in a NAM and a PAM.⁴⁶⁵

4.13 Signal transducer and activator of transcription proteins

Signal transducer and activator of transcription 3

Signal transducer and activator of transcription 3 (STAT3) is a transcription factor implicated in cancer and inflammatory and cardiovascular diseases.^{467, 468} Allosteric drug discovery on STAT3 has been performed using Allofinder, a platform consisting of software tools for drug discovery.¹⁸⁵ Allosite was first employed to predict five putative allosteric sites in STAT3 (PDB: 3CWG).⁴⁶⁹ One of these sites is located in the CCD domain implicated in STAT3 regulation, far from the STAT3–DNA interface. Virtual screening was performed in this site with AutoDock Vina³³⁸ and the SPECS²⁹³ compound library. Compounds were ranked by a binding scoring method for affinity prediction of allosteric ligand–protein interactions, Alloscore.¹⁸⁷ The top 15 hits were assayed, with one compound inhibiting STAT3. Finally, site-directed mutagenesis confirmed the binding of this compound in the predicted allosteric pocket.

4.14 Peptidase C1 proteins

Cathepsin K

Cathepsin K is a protease responsible for bone resorption, and is a prime therapeutic target for osteoporosis.^{470, 471} The SCA method was performed in the MSA of an ensemble of 1,239 catalytic domains from the papain-like cysteine peptidases family followed by hierarchical clustering, revealing a protein sector of coevolving residues with a continuous residue network.⁴⁷² Alanine-scanning of 15 single-substitution mutants verified this residue network as allosteric. Using AutoLigand⁴⁷³ on Cathepsin K (PDB: 1ATK)⁴⁷⁴ predicted seven putative allosteric pockets in contact with sector residues. Compound libraries from the ZINC^{376, 377} database were virtual screened in all seven predicted binding sites using DOCK,^{294, 295} and the top-scoring 10% compounds were subsequently virtually screened with AutoDock.^{296, 297} More than 200 compounds were assayed, 15 showed potency and one was crystallized identifying one of the predicted sites as a novel allosteric site (PDB: 5J94). Further experiments showed that this compound is a potent and selective Cathepsin K allosteric inhibitor.

4.15 Ras proteins

K-Ras

Ras proteins are key regulators of cell growth signaling pathways that are switched on/off in a GTPase cycle between the active GTP-bound and the inactive GDP-bound states. Dysregulation of Ras proteins occurs in ~25% of human cancers.^{475, 476} The K-Ras protein, which is a member of the Ras family and one of the most common human oncogenes, was computation-

ally studied by performing Mg^{2+} /GTP bound and Mg^{2+} /GDP bound K-Ras MD simulations using the AMBER^{477, 478} software and force field.⁴⁷⁹ The K-Ras bound states were modeled using the human K-Ras crystal structure in complex with a GTP analog (PDB: 3GFT). Subsequently, a protein conformational ensemble was produced from Ras crystal structures and MD snapshots to account for K-Ras flexibility using PCA and RMSD clustering with the Bio3D⁴⁸⁰ R package. The FTMap^{83, 85} program and the AutoLigand⁴⁷³ module were used in this conformational ensemble to identify novel binding pockets. In addition, blind docking was conducted with known Ras inhibitors derived from HTS using AutoDock^{296, 297} and a grid covering the whole crystal structure. Five non-substrate pockets were identified, named p1, p2, p3, p3b, and p4, and a virtual screening exercise was performed in all of them and all conformers using the NCI and ZINC^{376, 377} compound libraries and Glide^{26, 228-230}. The top compounds were rescored with eight other scoring functions and were then filtered with Lipinski's rule of 5.⁴⁸¹ 19 top-scoring compounds targeting the p3 site, which was the only one present in all three pocket discovery methods applied in this study, were assayed; hits displaying moderate affinity and selectivity serving as starting points for lead optimization were discovered.

The same research group also performed a large scale MD simulation (1.76 μ s in total) of GTP-bound Q61H mutant K-Ras (PDB: 3GFT) using the NAMD⁴⁸² program and the CHARMM^{219, 220} force field.⁴⁸³ A conformational ensemble of 75 protein structures were extracted based on RMSD clustering, and andrographolide and derivatives were blind-docked

identifying three putative binding sites.⁴⁸⁴ The binding stability of a chosen ligand was tested in two of these pockets with five independent MD simulations for each pocket resulting in a preferred binding pocket. In vitro studies of these compounds established K-Ras inhibition for two compounds. Then, authors focused on G12D K-Ras and performed 300 ns MD simulations (PDB: 4DSO)⁴⁸⁵ to generate an ensemble of conformations with an open allosteric site p1.⁴⁸⁶ Six million compounds were virtually screened in the conformation with the most open p1 site, using AutoDock^{296, 297} and the ZINC^{376, 377} database, and top-scoring compounds were re-scored with AutoDock Vina³³⁸. The top 500 hits from each screen were filtered based on their interactions with the protein, and 11 compounds were assayed. Two were found to inhibit K-Ras by disrupting the K-Ras-Raf interaction.

Concurrently, MD simulations were performed in the WT K-Ras, and in the four major mutants G12D (PDB: 4DSO),⁴⁸⁵ G12V, G13D, and Q61H (PDB: 3GFT) K-Ras for 200–400 ns each.⁴⁸⁷ The G12V and G13D K-Ras mutants were created from PDB ID 4DSO. 8–12 representative conformations were selected for each of the p1, p2, p3, p4 allosteric pockets and each of the WT and mutant proteins, based on RMSD clustering and pocket analysis with MDPocket,⁴⁸⁸ resulting in 162 final structures. 23 million compounds from the ZINC^{376, 377} database were filtered based on drug-like properties and many other features, resulting in ~350,000–700,000 ligands per mutant per pocket, which were virtually screened (76 million docking runs) using Glide^{26, 228–230}. For each pocket, docking results were combined and the top-scoring 10% compounds

were clustered and post processed with the DataWarrior⁴⁸⁹ program, resulting in 785 hits, with 87% populating the p1 and p2 allosteric sites. Although clustering of the 785 hits displayed high diversity, scaffold diversity analysis revealed that more than half of them contain similar scaffolds, including pyrazole, indole, and thiazole. 90 hits from the p1 and p2 allosteric sites were assayed with NMR, resulting in nine compounds (10% success rate) causing NMR amide chemical shift perturbations, and one was shown to bind to p1 with low μM affinity.

In another study targeting the G12D K-Ras mutant, virtual screening of 1.36 million compounds from the Chemdiv⁴⁹⁰ library resulted in a hit compound, 0375-0604, which was selected for further study.⁴⁹¹ The G12D K-Ras mutant (PDB: 4DSU)⁴⁸⁵ was used to create the G12C and Q61H K-Ras mutants, and 0375-0604 was docked in a hydrophobic binding pocket adjacent to the switch I and switch II regions in all mutant structures using Glide^{26, 228–230}. *In vitro* experiments showed binding affinity to K-Ras, selectivity for the mutant forms of K-Ras over the WT, and the potential to block the binding of GTP.

Moreover, the G12C mutation of K-Ras provides with the opportunity of covalent allosteric ligand design. The advantages of this irreversible binding, as well as, the progress in designing covalent allosteric drugs rationally for K-Ras are described below.

4.16 Covalent allosteric modulators

Small molecule ligands can be grouped into two major categories based on their interactions with the biological target. Non-covalent ligands interact with the binding site in a reversible

manner, while covalent ligands bind irreversibly with protein aminoacids containing nucleophiles such as hydroxyl or sulfhydryl groups found in serine, cysteine, threonine, or tyrosine. This irreversible binding is transcribed in lower administered dosage as covalent ligands do not detach from their targets. Subsequently, this leads to higher potency and high energy barriers between active and inactive conformations,⁴⁹² which together with the aforementioned advantages of allosteric modulators such as the high specificity and the noncompetitive inhibition imply that covalent allosteric ligands are worthy of exploration.

Examples of rational covalent allosteric modulator design have been reviewed in ref.⁴⁸ An intriguing case is the oncogenic G12C mutation of GTPase K-Ras4B, for which SAR and crystallographic studies identified covalent allosteric inhibitors forming a disulfide bond with the mutant residue G12C (PDBs: 4LYJ, 4M22, 4M1Y, 4M1W, 4M1T, 4M1S, 4M1O, 4LYH, 4LYF, 4LV6, 4LUC); these inhibitors displayed significant *in vitro* potency.⁴⁹³ Further iterative structure-based design in one of these inhibitors led to the discovery of a very potent and efficacious

covalent allosteric inhibitor, named ARS-853, which stabilizes the inactive state of GDP-bound G12C mutant K-Ras4B (PDB: 5F2E).^{494, 495} Further scaffold and SAR optimizations led to the development of ARS-1620, which was also co-crystallized with K-Ras G12C (PDB: 5V9U).⁴⁹⁶ ARS-1620 exhibited *in vivo* potency in K-Ras tumors.⁴⁹⁶ By exploiting the H95/Y96/Q99 cryptic pocket,⁴⁹⁷ ARS-1620 was further optimized with iterative substitutions, SAR optimizations, and crystallography, leading to AMG 510 (PDB 6OIM, see Figure 5),⁴⁹⁸ which significantly inhibited tumor growth *in vivo*, and is first G12C K-Ras inhibitor to enter clinical trials by Amgen .Inc.^{498, 499} AMG 510 (sotorasib) was granted accelerated approval (Lumakras™, Amgen, Inc.) by the FDA on May 28 2021, for adult patients with KRAS G12C mutated locally advanced or metastatic non-small cell lung cancer, who have received at least one prior systemic therapy. This application was granted priority review, fast-track, breakthrough therapy and orphan drug designation. Information about the clinical trials of sotorasib can be accessed at <https://clinicaltrials.gov> under the identifier NCT03600883.

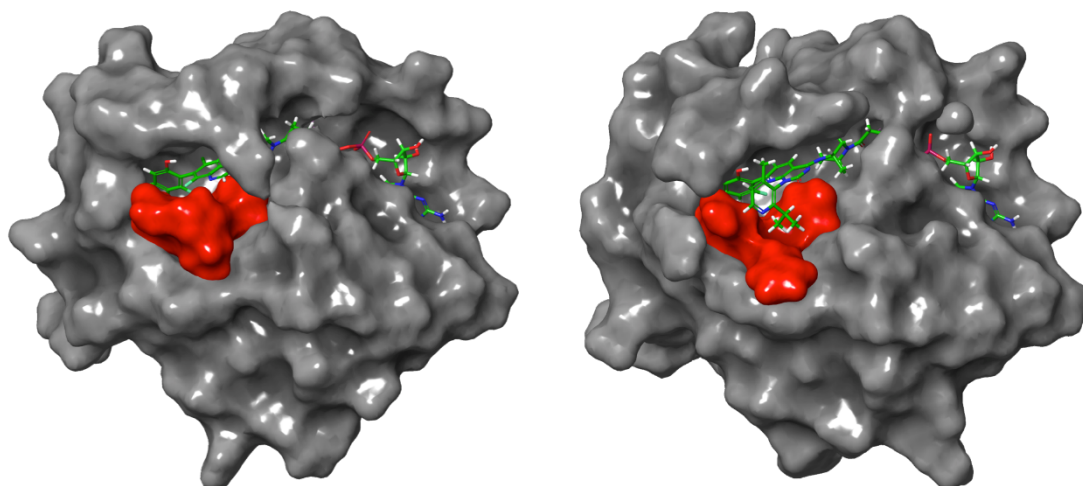


Figure 5. On the left panel the crystal structure of K-Ras G12C mutant co-crystallized with allosteric covalent inhibitor ARS-1620 and GDP (PDB ID: 5V9U) is depicted. On the right panel the crystal structure of K-Ras G12C mutant co-crystallized with allosteric covalent inhibitor AMG 510 (sotorasib) and GDP (PDB ID: 6OIM) is seen. Binding of AMG 510 opens up the cryptic pocket enclosed by H95/Y96/Q99, which are depicted in red.

Another covalent allosteric inhibitor case is the rational design and synthesis of novel allosteric inhibitors that covalently modify the protein kinase Akt.⁵⁰⁰ Co-crystal structures of these inhibitors with Akt can be found in PDB: 6HHF,⁵⁰¹ as well as another four structure-based designed and synthesized covalent allosteric inhibitors (PDBs: 6HHJ, 6HHG, 6HHI, 6HHH), identified as potent candidates for in vivo studies and further lead optimization.⁵⁰²

In an allosteric communication computational study based on evolutionary data performed by Tang *et al.*⁵⁰³ for the Myosin-2 motor protein, a pathway connecting the ATP site with the lever arm of the protein was discovered using MSA and conservation weights. To predict new putative allosteric binding sites near this pathway, we used the fragment-based computational mapping server FTMap, which predicts binding

hot spots of macromolecules,^{83, 504} in the crystallographic structure PDB: 2XO8⁵⁰⁵ (Figure 6). Indeed, we identify a pocket near the allosteric pathway, and specifically next to Met486; this finding could open up the possibility of allosterically, and possibly covalently, targeting Myosin-2 by modulating the ATP site through this allosteric pathway.⁵⁰⁶

Several other covalent allosteric inhibitors have been co-crystallized with their protein targets such as the ubiquitin-like modifier SUMO E1 in complex with a covalent allosteric inhibitor targeting a cryptic pocket with high specificity (PDB: 6CWY)⁵⁰⁷ and the natural product novolactone bound covalently and allosterically to the Hsp70 (PDB: 4WV7)⁵⁰⁸ paving the way for further structure-based design.

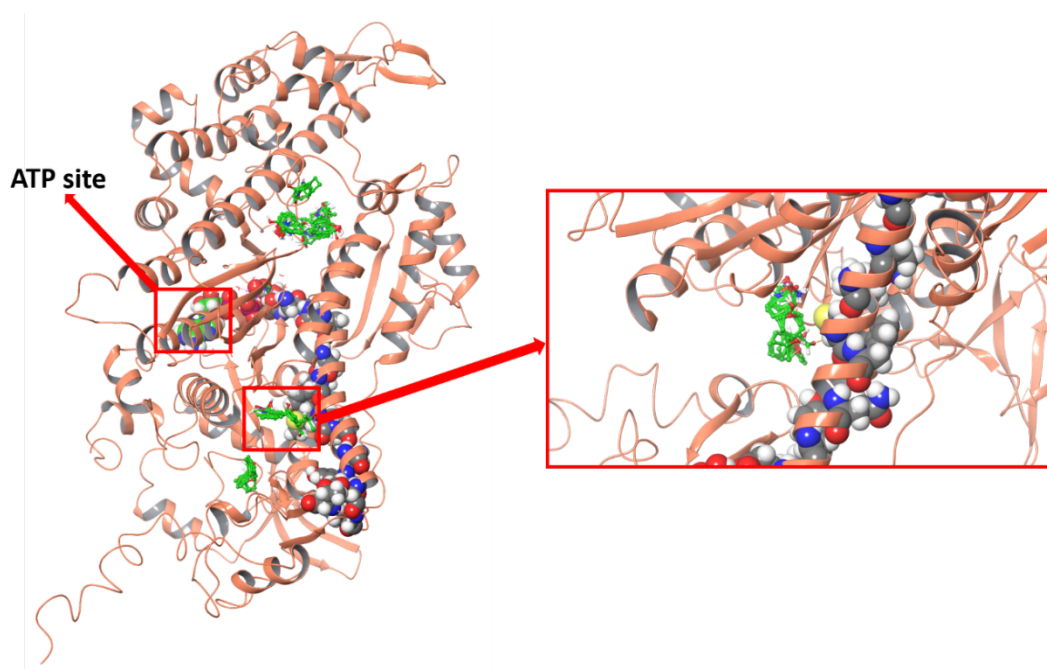


Figure 6. The crystal structure of Myosin-2 (PDB: 2XO8) and the calculated allosteric pathway shown in CPK representation. With green we show the fragments produced by FTMap. In the inset, a close-up of the predicted binding site next to Met486 is shown (the sulfur atom of Met486 that could facilitate allosteric binding is shown in yellow).

Table 2. Proteins for which allosteric modulators have been rationally designed, methods and tools utilized, and synopsis of the results.

Protein	Methods	Tools	Results	Refs
M2 muscarinic acetylcholine receptor (mAChR)	MD simulations, spontaneous binding. Accelerated MD simulations, clustering, ensemble docking, HTVS, IFD. Homology modeling, BPMC docking	NAMD ^{482, 509} , GROMACS ^{351, 510, 511} clustering, GLIDE ²²⁸⁻²³¹ ICM ^{261, 262}	PAMs and NAMs act via two different allosteric mechanisms. 12 PAMS and NAMs were rationally discovered with binding affinity $\leq 30 \mu\text{M}$. Agonist McN-A-343 is a bitopic ligand with the allosteric moiety showing the probe dependence effect	67, 222, 233
Complement component 5a receptor (C5aR)	Homology modeling, MD simulations, virtual screening	Discovery Studio ²⁴² , LiGenDock ^{243, 244}	Discovery of DF2593A as a potent and orally active C5a non-competitive allosteric antagonist	205
Ovarian cancer G-protein coupled receptor 1 (OGR1 or GPR68), Psychosine receptor	Homology modeling, ENM, virtual screening, <i>in silico</i> lead profiling	MODELLER ²⁴⁸ , 3K-ENM ²⁵⁰ , DOCK ^{251, 252} , SEA ²⁵⁴	Rational design of ogerin allosteric PAM and ogerin PAM analogs for GPR68 and allosteric modulators for GPR65	90

Rational design of allosteric modulators: challenges and successes

(GPR65)				
Dopamine receptor D ₃ (D3R), Dopamine receptor D ₂ (D2R)	NMA, virtual screening, ligand-guided receptor optimization, clustering. SAR optimizations, BPMC docking	LiBERO ²⁶⁰ , ICM ^{261, 262}	Discovered two potent NAMs for D3R. Discovery of three ligands, one many-fold more selective for D2R	259, 263
Glucagon receptor (GCGR or GLR)	Homology modeling, MD simulations, clustering, virtual screening, ligand-based similarity search, filtering	AMBER ⁵¹² , GROMACS ^{351, 510, 511} , clustering, Gold ²⁷¹ , Pipeline Pilot ²⁷² , ROCS ^{273, 274} , IFP ²⁷⁵	Discovery of two allosteric inhibitors	91
15-lipoxygenase (ALOX15)	Homology modeling, MD simulations, clustering, pocket detection, residue motion-al cross-correlation, virtual screening	PRIME ²⁸⁵⁻²⁸⁷ , Desmond ^{288, 289} , GROMACS ^{351, 510, 511} , clustering, CAVITY ^{86, 87} , MutInf ¹¹¹ , DOCK ^{294, 295} , AutoDock ^{296, 297} , Glide ²²⁸⁻²³¹	Discovery of three allosteric activators	283
Human immunodeficiency virus type 1 integrase (HIV-1 integrase)	MD simulations, docking	AMBER ⁵¹² , AutoDock ^{296, 297}	Discovery of an allosteric pocket adjacent to the active site with MD and rational design of 10 bitopic ligands	300
Human immunodeficiency virus type 1 protease (HIV-1 protease)	Receptor-based pharmacophore modeling, MD simulations, LD simulations, virtual screening, ligand-based chemical search, ligand-based virtual screening, docking, essential dynamics	AMBER ⁵¹² , MOE ³¹⁰ , SYBYL-X ³¹⁴ , ROCS ^{273, 274} , EON ³¹⁵ , Glide ²²⁸⁻²³¹	Discovery of one allosteric inhibitor with IC ₅₀ of 18 ± 3 µM and an allosteric inhibitor equipotent in the WT and the MDR HIV-1p	92, 306, 311
Human immunodeficiency virus type 1 reverse transcriptase (HIV-1 RT)	Virtual screening, de novo ligand design, MC/FEP	Glide ²²⁸⁻²³¹ , BOMB ³²² , MCPRO ³²³	Discovery of several allosteric inhibitors (NNRTIs) with pM IC ₅₀ in an allosteric pocket highly selective for HIV-1 RT	321
Flavivirus NS2B-NS3 protease	Virtual screening	AutoDock Vina ³³⁸	Discovery of three allosteric inhibitors in an allosteric pocket highly conserved among flaviviruses	337
Non-structural protein 5B (Hepatitis C virus)	Structure-based pharmacophore modeling, 3D-QSAR, virtual screening, coarse-grained MD simulations	MOE ³¹⁰ , Discovery Studio ²⁴² , Gold ²⁷¹ , SYBYL-X ³¹⁴ , GLIDE ²²⁸⁻²³¹ , GROMACS ^{351, 510, 511}	Five allosteric sites and rational design of potent ligands able to inhibit RdRp-NS5B allosterically	344-346
Heat shock protein 90	MD simulations, residue motion-al cross-correlation, es-	GROMACS ^{351, 510, 511} , ICM ^{261, 262} , AutoDock ²⁹⁶	Discovery of biased allosteric	353-356

(Hsp90)	sentinal dynamics, GNM, clustering, pocket detection, receptor-based 3D pharmacophore modeling, ligand-based virtual screening, blind docking, rational optimizations	²⁹⁷ , GLIDE ²²⁸⁻²³¹	inhibitors	
Heat shock protein 70 (Hsp70)	Homology modeling, pocket detection, rational ligand design, docking, SAR optimizations	PRIME ²⁸⁵⁻²⁸⁷ , SiteMap ³⁶²⁻³⁶⁴ , GLIDE ²²⁸⁻²³¹	Discovery of a novel allosteric pocket and novel anticancer allosteric inhibitors	357, 361, 365-367
3-phosphoinositide-dependent protein kinase 1 (PDK1 or PDPK1)	Ligand-based virtual screening. Chemical library generation, ensemble docking	SYBYL-X ³¹⁴ , MODELLER ²⁴⁸ , DUD-E ³⁷⁸ , DOCK ^{251, 252}	Discovery of two PAMS and allosteric modulators; the best was crystallized bound to ATP (PDB: 4XX9, Figure 3)	98, 374
Epidermal growth factor receptor (EGFR)	Medicinal chemistry optimizations		Discovery of an allosteric inhibitor, 1000-fold more selective for the mutant type and non-selective for 250 other kinases. Crystal structure of EGFR T790M/C797S/V948R in complex with an allosteric inhibitor was reported (PDB: 5ZWJ)	52, 380
Tropomyosin receptor kinase A (TrkA)	Water analysis, virtual screening, lead optimization	WaterMap ³⁸⁴⁻³⁸⁷ , GLIDE ²²⁸⁻²³¹	Rational lead optimization resulted in an orally non-toxic highly selective and potent allosteric inhibitor (PDB: 6D20)	383
Tyrosine-protein phosphatase non-receptor type 11 (PTPN11 or SHP2)	Pharmacophore modeling, ligand docking, chemical library generation, virtual screening, MD simulations. Pocket detection, SAR optimizations	Discovery Studio ²⁴² , GROMACS ^{351, 510, 511} , SiteMap ³⁶²⁻³⁶⁴	Discovery of an allosteric inhibitor with the same inhibiting function as the known allosteric inhibitor SHP099 with a more favorable binding conformation. Novel orally bioavailable allosteric inhibitors were rationally designed, demonstrating high potency and selectivity, some of them were crystalized with SHP2 (PDB IDs: 6MDB, 6MDC, 6MDD, 6MD7)	96, 395-397
γ -aminobutyric acid type A receptor (GABA _A R)	Homology modeling, ligand docking, pharmacophore modeling, virtual screening. MD simulations, ligand dock-	FlexX ⁴⁰⁰ and FlexE ⁴⁰¹ , LigandScout ⁴⁰³ , DUD-E ³⁷⁸ , PLANTS ⁴⁰⁴ , GROMACS ³⁵¹ , DOCK ²⁵¹	Two allosteric modulators inhibiting the benzodiazepine-binding site.	94, 402, 405

Rational design of allosteric modulators: challenges and successes

	ing, virtual screening. Pharmacophore modeling, virtual screening	²⁵²	GABA _A R and GLIC modulators. Design of two allosteric modulators displaying low-dose anti-convulsant activity and GABA _A R selectivity	
Glycine receptors (GlyRs)	MD simulations, ensemble-based virtual screening. SAR optimizations, pharmacophore modeling, virtual screening	GROMACS ³⁵¹ , AutoDock Vina ³³⁸ , MOE ³¹⁰	Discovery of 12 FDA-approved drugs acting as selective allosteric modulators. Novel class of allosteric modulators with 17 hits.	410, 414
Acid-sensing ion channel 3 (ASIC3)	Ligand-based virtual screening, homology modeling, blind docking	ROCS ^{273, 274} , AutoDock ^{296, 297}	Discovery of two FDA-approved drugs acting as PAMs	417
$\alpha 7$ nicotinic acetylcholine receptor ($\alpha 7$ nAChR)	Pharmacophore modeling, virtual screening	ROCS ^{273, 274} , Decoy-Finder ⁴²¹	Discovery of four FDA-approved drugs acting as allosteric modulators	420
Cysteine-aspartic protease 3 (Caspase-3), Cysteine-aspartic protease 7 (Caspase-7)	Virtual screening	DOCK ^{251, 252}	Discovery of four already FDA-approved drugs that can inhibit caspase-3 and -7 allosterically	428
D-3-phosphoglycerate dehydrogenase (PHGDH)	Coarse-grained two-state Gō model, LD simulations, pocket detection, virtual screening, 3D QSAR, docking	Cafemol ⁴³⁴ , CAVITY ^{86, 87} , DOCK ^{251, 252} , AutoDock Vina ³³⁸ , PHASE ⁴³⁶ , GLIDE ²²⁸⁻²³¹	Discovery of three novel allosteric inhibitors with the best IC ₅₀ = 21.6 μ M for a predicted allosteric site; seven allosteric inhibitors were discovered for another predicted allosteric site	431, 435
Glutathione peroxidase 4 (GPX4)	Pocket detection, residue motional cross-correlation, MD simulations, virtual screening, SAR optimizations	CAVITY ^{86, 87} , CorrSite ¹⁰⁹ , GLIDE ²²⁸⁻²³¹	Rational design of nine GPX4 activators	440
Sirtuin 6 (SIRT6)	Allosteric pocket detection, virtual screening, medicinal chemistry optimizations	Allosite ^{145, 149} , GLIDE ²²⁸⁻²³¹	Discovery of allosteric activators with one them crystallized (PDB: 5Y2F)	445
High-temperature requirement A protein (HtrA)	Homology modeling, pocket detection, virtual screening, ligand-based similarity search	Modeller ²⁴⁸ , PocketPicker ⁴⁵⁵ , PoLiMorph ⁴⁵⁶⁻⁴⁵⁸	Discovery of an allosteric inhibitor	93
TEM β -lactamase	MD simulations, MSMs, pocket detection, virtual screening, Boltzmann-weighted docking	GROMACS ^{351, 510, 511} , MSMBuilder ⁴⁶² , LIGSITE ⁴⁶³ , Surflex-dock ⁴⁶⁴	Discovery of a NAM and two PAMs	174, 175, 465, 466

Signal transducer and activator of transcription 3 (STAT3)	Allosteric drug design, allosteric pocket detection, virtual screening	Allofinder ¹⁸⁵ , Allosite ^{145, 149} , AutoDock Vina ³³⁸	Discovery of an allosteric inhibitor	185
Cathepsin K	SCA, pocket detection, virtual screening	pySCA ¹⁰³ , AutoLigand ⁴⁷³ , DOCK ^{251, 252} , AutoDock ^{296, 297}	Discovery of 15 allosteric modulators; one as a selective allosteric inhibitor (PDB: 5J94) identifying one of the predicted sites as being a novel allosteric site	472
K-Ras, K-Ras G12C	MD simulations, PCA, clustering, pocket detection, blind docking, ensemble virtual screening. MD simulations, ensemble virtual screening. MD simulations, pocket analysis, ensemble virtual screening. Virtual screening, ligand docking. SAR studies, iterative structure-based design, covalent structure-based design	AMBER ⁵¹² , Bio3D ⁴⁸⁰ , FTMap ^{83, 85} , AutoLigand ⁴⁷³ , AutoDock ^{296, 297} , GLIDE ²²⁸⁻²³¹ , NAMD ⁴⁸² , MDPocket ⁴⁸⁸ , AutoDock Vina ³³⁸ , DataWarrior ⁴⁸⁹	Discovery of 19 allosteric modulators displaying moderate affinity and selectivity serving as starting points for lead optimization. Discovery of two allosteric inhibitors blocking the GTPase cycle. Discovery of two allosteric inhibitors; one disrupts the K-Ras-Raf interaction. Discovery of nine potent compounds; one binds with low μ M affinity. Discovery of one selective inhibitor for the mutant K-Ras and the potential to block GTP binding. SAR and crystallographic studies identified covalent allosteric inhibitors bound to G12C. Iterative structure-based design led to a covalent FDA-approved allosteric inhibitor	479, 483, 484, 486, 487, 491, 493, 494, 496, 498, 499
Protein kinase Akt	SAR studies, covalent structure-based design		Rational design and synthesis of novel allosteric inhibitors that covalently modify the protein kinase Akt. One inhibitor was crystallized with Akt (PDB: 6HHF); another four covalent allosteric inhibitors were designed and synthesized (PDBs: 6HHJ, 6HHG, 6HHI, 6HHH)	500, 502

5 Discussion and Conclusions

Rational design of allosteric modulators is gaining increasing attention in the last decade. Traditionally, targeting orthosteric sites has been the primary approach for drugging proteins; although orthosteric drug discovery always remains an attractive practice, allosteric inhibition now offers a new paradigm to modulate receptor function. Allosteric or noncompetitive inhibition allows for modulation rather than complete inhibition, and unique allosteric sites among protein family members for higher selectivity, lower toxicity, and fewer side effects. The advantages of allosteric drug design outmatch the hurdles, and a continuous stream of studies has emerged for the development of allosteric modulators in the last decade. Although to date most allosteric bioactive ligands and drugs have been discovered through HTS, technological improvements and advances in understanding allosteric mechanisms have led to new structural allosteric data and rational procedures for targeting biological targets allosterically and to the emergence of new tools specifically for allosteric ligand design.

A general process for allosteric ligand design cannot be standardized as demonstrated in the different approaches in cases studies presented herein. Depending on the available data of the biological target, *e.g.* availability of 3D structure, known allosteric site, known allosteric modulators, different strategies can be adopted. When the protein 3D structure is not known, homology modeling can be utilized to create a model (or several models) of the protein.^{90, 91, 93, 205, 361} Usually, homology models are then validated for their proximity to the real structure by successfully docking known active

ligands with better predictive score than inactive ligands and decoys,^{90, 91} or other techniques such as constructing the average structure from MD simulations,²⁰⁵ and evaluating it based on experimental data.⁹¹ When the 3D protein structure is unknown but allosteric modulators are known, *i.e.* from HTS, or when the allosteric site is known, ligand-based and receptor-based pharmacophore modeling is another option.^{91-96, 98, 344, 345, 354}

The basic difference between allosteric and orthosteric ligand design is that in most cases the allosteric site is undetermined. When the allosteric site location is known from literature or crystallography, as in several studies discussed herein,^{95, 96, 98, 222, 344, 345, 374, 383, 428} one can proceed with a standard rational drug design procedure including simulations, virtual screening, ensemble docking, and lead optimization. When the protein target contains multiple pockets on its surface, most commonly it is not known whether small molecule ligands in these sites could modulate the activity of the distal active site or whether they could reorder the protein conformational landscape. Various methodologies and tools specific to allosteric site prediction have been designed and applied based on residue coevolution,⁴⁷² correlated residue motions,^{283, 353, 440} perturbations,⁴³¹ and machine learning,^{185, 445} with many of them being combined with MD, MC, or NMA, as discussed in the Methods section and in other reviews.^{30, 32, 33, 60, 105, 110, 129, 135, 180-183} Although these tools can correctly predict allosteric sites, they have been utilized only in a few allosteric modulator design cases and mostly by their authors.^{185, 283, 440, 445, 472} Other methods for detecting allosteric sites are blind docking,^{417, 479, 484} where the whole protein surface is docked by known allosteric modulators, and spontane-

ous binding,⁶⁷ where the ligand locates the allosteric binding site by exploring the receptor surface in MD simulations, although these approaches are computationally expensive.

Considering that allostery is a property of the protein conformational landscape, the protein conformational space of the apo and the holo structures can be explored using simulations in order to generate an ensemble of conformations.^{174, 222, 353, 431, 479} By examining this conformational ensemble it is possible to discover cryptic sites not visible in the original crystal structure. Targeting such cryptic sites may result in modifying allosterically the protein function.^{174, 301, 465, 507} Although a plethora of methodologies and software programs have been designed for the discovery and druggability assessment of cryptic pockets (Table 1), the investigation of whether these cryptic pockets act

allosterically is not explored, leaving room for improvement in the cryptic allosteric binding site prediction and drug design. Furthermore, it was recently demonstrated that cryptic sites lie in flexible regions and can be open in apo structures. Using a conformational selection mechanism (Figure 7A), the protein adopts a conformation in which the cryptic pocket is favorable for ligand binding. With the induced-fit mechanism (Figure 7B), which was until recently considered as the most probable mechanism of cryptic site detection, the cryptic binding pocket opens only when the ligand encounters the pocket.⁵¹³ Previously, it was shown that an interplay between these mechanisms may take place for the formation of cryptic sites (Figure 7C).⁶⁶ It is possible that in the apo structures cryptic sites may acquire a semi-open form or in rare events an open form but further research is needed.

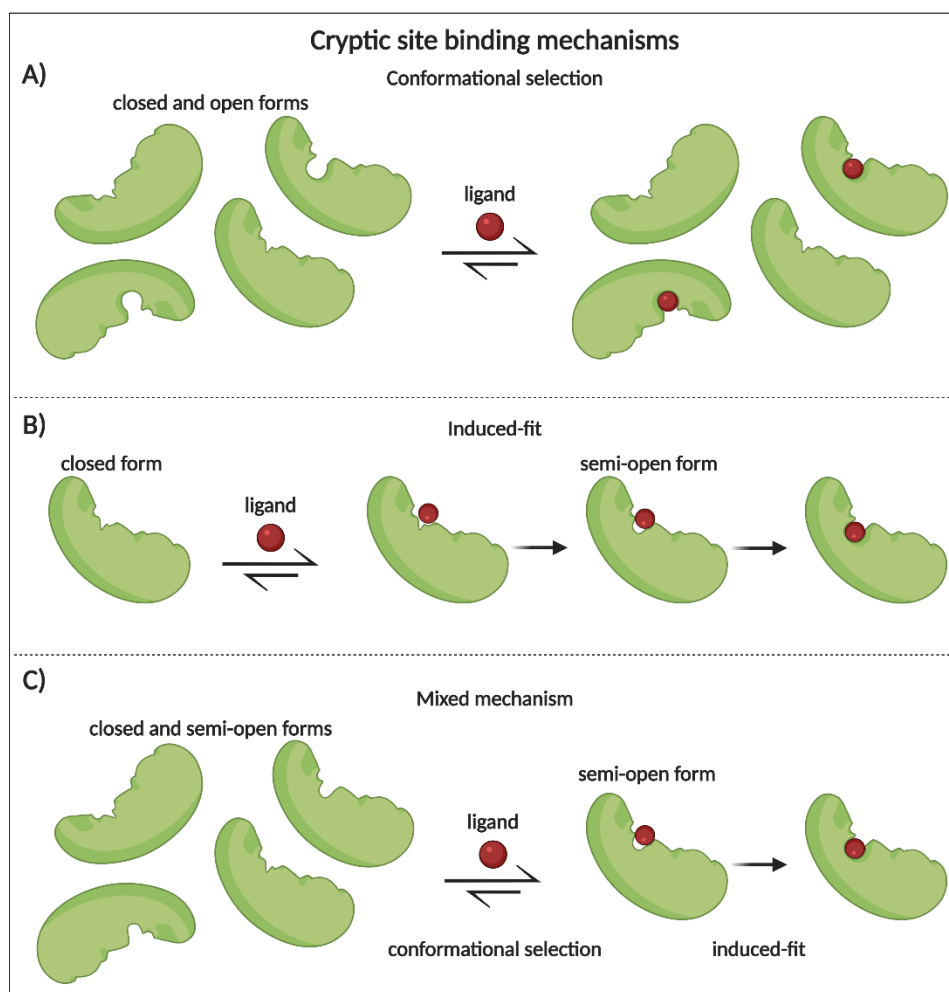


Figure 7. Possible mechanisms describing the binding of a ligand or a probe in a cryptic site. (a) In the conformational selection mechanism the protein must adopt a conformation in which the cryptic pocket is open in order for the ligand to bind. (b) In the induced-fit mechanism the cryptic binding pocket is closed and conformational changes are only observed when the ligand encounters the pocket. (c) A mixed approach combines both mechanisms; first the cryptic pocket adopts a semi-open form with the conformational selection mechanism, and then, the ligand selects these conformations and binds with the induced-fit mechanism, fully opening the cryptic binding site.^{66, 513}

Moreover, in a few cases presented herein, an allosteric pocket was discovered adjacent to the orthosteric pocket.^{233, 259, 301} The proximity of such sites provides the opportunity and the possibility to create bitopic ligands, consisting of a moiety interacting with the orthosteric site and an allosteric moiety interacting with the extended allosteric part of the pocket.²³² A few covalent allosteric drugs

have also been discovered. In the putative allosteric site, detection of a druggable cysteine offers the opportunity of covalent allosteric modulator design,^{119, 194, 500} and these may offer additional advantages such as smaller drug dosages and more efficacy.

After the identification of putative allosteric sites, the drug design process of allosteric bioactive lig-

ands is fairly traditional. Although allosteric modulators have different biological response than orthosteric ligands,^{62, 187, 514} standard procedures of structure-based or ligand-based virtual screening using docking or ensemble docking for the most representative protein conformers, pharmacophore modeling of large databases counting millions of compounds, followed by filtering and clustering, are usually followed as evident from the case studies discussed herein. The general chemical characteristics that allosteric modulators have, for example, low molecular weight, being hydrophobic, only a few rotatable bonds, can be taken into account for manual inspection of the top scoring compounds that will be selected for assaying. A simplified workflow for rational allosteric ligand design is presented in Figure 8, and a variety of available tools predicting allosteric sites and pathways is presented in Table 1.

One major point that is often overlooked in allosteric ligand design is the communication of the discovered pocket with the active/orthosteric site or other functionally important regions of the protein. It is not enough to identify and verify the location of a new protein binding pocket; the association of these putative allosteric binding sites with the orthosteric site should then be examined.⁵¹ The conformation

and sequenced-based tools, outlined in “Methods” section, can identify binding sites as well as predict their association with the orthosteric site. Although conformation and sequenced-based approaches are seemingly not connected, they could actually be two sides of the same coin. The ensemble view of allostery supports both the population shift through change in conformational dynamics but also matches evolution. This relationship was recently discussed in refs.^{515, 516}

Rational allosteric drug design has clearly advanced in the last decade, but on the other hand, there is plenty of room for improvement. The studies presented herein demonstrate successful rational design approaches and principles for the discovery of potent allosteric modulators even for targets that were previously thought to be undruggable, e.g., K-Ras. Moreover, the diversity of the proteins that were subjected to rational design of allosteric modulators supports the fact that allostery is a property of the conformational ensemble, and thus all proteins may be considered having an allosteric nature. The advances in computational power, and structural and computational advancements are expected to lead the rational design of allosteric modulators to a more mature stage, holding an auspicious future in drug design.

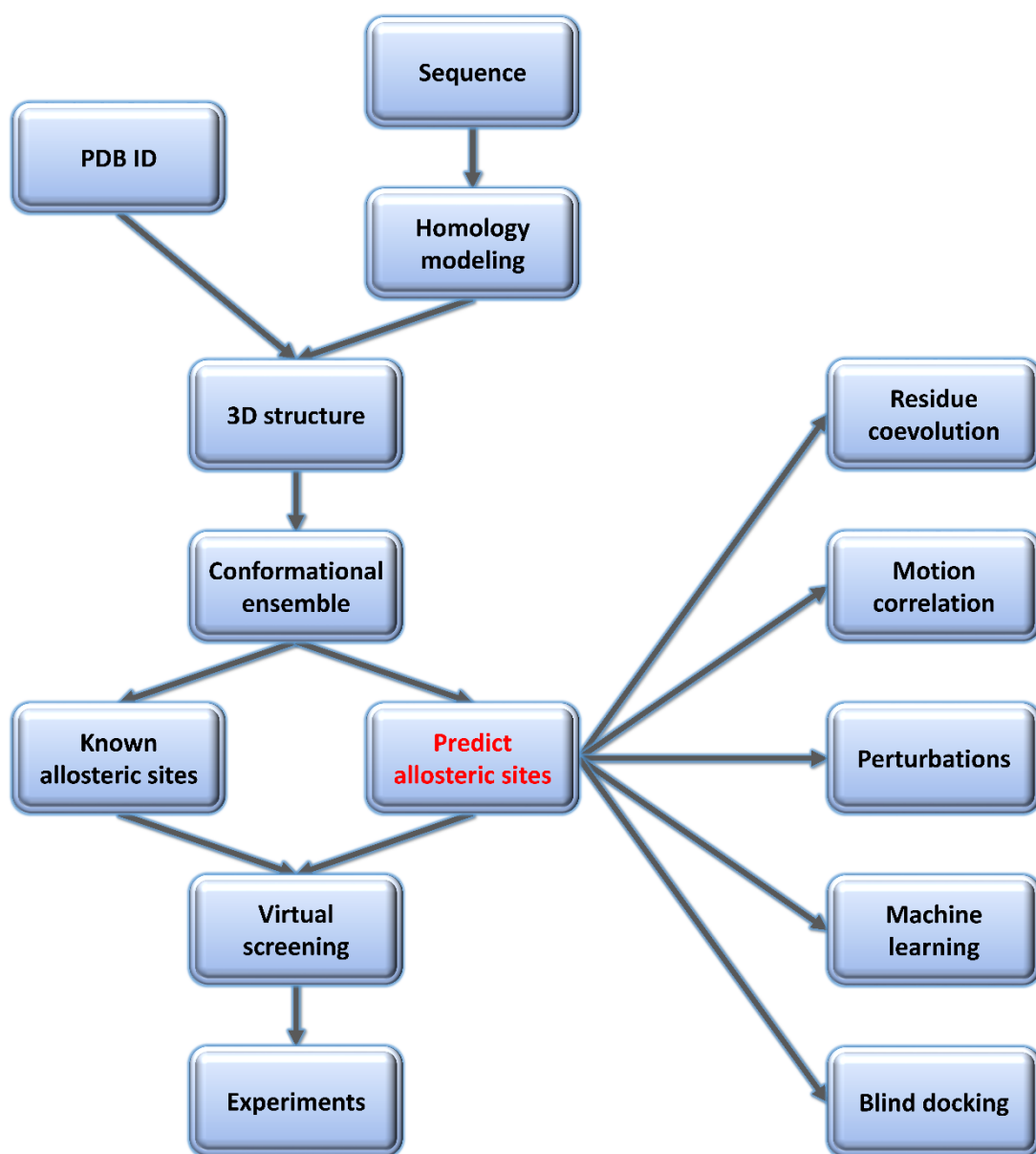


Figure 8. Proposed workflow for computational allosteric ligand design.

Table 3. Abbreviation list

Abbreviation	Definition	Abbreviation	Definition
A ₃ AR	Adenosine A3 receptor	LiBERO	Ligand-guided receptor optimization
ADMET	Absorption, distribution, metabolism, excretion, and toxicity	mAChR	Muscarinic acetylcholine receptor
ALOX15	15-lipoxygenase	MC	Monte Carlo
aMD	Accelerated molecular dynamics	MD	Molecular dynamics
ASIC3	Acid-sensing ion channel 3	MPS	Multiple protein structures
BPMC	Biased probability Monte Carlo	MSA	Multiple sequence alignment
C5aR	Complement component 5a receptor	MSM	Markov state model
Caspase	Cysteine-aspartic protease	nAChR	Nicotinic acetylcholine receptor
CNS	Central nervous system	NAM	Negative allosteric modulator
CRFR1	Corticotropin-releasing factor type 1 receptor	NCI	National Cancer Institute
CTD	C-terminal domain	NMA	Normal mode analysis
D2R	Dopamine receptor D ₂	NNRTI	Non-nucleoside reverse transcriptase inhibitor
D3R	Dopamine receptor D ₃	OGR1	Ovarian cancer G-protein coupled receptor 1
EGFR	Epidermal growth factor receptor	PAM	Positive allosteric modulator
ENM	Elastic network model	PCA	Principal component analysis
FDA	US Food and Drug Administration	PDK1	3-phosphoinositide-dependent protein kinase 1
FEP	Free energy perturbations	pLGICs	Pentameric ligand-gated ion channels
GABA _A R	γ-Aminobutyric acid type A receptor	PHGDH	D-3-phosphoglycerate dehydrogenase
GCGR	Glucagon receptor	PIF	PDK1-interacting fragment
GLIC	<i>Gloeobacter violaceus</i> ligand-gated ion channel	POPC	1-palmitoyl-2-oleoylphosphatidylcholine
GLP-1R	Glucagon-like peptide-1 receptor	PTP	Protein tyrosine phosphatase
GlyRs	Glycine receptors	RdRp	RNA-dependent RNA polymerase
GMQ	2-guanidine-4-methylquinazoline	RT	Reverse transcriptase
GNM	Gaussian network model	RTK	Receptor tyrosine kinase
GPCR	G-protein-coupled receptor	SAM	Silent allosteric modulator
GPX4	Glutathione peroxidase 4	SAR	Structure-activity relationship
HCV	Hepatitis C virus	SBSMMA	Statistical mechanical model of allostery
HIV-1	Human immunodeficiency virus type 1	SCA	Statistical coupling analysis
HIVp	Human immunodeficiency virus type 1 protease	SHP2	Tyrosine-protein phosphatase non-receptor type 11
Hsp	Heat shock protein	SIRT6	Sirtuin 6
HtrA	High-temperature requirement A protein	STAT3	Signal transducer and activator of transcription 3
HTS	High-throughput screening	TMD	Transmembrane domain
HTVS	High-throughput virtual screening	TNM	Torsional network model
IFD	Induced-fit docking	TrkA	Tropomyosin receptor kinase A
LD	Langevin dynamics	WT	Wild type

Funding

A.C. is co-financed by Greece and the European Union (European Social Fund- ESF) through the Operational Programme «Human Resources Development, Education and Lifelong Learning» in the context of the project “Strengthening Human Resources Research Potential via Doctorate Research” (MIS-5000432), implemented by the State Scholarships Foundation (IKY). Z.C. was supported by the Hellenic Foundation for Research and Innovation (H.F.R.I.) under the “First Call for H.F.R.I. Research Projects to support Faculty members and Researchers and the procurement of high-cost research equipment grant” (Project Number: 1780).

Conflict of Interest: none declared.

References

1. del Sol A, Tsai CJ, Ma B, Nussinov R. The origin of allosteric functional modulation: multiple pre-existing pathways. *Structure*. 2009;17(8):1042–50.
2. Bohr C, Hasselbalch K, Krogh A. Ueber einen in biologischer Beziehung wichtigen Einfluss, den die Kohlensäurespannung des Blutes auf dessen Sauerstoffbindung übt. *Skand Arch Physiol*. 1904;16(2):402–12.
3. Hill AV. The possible effects of the aggregation of the molecules of haemoglobin on its dissociation curves. *J Physiol*. 1910;40:i–vii.
4. Adair GS. The hemoglobin system. IV. The reproduction of the carbon dioxide curves of blood with an artificial mixture of hemoglobin and sodium bicarbonate. *J Biol Chem*. 1925;63(2):515–6.
5. Pauling L. The oxygen equilibrium of hemoglobin and its structural interpretation. *Proc Natl Acad Sci U S A*. 1935;21(4):186–91.
6. Klotz IM. The application of the law of mass action to binding by proteins; interactions with calcium. *Arch Biochem*. 1946;9(1):109–17.
7. Monod J, Wyman J, Changeux JP. On the nature of allosteric transitions: a plausible model. *J Mol Biol*. 1965;12:88–118.
8. Koshland D Jr, Némethy G, Filmer D. Comparison of experimental binding data and theoretical models in proteins containing subunits. *Biochemistry*. 1966;5(1):365–85.
9. Cui Q, Karplus M. Allostery and cooperativity revisited. *Protein Sci*. 2008;17(8):1295–307.
10. Motlagh HN, Wrabl JO, Li J, Hilser VJ. The ensemble nature of allostery. *Nature*. 2014;508(7496):331–9.
11. Tsai CJ, Nussinov R. A unified view of “how allostery works”. *PLoS Comput Biol*. 2014;10(2):e1003394.
12. Gunasekaran K, Ma B, Nussinov R. Is allostery an intrinsic property of all dynamic proteins? *Proteins*. 2004;57(3):433–43.
13. Changeux JP, Christopoulos A. Allosteric modulation as a unifying mechanism for receptor function and regulation. *Cell*. 2016;166(5):1084–102.
14. Kar G, Keskin O, Gursoy A, Nussinov R. Allostery and population shift in drug discovery. *Curr Opin Pharmacol*. 2010;10(6):715–22.
15. Hilser VJ, Wrabl JO, Motlagh HN. Structural and energetic basis of allostery. *Annu Rev Biophys*. 2012;41(1):585–609.
16. Motlagh HN, Hilser VJ. Agonism/antagonism switching in allosteric ensembles. *Proc Natl Acad Sci U S A*. 2012;109(11):4134–9.
17. Changeux JP. Allostery and the Monod–Wyman–Changeux model after 50 years. *Annu Rev Biophys*. 2012;41(1):103–33.
18. Christopoulos A, Changeux JP, Catterall WA, Fabbro D, Burris TP, Cidlowski JA, et al. International Union of Basic and Clinical Pharmacology. XC. Multisite pharmacology: recommendations for the nomenclature of receptor allostery and allosteric ligands. *Pharmacol Rev*. 2014;66(4):918–47.
19. Cournia Z, Chatzigeorgoulas A. Allostery in membrane proteins. *Curr Opin Struct Biol*. 2020;62:197–204.
20. Schann S, Mayer S, Franchet C, Frauli M, Steinberg E, Thomas M, et al. Chemical switch of a metabotropic glutamate receptor 2 silent allosteric modulator into dual metabotropic glutamate receptor 2/3 negative/positive allosteric modulators. *J Med Chem*. 2010;53(24):8775–9.
21. Kenakin TP. Chapter 5 – allosteric drug effects. In: Kenakin TP, editor. *Pharmacology in drug discovery and development*. 2nd ed. New York, NY, USA:Academic Press; 2017. p. 101–29.
22. Schwartz TW, Holst B. Ago-allosteric modulation and other types of allostery in dimeric 7TM receptors. *J Recept Signal Transduct Res*. 2006;26(1–2):107–28.
23. Schwartz TW, Holst B. Allosteric enhancers, allosteric agonists and ago-allosteric modulators: where do they bind and how do they act? *Trends Pharmacol Sci*. 2007;28(8):366–73.
24. Wenthur CJ, Gentry PR, Mathews TP, Lindsley CW. Drugs for allosteric sites on receptors. *Annu Rev Pharmacol Toxicol*. 2014;54:165–84.
25. Fang Z, Grütter C, Rauh D. Strategies for the selective regulation of kinases with allosteric modulators: exploiting exclusive structural features. *ACS Chem Biol*. 2013;8(1):58–70.
26. Hardy JA, Wells JA. Searching for new allosteric sites in enzymes. *Curr Opin Struct Biol*. 2004;14(6):706–15.
27. Feher VA, Durrant JD, Van Wart AT, Amaro RE. Computational approaches to mapping allosteric pathways. *Curr Opin Struct Biol*. 2014;25:98–103.
28. Shen Q, Wang G, Li S, Liu X, Lu S, Chen Z, et al. ASD v3.0: unraveling allosteric regulation with structural mechanisms and biological networks. *Nucleic Acids Res*. 2016;44(D1):D527–35.
29. Wagner JR, Lee CT, Durrant JD, Malmstrom RD, Feher VA, Amaro RE. Emerging computational methods for the rational discovery of allosteric drugs. *Chem Rev*. 2016;116(11):6370–90.
30. Schueler-Furman O, Wodak SJ. Computational approaches to investigating allostery. *Curr Opin Struct Biol*. 2016;41:159–71.
31. Lu S, Ji M, Ni D, Zhang J. Discovery of hidden allosteric sites as novel targets for allosteric drug design. *Drug Discov Today*. 2018;23(2):359–65.
32. Greener JG, Sternberg MJ. Structure-based prediction of protein allostery. *Curr Opin Struct Biol*. 2018;50:1–8.

33. Lu S, He X, Ni D, Zhang J. Allosteric modulator discovery: from serendipity to structure-based design. *J Med Chem.* 2019;62:6405–21.
34. Davenport J, Manjarrez JR, Peterson L, Krumm B, Blagg BS, Matts RL. Gambogic acid, a natural product inhibitor of Hsp90. *J Nat Prod.* 2011;74(5):1085–92.
35. Feldman T, Kabaleeswaran V, Jang SB, Antczak C, Djaballah H, Wu H, et al. A class of allosteric caspase inhibitors identified by highthroughput screening. *Mol Cell.* 2012;47(4):585–95.
36. Lewis MA, Hunihan L, Watson J, Gentles RG, Hu S, Huang Y, et al. Discovery of D1 dopamine receptor positive allosteric modulators: characterization of pharmacology and identification of residues that regulate species selectivity. *J Pharmacol Exp Ther.* 2015;354(3):340–9.
37. Luderman KD, Conroy JL, Free RB, Southall N, Ferrer M, Sanchez-Soto M, et al. Identification of positive allosteric modulators of the D1 dopamine receptor that act at diverse binding sites. *Mol Pharmacol.* 2018;94(4):1197–209.
38. Saalau-Bethell SM, Woodhead AJ, Chessari G, Carr MG, Coyle J, Graham B, et al. Discovery of an allosteric mechanism for the regulation of HCV NS3 protein function. *Nat Chem Biol.* 2012;8(11):920–5.
39. Hackos DH, Lupardus PJ, Grand T, Chen Y, Wang TM, Reynen P, et al. Positive allosteric modulators of GluN2A-containing NMDARs with distinct modes of action and impacts on circuit function. *Neuron.* 2016;89(5):983–99.
40. Volgraf M, Sellers BD, Jiang Y, Wu G, Ly CQ, Villemure E, et al. Discovery of GluN2A-selective NMDA receptor positive allosteric modulators (PAMs): tuning deactivation kinetics via structure-based design. *J Med Chem.* 2016;59(6):2760–79.
41. Davoren JE, Nason D, Coe J, Dlugolenski K, Helal C, Harris AR, et al. Discovery and lead optimization of atropisomer D1 agonists with reduced desensitization. *J Med Chem.* 2018;61(24):11384–97.
42. Wold EA, Chen J, Cunningham KA, Zhou J. Allosteric modulation of class A GPCRs: targets, agents, and emerging concepts. *J Med Chem.* 2019;62(1):88–127.
43. Lu S, Zhang J. Small molecule allosteric modulators of G-protein-coupled receptors: drug–target interactions. *J Med Chem.* 2018;62:24–45.
44. Haskell-Luevano C, Meanwell NA. Allosteric modulators of drug targets. *J Med Chem.* 2019;62(1):1–2.
45. Nussinov R, Tsai CJ, Csermely P. Allo-network drugs: harnessing allostery in cellular networks. *Trends Pharmacol Sci.* 2011;32(12):686–93.
46. Nussinov R, Tsai CJ. The different ways through which specificity works in orthosteric and allosteric drugs. *Curr Pharm Des.* 2012;18(9):1311–6.
47. Wootten D, Christopoulos A, Sexton PM. Emerging paradigms in GPCR allostery: implications for drug discovery. *Nat Rev Drug Discov.* 2013;12(8):630–44.
48. Lu SY, Zhang J. Designed covalent allosteric modulators: an emerging paradigm in drug discovery. *Drug Discov Today.* 2017;22(2):447–53.
49. Panjkovich A, Daura X. Assessing the structural conservation of protein pockets to study functional and allosteric sites: implications for drug discovery. *BMC Struct Biol.* 2010;10:9.
50. Wei GH, Xi WH, Nussinov R, Ma BY. Protein ensembles: how does nature harness thermodynamic fluctuations for life? The diverse functional roles of conformational ensembles in the cell. *Chem Rev.* 2016;116(11):6516–51.
51. Gkeka P, Papafotika A, Christoforidis S, Cournia Z. Exploring a non-ATP pocket for potential allosteric modulation of PI3K α . *J Phys Chem B.* 2015;119(3):1002–16.
52. Jia Y, Yun CH, Park E, Ercan D, Manuia M, Juarez J, et al. Overcoming EGFR(T790M) and EGFR(C797S) resistance with mutant-selective allosteric inhibitors. *Nature.* 2016;534(7605):129–32.
53. Wylie AA, Schoepfer J, Jahnke W, Cowan-Jacob SW, Loo A, Furet P, et al. The allosteric inhibitor ABL001 enables dual targeting of BCR-ABL1. *Nature.* 2017;543(7647):733–7.
54. Christopoulos A, Kenakin T. G protein-coupled receptor allostery and complexing. *Pharmacol Rev.* 2002;54(2):323–74.
55. Christopoulos A. Allosteric binding sites on cell-surface receptors: novel targets for drug discovery. *Nat Rev Drug Discov.* 2002;1(3):198–210.
56. Digby GJ, Conn PJ, Lindsley CW. Orthosteric- and allosteric-induced ligand-directed trafficking at GPCRs. *Curr Opin Drug Discov Dev.* 2010;13(5):587–94.
57. Bartuzi D, Kaczor AA, Matosiuk D. Molecular mechanisms of allosteric probe dependence in μ opioid receptor. *J Biomol Struct Dyn.* 2019;37(1):36–47.
58. Thum S, Kokornaczyk AK, Seki T, De Maria M, Ortiz Zacarias NV, de Vries H, et al. Synthesis and biological evaluation of chemokine receptor ligands with 2-benzazepine scaffold. *Eur J Med Chem.* 2017;135:401–13.
59. Valant C, Felder CC, Sexton PM, Christopoulos A. Probe dependence in the allosteric modulation of a G protein-coupled receptor: implications for detection and validation of allosteric ligand effects. *Mol Pharmacol.* 2012;81(1):41–52.
60. Guo J, Zhou HX. Protein allostery and conformational dynamics. *Chem Rev.* 2016;116(11):6503–15.
61. Kenakin TP. Biased signalling and allosteric machines: new vistas and challenges for drug discovery. *Br J Pharmacol.* 2012;165(6):1659–69.
62. van Westen GJ, Gaulton A, Overington JP. Chemical, target, and bioactive properties of allosteric modulation. *PLoS Comput Biol.* 2014;10(4):e1003559.
63. Johnstone S, Albert JS. Pharmacological property optimization for allosteric ligands: a medicinal chemistry perspective. *Bioorg Med Chem Lett.* 2017;27(11):2239–58.
64. Sadowsky JD, Burlingame MA, Wolan DW, McClendon CL, Jacobson MP, Wells JA. Turning a protein kinase on or off from a single allosteric site via disulfide trapping. *Proc Natl Acad Sci U S A.* 2011;108(15):6056–61.
65. Wood MR, Hopkins CR, Brogan JT, Conn PJ, Lindsley CW. “Molecular switches” on mGluR allosteric ligands that modulate modes of pharmacology. *Biochemistry.* 2011;50(13):2403–10.

66. Oleinikovas V, Saladino G, Cossins BP, Gervasio FL. Understanding cryptic pocket formation in protein targets by enhanced sampling simulations. *J Am Chem Soc.* 2016;138(43):14257–63.
67. Dror RO, Green HF, Valant C, Borhani DW, Valcourt JR, Pan AC, et al. Structural basis for modulation of a G-protein-coupled receptor by allosteric drugs. *Nature.* 2013;503(7475):295–9.
68. Malmstrom RD, Kornev AP, Taylor SS, Amaro RE. Allostery through the computational microscope: cAMP activation of a canonical signalling domain. *Nat Commun.* 2015;6:7588.
69. Pontiggia F, Pachov DV, Clarkson MW, Villali J, Hagan MF, Pande VS, et al. Free energy landscape of activation in a signalling protein at atomic resolution. *Nat Commun.* 2015;6:7284.
70. Lipchock JM, Loria JP. Nanometer propagation of millisecond motions in V-type allostery. *Structure.* 2010;18(12):1596–607.
71. Gasper PM, Fuglestad B, Komives EA, Markwick PR, McCammon JA. Allosteric networks in thrombin distinguish procoagulant vs. anticoagulant activities. *Proc Natl Acad Sci U S A.* 2012;109(52):21216–22.
72. Srivastava AK, McDonald LR, Cembran A, Kim J, Masterson LR, McClendon CL, et al. Synchronous opening and closing motions are essential for cAMP-dependent protein kinase A signaling. *Structure.* 2014;22(12):1735–43.
73. Oyen D, Fenwick RB, Stanfield RL, Dyson HJ, Wright PE. Cofactor-mediated conformational dynamics promote product release from *Escherichia coli* dihydrofolate reductase via an allosteric pathway. *J Am Chem Soc.* 2015;137(29):9459–68.
74. Urwyler S. Allosteric modulation of family C G-protein-coupled receptors: from molecular insights to therapeutic perspectives. *Pharmacol Rev.* 2011;63(1):59–126.
75. Hall A, Provins L, Valade A. Novel strategies to activate the dopamine D1 receptor: recent advances in orthosteric agonism and positive allosteric modulation. *J Med Chem.* 2018;62(1):128–40.
76. Laio A, Parrinello M. Escaping free-energy minima. *Proc Natl Acad Sci U S A.* 2002;99(20):12562–6.
77. Karplus M, Kuriyan J. Molecular dynamics and protein function. *Proc Natl Acad Sci U S A.* 2005;102(19):6679–85.
78. Paquet E, Viktor HL. Molecular dynamics, Monte Carlo simulations, and Langevin dynamics: a computational review. *Biomed Res Int.* 2015;2015:183918.
79. Kmiecik S, Gront D, Kolinski M, Wieteska L, Dawid AE, Kolinski A. Coarse-grained protein models and their applications. *Chem Rev.* 2016;116(14):7898–936.
80. Husic BE, Pande VS. Markov state models: from an art to a science. *J Am Chem Soc.* 2018;140(7):2386–96.
81. Yang YI, Shao Q, Zhang J, Yang L, Gao YQ. Enhanced sampling in molecular dynamics. *J Chem Phys.* 2019;151(7):070902.
82. Le Guilloux V, Schmidtke P, Tuffery P. Fpocket: an open source platform for ligand pocket detection. *BMC Bioinformatics.* 2009;10:168.
83. Brenke R, Kozakov D, Chuang GY, Beglov D, Hall D, Landon MR, et al. Fragment-based identification of druggable ‘hot spots’ of proteins using Fourier domain correlation techniques. *Bioinformatics.* 2009;25(5):621–7.
84. Barducci A, Bonomi M, Parrinello M. Metadynamics. *Wires Comput Mol Sci.* 2011;1(5):826–43.
85. Kozakov D, Grove LE, Hall DR, Bohnuud T, Mottarella SE, Luo L, et al. The FTMap family of web servers for determining and characterizing ligand-binding hot spots of proteins. *Nat Protoc.* 2015;10(5):733–55.
86. Yuan Y, Pei J, Lai L. LigBuilder 2: a practical de novo drug design approach. *J Chem Inf Model.* 2011;51(5):1083–91.
87. Yuan Y, Pei J, Lai L. Binding site detection and druggability prediction of protein targets for structure-based drug design. *Curr Pharm Des.* 2013;19(12):2326–33.
88. Amaro RE, Baudry J, Chodera J, Demir O, McCammon JA, Miao Y, et al. Ensemble docking in drug discovery. *Biophys J.* 2018;114(10):2271–8.
89. Evangelista Falcon W, Ellingson SR, Smith JC, Baudry J. Ensemble docking in drug discovery: how many protein configurations from molecular dynamics simulations are needed to reproduce known ligand binding? *J Phys Chem B.* 2019;123(25):5189–95.
90. Huang XP, Karpiak J, Kroeze WK, Zhu H, Chen X, Moy SS, et al. Allosteric ligands for the pharmacologically dark receptors GPR68 and GPR65. *Nature.* 2015;527(7579):477–83.
91. de Graaf C, Rein C, Piwnica D, Giordanetto F, Rognan D. Structure-based discovery of allosteric modulators of two related class B G-protein-coupled receptors. *ChemMedChem.* 2011;6(12):2159–69.
92. Ung PM, Dunbar JB Jr, Gestwicki JE, Carlson HA. An allosteric modulator of HIV-1 protease shows equipotent inhibition of wild-type and drug-resistant proteases. *J Med Chem.* 2014;57(15):6468–78.
93. Perna AM, Reisen F, Schmidt TP, Geppert T, Pillong M, Weisel M, et al. Inhibiting *Helicobacter pylori* HtrA protease by addressing a computationally predicted allosteric ligand binding site. *Chem Sci.* 2014;5:3583–90.
94. Stadler M, Monticelli S, Seidel T, Luger D, Salzer I, Boehm S, et al. Design, synthesis, and pharmacological evaluation of novel $\beta 2/3$ subunit-selective γ -aminobutyric acid type A (GABAA) receptor modulators. *J Med Chem.* 2018;62(1):317–41.
95. Meagher KL, Lerner MG, Carlson HA. Refining the multiple protein structure pharmacophore method: consistency across three independent HIV-1 protease models. *J Med Chem.* 2006;49(12):3478–84.
96. Jin WY, Ma Y, Li WY, Li HL, Wang RL. Scaffold-based novel SHP2 allosteric inhibitors design using receptor-ligand pharmacophore model, virtual screening and molecular dynamics. *Comput Biol Chem.* 2018;73:179–88.
97. Schaller D, Sribar D, Noonan T, Deng LH, Nguyen TN, Pach S, et al. Next generation 3D pharmacophore modeling. *WIREs Comput Mol Sci.* 2020;10(4):e1468.
98. Engel M, Hindie V, Lopez-Garcia LA, Stroba A, Schaeffer F, Adrian I, et al. Allosteric activation of the protein kinase PDK1

- p>with low molecular weight compounds.
- EMBO J.*
- 2006;25(23):5469–80.
99. Lockless SW, Ranganathan R. Evolutionarily conserved pathways of energetic connectivity in protein families. *Science.* 1999;286(5438):295–9.
 100. Suel GM, Lockless SW, Wall MA, Ranganathan R. Evolutionarily conserved networks of residues mediate allosteric communication in proteins. *Nat Struct Biol.* 2003;10(1):59–69.
 101. Halabi N, Rivoire O, Leibler S, Ranganathan R. Protein sectors: evolutionary units of three-dimensional structure. *Cell.* 2009;138(4):774–86.
 102. Reynolds KA, McLaughlin RN, Ranganathan R. Hot spots for allosteric regulation on protein surfaces. *Cell.* 2011;147(7):1564–75.
 103. Rivoire O, Reynolds KA, Ranganathan R. Evolution-based functional decomposition of proteins. *PLoS Comput Biol.* 2016;12(6):e1004817.
 104. Pincus D, Resnekov O, Reynolds KA. An evolution-based strategy for engineering allosteric regulation. *Phys Biol.* 2017;14(2):025002.
 105. Dokholyan NV. Controlling allosteric networks in proteins. *Chem Rev.* 2016;116(11):6463–87.
 106. Chennubhotla C, Bahar I. Signal propagation in proteins and relation to equilibrium fluctuations. *PLoS Comput Biol.* 2007;3(9):1716–26.
 107. Chennubhotla C, Yang Z, Bahar I. Coupling between global dynamics and signal transduction pathways: a mechanism of allostery for chaperonin GroEL. *Mol Biosyst.* 2008;4(4):287–92.
 108. Vanwart AT, Eargle J, Luthey-Schulten Z, Amaro RE. Exploring residue component contributions to dynamical network models of allostery. *J Chem Theory Comput.* 2012;8(8):2949–61.
 109. Ma X, Meng H, Lai L. Motions of allosteric and orthosteric ligand-binding sites in proteins are highly correlated. *J Chem Inf Model.* 2016;56(9):1725–33.
 110. Zhang W, Xie J, Lai L. Correlation between allosteric and Orthosteric sites. *Adv Exp Med Biol.* 2019;1163:89–105.
 111. McClendon CL, Friedland G, Mobley DL, Amirkhani H, Jacobson MP. Quantifying correlations between allosteric sites in thermodynamic ensembles. *J Chem Theory Comput.* 2009;5(9):2486–502.
 112. McClendon CL, Hua L, Barreiro A, Jacobson MP. Comparing conformational ensembles using the Kullback–Leibler divergence expansion. *J Chem Theory Comput.* 2012;8(6):2115–26.
 113. LeVine MV, Weinstein H. NbIT – a new information theory-based analysis of allosteric mechanisms reveals residues that underlie function in the leucine transporter LeuT. *PLoS Comput Biol.* 2014;10(5):e1003603.
 114. Lin MM. Timing correlations in proteins predict functional modules and dynamic allostery. *J Am Chem Soc.* 2016;138(15):5036–43.
 115. Singh S, Bowman GR. Quantifying allosteric communication via both concerted structural changes and conformational disorder with CARDS. *J Chem Theory Comput.* 2017;13(4):1509–17.
 116. Long SY, Wang JW, Tian P. Significance of triple torsional correlations in proteins. *RSC Adv.* 2019;9(24):13949–58.
 117. Kaya C, Armutlulu A, Ekesan S, Haliloglu T. MCPPath: Monte Carlo path generation approach to predict likely allosteric pathways and functional residues. *Nucleic Acids Res.* 2013;41(Web Server issue):W249–55.
 118. Clarke D, Sethi A, Li S, Kumar S, Chang RWF, Chen J, et al. Identifying allosteric hotspots with dynamics: application to inter- and intra-species conservation. *Structure.* 2016;24(5):826–37.
 119. Xu Y, Wang S, Hu Q, Gao S, Ma X, Zhang W, et al. CavityPlus: a web server for protein cavity detection with pharmacophore modelling, allosteric site identification and covalent ligand binding ability prediction. *Nucleic Acids Res.* 2018;46(W1):W374–W9.
 120. Yu M, Ma X, Cao H, Chong B, Lai L, Liu Z. Singular value decomposition for the correlation of atomic fluctuations with arbitrary angle. *Proteins.* 2018;86(10):1075–87.
 121. Mendez R, Bastolla U. Torsional network model: normal modes in torsion angle space better correlate with conformation changes in proteins. *Phys Rev Lett.* 2010;104(22):228103.
 122. Alfayate A, Rodriguez Caceres C, Gomes Dos Santos H, Bastolla U. Predicted dynamical couplings of protein residues characterize catalysis, transport and allostery. *Bioinformatics.* 2019;35(23):4971–8.
 123. Amor BR, Schaub MT, Yaliraki SN, Barahona M. Prediction of allosteric sites and mediating interactions through bond-to-bond propensities. *Nat Commun.* 2016;7:12477.
 124. Sethi A, Eargle J, Black AA, Luthey-Schulten Z. Dynamical networks in tRNA:protein complexes. *Proc Natl Acad Sci U S A.* 2009;106(16):6620–5.
 125. Piovesan D, Minervini G, Tosatto SC. The RING 2.0 web server for high quality residue interaction networks. *Nucleic Acids Res.* 2016;44(W1):W367–74.
 126. Aydinl RM, Sercinoglu O, Ozbek P. ProSNEx: a web-based application for exploration and analysis of protein structures using network formalism. *Nucleic Acids Res.* 2019;47(W1):W471–W6.
 127. Rivalta I, Sultan MM, Lee NS, Manley GA, Loria JP, Batista VS. Allosteric pathways in imidazole glycerol phosphate synthase. *Proc Natl Acad Sci U S A.* 2012;109(22):E1428–36.
 128. Bhattacharya S, Vaidehi N. Differences in allosteric communication pipelines in the inactive and active states of a GPCR. *Biophys J.* 2014;107(2):422–34.
 129. O'Rourke KF, Gorman SD, Boehr DD. Biophysical and computational methods to analyze amino acid interaction networks in proteins. *Comput Struct Biotechnol J.* 2016;14:245–51.
 130. Negre CFA, Morzan UN, Hendrickson HP, Pal R, Lisi GP, Loria JP, et al. Eigenvector centrality for characterization of protein allosteric pathways. *Proc Natl Acad Sci U S A.* 2018;115(52):E12201–E8.

131. Botello-Smith WM, Luo Y. Robust determination of protein allosteric signaling pathways. *J Chem Theory Comput.* 2019;15(4):2116–26.
132. Lake PT, Davidson RB, Klem H, Hocky GM, McCullagh M. Residue-level allostery propagates through the effective coarse-grained Hessian. *J Chem Theory Comput.* 2020;16(5):3385–95.
133. Dijkstra EW. A note on two problems in connexion with graphs. *Numer Math.* 1959;1(1):269–71.
134. Bellman R. On a routing problem. *Quart Appl Math.* 1958;16(1):87–90.
135. Liang Z, Verkhivker GM, Hu G. Integration of network models and evolutionary analysis into high-throughput modeling of protein dynamics and allosteric regulation: theory, tools and applications. *Brief Bioinform.* 2020;21(3):815–35.
136. Lange OF, Grubmüller H. Full correlation analysis of conformational protein dynamics. *Proteins.* 2008;70(4):1294–312.
137. Lange OF, Grubmüller H. Generalized correlation for biomolecular dynamics. *Proteins.* 2006;62(4):1053–61.
138. Gervasio FL, Laio A, Parrinello M. Flexible docking in solution using metadynamics. *J Am Chem Soc.* 2005;127(8):2600–7.
139. Saleh N, Ibrahim P, Saladino G, Gervasio FL, Clark T. An efficient metadynamics-based protocol to model the binding affinity and the transition state ensemble of G-protein-coupled receptor ligands. *J Chem Inf Model.* 2017;57(5):1210–7.
140. Fusani L, Palmer DS, Somers DO, Wall ID. Exploring ligand stability in protein crystal structures using binding pose metadynamics. *J Chem Inf Model.* 2020;60(3):1528–39.
141. Söldner CA, Horn AHC, Sticht H. A metadynamics-based protocol for the determination of GPCR-ligand binding modes. *Int J Mol Sci.* 2019;20(8):1970.
142. Ansari SM, Coletta A, Kirkeby Skeby K, Sørensen J, Schiøtt B, Palmer DS. Allosteric-activation mechanism of bovine chymosin revealed by bias-exchange metadynamics and molecular dynamics simulations. *J Phys Chem B.* 2016;120(40):10453–62.
143. Cavalli A, Spitaleri A, Saladino G, Gervasio FL. Investigating drug-target association and dissociation mechanisms using metadynamics-based algorithms. *Acc Chem Res.* 2015;48(2):277–85.
144. Demerdash ON, Daily MD, Mitchell JC. Structure-based predictive models for allosteric hot spots. *PLoS Comput Biol.* 2009;5(10):e1000531.
145. Huang W, Lu S, Huang Z, Liu X, Mou L, Luo Y, et al. Allosite: a method for predicting allosteric sites. *Bioinformatics.* 2013;29(18):2357–9.
146. Greener JG, Sternberg MJ. AlloPred: prediction of allosteric pockets on proteins using normal mode perturbation analysis. *BMC Bioinformatics.* 2015;16(1):335.
147. Chen AS, Westwood NJ, Brear P, Rogers GW, Mavridis L, Mitchell JB. A random forest model for predicting allosteric and functional sites on proteins. *Mol Inform.* 2016;35(3–4):125–35.
148. Cimermancic P, Weinkam P, Rettenmaier TJ, Bichmann L, Keedy DA, Woldeyes RA, et al. CryptoSite: expanding the druggable proteome by characterization and prediction of cryptic binding sites. *J Mol Biol.* 2016;428(4):709–19.
149. Song K, Liu X, Huang W, Lu S, Shen Q, Zhang L, et al. Improved method for the identification and validation of allosteric sites. *J Chem Inf Model.* 2017;57(9):2358–63.
150. Akbar R, Helms V. ALLO: a tool to discriminate and prioritize allosteric pockets. *Chem Biol Drug Des.* 2018;91(4):845–53.
151. Yan W, Hu G, Liang Z, Zhou J, Yang Y, Chen J, et al. Node-weighted amino acid network strategy for characterization and identification of protein functional residues. *J Chem Inf Model.* 2018;58(9):2024–32.
152. Botlani M, Siddiqui A, Varma S. Machine learning approaches to evaluate correlation patterns in allosteric signaling: a case study of the PDZ2 domain. *J Chem Phys.* 2018;148(24):241726.
153. Zhou H, Dong Z, Tao P. Recognition of protein allosteric states and residues: machine learning approaches. *J Comput Chem.* 2018;39(20):1481–90.
154. Tsuchiya Y, Taneishi K, Yonezawa Y. Autoencoder-based detection of dynamic allostery triggered by ligand binding based on molecular dynamics. *J Chem Inf Model.* 2019;59(9):4043–51.
155. Hayatshahi HS, Ahuactzin E, Tao P, Wang S, Liu J. Probing protein allostery as a residue-specific concept via residue response maps. *J Chem Inf Model.* 2019;59(11):4691–705.
156. Mishra SK, Kandoi G, Jernigan RL. Coupling dynamics and evolutionary information with structure to identify protein regulatory and functional binding sites. *Proteins.* 2019;87(10):850–68.
157. Huang WK, Wang GQ, Shen QC, Liu XY, Lu SY, Geng L, et al. ASBench: benchmarking sets for allosteric discovery. *Bioinformatics.* 2015;31(15):2598–600.
158. Guarnera E, Berezovsky IN. Structure-based statistical mechanical model accounts for the causality and energetics of allosteric communication. *PLoS Comput Biol.* 2016;12(3):e1004678.
159. Tee WV, Guarnera E, Berezovsky IN. Reversing allosteric communication: from detecting allosteric sites to inducing and tuning targeted allosteric response. *PLoS Comput Biol.* 2018;14(6):e1006228.
160. Yao XQ, Hamelberg D. Detecting functional dynamics in proteins with comparative perturbed-ensembles analysis. *Acc Chem Res.* 2019;52(12):3455–64.
161. Yao XQ, Momin M, Hamelberg D. Elucidating allosteric communications in proteins with difference contact network analysis. *J Chem Inf Model.* 2018;58(7):1325–30.
162. Seco J, Luque FJ, Barril X. Binding site detection and druggability index from first principles. *J Med Chem.* 2009;52(8):2363–71.
163. Alvarez-Garcia D, Barril X. Molecular simulations with solvent competition quantify water displaceability and provide accurate interaction maps of protein binding sites. *J Med Chem.* 2014;57(20):8530–9.
164. Lexa KW, Carlson HA. Full protein flexibility is essential for proper hot-spot mapping. *J Am Chem Soc.* 2011;133(2):200–2.

165. Ghanakota P, Carlson HA. Moving beyond active-site detection: MixMD applied to allosteric systems. *J Phys Chem B*. 2016;120(33):8685–95.
166. Graham SE, Leja N, Carlson HA. MixMD Probeview: robust binding site prediction from cosolvent simulations. *J Chem Inf Model*. 2018;58(7):1426–33.
167. Guvench O, MacKerell AD Jr. Computational fragment-based binding site identification by ligand competitive saturation. *PLoS Comput Biol*. 2009;5(7):e1000435.
168. Lakkaraju SK, Yu W, Raman EP, Hershfeld AV, Fang L, Deshpande DA, et al. Mapping functional group free energy patterns at protein occluded sites: nuclear receptors and G-protein coupled receptors. *J Chem Inf Model*. 2015;55(3):700–8.
169. Raman EP, Lakkaraju SK, Denny RA, MacKerell AD Jr. Estimation of relative free energies of binding using pre-computed ensembles based on the single-step free energy perturbation and the site-identification by ligand competitive saturation approaches. *J Comput Chem*. 2017;38(15):1238–51.
170. Kokh DB, Richter S, Henrich S, Czodrowski P, Rippmann F, Wade RC. TRAPP: a tool for analysis of transient binding pockets in proteins. *J Chem Inf Model*. 2013;53(5):1235–52.
171. Kokh DB, Czodrowski P, Rippmann F, Wade RC. Perturbation approaches for exploring protein binding site flexibility to predict transient binding pockets. *J Chem Theory Comput*. 2016;12(8):4100–13.
172. Yuan JH, Han SB, Richter S, Wade RC, Kokh DB. Druggability assessment in TRAPP using machine learning approaches. *J Chem Inf Model*. 2020;60(3):1685–99.
173. Cuchillo R, Pinto-Gil K, Michel J. A collective variable for the rapid exploration of protein druggability. *J Chem Theory Comput*. 2015;11(3):1292–307.
174. Bowman GR, Geissler PL. Equilibrium fluctuations of a single folded protein reveal a multitude of potential cryptic allosteric sites. *Proc Natl Acad Sci U S A*. 2012;109(29):11681–6.
175. Bowman GR, Bolin ER, Hart KM, Maguire BC, Marqusee S. Discovery of multiple hidden allosteric sites by combining Markov state models and experiments. *Proc Natl Acad Sci U S A*. 2015;112(9):2734–9.
176. Ferruz N, Doerr S, Vanase-Frawley MA, Zou Y, Chen X, Marr ES, et al. Dopamine D3 receptor antagonist reveals a cryptic pocket in aminergic GPCRs. *Sci Rep*. 2018;8(1):897.
177. Wagner JR, Sorensen J, Hensley N, Wong C, Zhu C, Perison T, et al. POVME 3.0: software for mapping binding pocket flexibility. *J Chem Theory Comput*. 2017;13(9):4584–92.
178. Sabanes Zariquiey F, de Souza JV, Bronowska AK. Cosolvent Analysis Toolkit (CAT): a robust hotspot identification platform for cosolvent simulations of proteins to expand the druggable proteome. *Sci Rep*. 2019;9(1):19118.
179. Vajda S, Beglov D, Wakefield AE, Egbert M, Whitty A. Cryptic binding sites on proteins: definition, detection, and druggability. *Curr Opin Chem Biol*. 2018;44:1–8.
180. Kuzmanic A, Bowman GR, Juarez-Jimenez J, Michel J, Gervasio FL. Investigating cryptic binding sites by molecular dynamics simulations. *Acc Chem Res*. 2020;53(3):654–61.
181. Daura X. Advances in the computational identification of allosteric sites and pathways in proteins. *Adv Exp Med Biol*. 2019;1163:141–69.
182. Wodak SJ, Paci E, Dokholyan NV, Berezhovsky IN, Horovitz A, Li J, et al. Allostery in its many disguises: from theory to applications. *Structure*. 2019;27(4):566–78.
183. Sheik Amamuddy O, Veldman W, Manyumwa C, Khairallah A, Agajanian S, Oluyemi O, et al. Integrated computational approaches and tools for allosteric drug discovery. *Int J Mol Sci*. 2020;21(3):847.
184. Song K, Li Q, Gao W, Lu S, Shen Q, Liu X, et al. AlloDriver: a method for the identification and analysis of cancer driver targets. *Nucleic Acids Res*. 2019;47(W1):W315–W21.
185. Huang M, Song K, Liu X, Lu S, Shen Q, Wang R, et al. AlloFinder: a strategy for allosteric modulator discovery and allosterome analyses. *Nucleic Acids Res*. 2018;46(W1):W451–W8.
186. Tan ZW, Tee WV, Guarnera E, Booth L, Berezhovsky IN. AlloMAPS: allosteric mutation analysis and polymorphism of signaling database. *Nucleic Acids Res*. 2019;47(D1):D265–D70.
187. Li S, Shen Q, Su M, Liu X, Lu S, Chen Z, et al. Alloscore: a method for predicting allosteric ligand-protein interactions. *Bioinformatics*. 2016;32(10):1574–6.
188. Guarnera E, Tan ZW, Zheng Z, Berezhovsky IN. AlloSigMA: allosteric signaling and mutation analysis server. *Bioinformatics*. 2017;33(24):3996–8.
189. Tan ZW, Guarnera E, Tee WV, Berezhovsky IN. AlloSigMA 2: paving the way to designing allosteric effectors and to exploring allosteric effects of mutations. *Nucleic Acids Res*. 2020;48(W1):W116–W24.
190. Weinkam P, Pons J, Sali A. Structure-based model of allostery predicts coupling between distant sites. *Proc Natl Acad Sci U S A*. 2012;109(13):4875–80.
191. Huang Z, Zhu L, Cao Y, Wu G, Liu X, Chen Y, et al. ASD: a comprehensive database of allosteric proteins and modulators. *Nucleic Acids Res*. 2011;39(Database issue):D663–9.
192. Huang Z, Mou L, Shen Q, Lu S, Li C, Liu X, et al. ASD v2.0: updated content and novel features focusing on allosteric regulation. *Nucleic Acids Res*. 2014;42(Database issue):D510–6.
193. Karami Y, Bitard-Feildel T, Laine E, Carbone A. “Infostery” analysis of short molecular dynamics simulations identifies highly sensitive residues and predicts deleterious mutations. *Sci Rep*. 2018;8(1):16126.
194. Zhang W, Pei J, Lai L. Statistical analysis and prediction of covalent ligand targeted cysteine residues. *J Chem Inf Model*. 2017;57(6):1453–60.
195. Li H, Chang YY, Lee JY, Bahar I, Yang LW. DynOmics: dynamics of structural proteome and beyond. *Nucleic Acids Res*. 2017;45(W1):W374–W80.
196. Porter JR, Zimmerman MI, Bowman GR. Enspara: modeling molecular ensembles with scalable data structures and parallel computing. *J Chem Phys*. 2019;150(4):044108.
197. Greener JG, Filippis I, Sternberg MJE. Predicting protein dynamics and allostery using multi-protein atomic distance constraints. *Structure*. 2017;25(3):546–58.

198. Cerdan AH, Sisquellas M, Pereira G, Barreto Gomes DE, Changeux JP, Cecchini M. The glycine receptor allosteric ligands library (GRALL). *Bioinformatics*. 2020;36(11):3379–84.
199. Panjkovich A, Daura X. PARS: a web server for the prediction of protein allosteric and regulatory sites. *Bioinformatics*. 2014;30(9):1314–5.
200. Goncarenco A, Mitternacht S, Yong T, Eisenhaber B, Eisenhaber F, Berezovsky IN. SPACER: server for predicting allosteric communication and effects of regulation. *Nucleic Acids Res*. 2013;41(Web Server issue):W266–72.
201. Seeber M, Felling A, Raimondi F, Mariani S, Fanelli F. WebPSN: a web server for high-throughput investigation of structural communication in biomacromolecules. *Bioinformatics*. 2015;31(5):779–81.
202. Felling A, Seeber M, Fanelli F. webPSN v2.0: a webserver to infer fingerprints of structural communication in biomacromolecules. *Nucleic Acids Res*. 2020;48(W1):W94–W103.
203. Comitani F, Gervasio FL. Exploring cryptic pockets formation in targets of pharmaceutical interest with SWISH. *J Chem Theory Comput*. 2018;14(6):3321–31.
204. Changeux JP, Edelstein SJ. Allosteric mechanisms of signal transduction. *Science*. 2005;308(5727):1424–8.
205. Moriconi A, Cunha TM, Souza GR, Lopes AH, Cunha FQ, Carneiro VL, et al. Targeting the minor pocket of C5aR for the rational design of an oral allosteric inhibitor for inflammatory and neuropathic pain relief. *Proc Natl Acad Sci U S A*. 2014;111(47):16937–42.
206. Jinushi M. Immune regulation of therapy-resistant niches: emerging targets for improving anticancer drug responses. *Cancer Metastasis Rev*. 2014;33(2–3):737–45.
207. Hauser AS, Attwood MM, Rask-Andersen M, Schioth HB, Gloriam DE. Trends in GPCR drug discovery: new agents, targets and indications. *Nat Rev Drug Discov*. 2017;16(12):829–42.
208. Wacker D, Stevens RC, Roth BL. How ligands illuminate GPCR molecular pharmacology. *Cell*. 2017;170(3):414–27.
209. Hauser AS, Chavali S, Masuho I, Jahn LJ, Martemyanov KA, Gloriam DE, et al. Pharmacogenomics of GPCR drug targets. *Cell*. 2018;172(1–2):41–54.e19.
210. Conn PJ, Kuduk SD, Doller D. Drug design strategies for GPCR allosteric modulators. *Annu Rev Med Chem*. 2012;47:441–57.
211. Kruse AC, Hu J, Pan AC, Arlow DH, Rosenbaum DM, Rosemond E, et al. Structure and dynamics of the M3 muscarinic acetylcholine receptor. *Nature*. 2012;482(7386):552–6.
212. Kruse AC, Ring AM, Manglik A, Hu J, Hu K, Eitel K, et al. Activation and allosteric modulation of a muscarinic acetylcholine receptor. *Nature*. 2013;504(7478):101–6.
213. Cianchetta A, Jacobson KA. Breakthrough in GPCR crystallography and its impact on computer-aided drug design. *Methods Mol Biol*. 2018;1705:45–72.
214. Andrews SP, Tehan B. Stabilised G protein-coupled receptors in structure-based drug design: a case study with adenosine A2A receptor. *MedChemComm*. 2013;4(1):52–67.
215. Rucktooa P, Cheng RKY, Segala E, Geng T, Errey JC, Brown GA, et al. Towards high throughput GPCR crystallography: in meso soaking of adenosine A2A receptor crystals. *Sci Rep*. 2018;8(1):41.
216. Wess J. Muscarinic acetylcholine receptor knockout mice: novel phenotypes and clinical implications. *Annu Rev Pharmacol Toxicol*. 2004;44:423–50.
217. Haga K, Kruse AC, Asada H, Yurugi-Kobayashi T, Shiroishi M, Zhang C, et al. Structure of the human M2 muscarinic acetylcholine receptor bound to an antagonist. *Nature*. 2012;482(7386):547–51.
218. Shaw DE, Deneroff MM, Dror RO, Kuskin JS, Larson RH, Salmon JK, et al. Anton, a special-purpose machine for molecular dynamics simulation. *Commun ACM*. 2008;51(7):91–7.
219. Mackerell AD, Bashford D, Bellott M, Dunbrack RL, Evanseck JD, Field MJ, et al. All-atom empirical potential for molecular modeling and dynamics studies of proteins. *J Phys Chem B*. 1998;102(18):3586–616.
220. Brooks BR, Brooks CL 3rd, Mackerell AD Jr, Nilsson L, Petrella RJ, Roux B, et al. CHARMM: the biomolecular simulation program. *J Comput Chem*. 2009;30(10):1545–614.
221. Hamelberg D, Mongan J, McCammon JA. Accelerated molecular dynamics: a promising and efficient simulation method for biomolecules. *J Chem Phys*. 2004;120(24):11919–29.
222. Miao Y, Goldfeld DA, Moo EV, Sexton PM, Christopoulos A, McCammon JA, et al. Accelerated structure-based design of chemically diverse allosteric modulators of a muscarinic G protein-coupled receptor. *Proc Natl Acad Sci U S A*. 2016;113(38):E5675–84.
223. Shi LM, Fan Y, Lee JK, Waltham M, Andrews DT, Scherf U, et al. Mining and visualizing large anticancer drug discovery databases. *J Chem Inf Comput Sci*. 2000;40(2):367–79.
224. Farid R, Day T, Friesner RA, Pearlstein RA. New insights about HERG blockade obtained from protein modeling, potential energy mapping, and docking studies. *Bioorg Med Chem*. 2006;14(9):3160–73.
225. Sherman W, Day T, Jacobson MP, Friesner RA, Farid R. Novel procedure for modeling ligand/receptor induced fit effects. *J Med Chem*. 2006;49(2):534–53.
226. Sherman W, Beard HS, Farid R. Use of an induced fit receptor structure in virtual screening. *Chem Biol Drug Des*. 2006;67(1):83–4.
227. Schrödinger: Schrödinger Suite Induced Fit Docking protocol; Glide, Schrödinger, LLC, New York, NY; Prime, Schrödinger, LLC, New York, NY.
228. Friesner RA, Banks JL, Murphy RB, Halgren TA, Klicic JJ, Mainz DT, et al. Glide: a new approach for rapid, accurate docking and scoring. 1. Method and assessment of docking accuracy. *J Med Chem*. 2004;47(7):1739–49.
229. Halgren TA, Murphy RB, Friesner RA, Beard HS, Frye LL, Pollard WT, et al. Glide: a new approach for rapid, accurate docking and scoring. 2. Enrichment factors in database screening. *J Med Chem*. 2004;47(7):1750–9.

230. Friesner RA, Murphy RB, Repasky MP, Frye LL, Greenwood JR, Halgren TA, et al. Extra precision Glide: docking and scoring incorporating a model of hydrophobic enclosure for protein-ligand complexes. *J Med Chem*. 2006;49(21):6177–96.
231. Schrödinger: Glide, Schrödinger, LLC, New York, NY.
232. Valant C, Robert Lane J, Sexton PM, Christopoulos A. The best of both worlds? Bitopic orthosteric/allosteric ligands of G protein-coupled receptors. *Annu Rev Pharmacol Toxicol*. 2012;52:153–78.
233. Valant C, Gregory KJ, Hall NE, Scammells PJ, Lew MJ, Sexton PM, et al. A novel mechanism of G protein-coupled receptor functional selectivity. Muscarinic partial agonist McN-A-343 as a bitopic orthosteric/allosteric ligand. *J Biol Chem*. 2008;283(43):29312–21.
234. Mohr K, Tränkle C, Kostenis E, Barocelli E, De Amici M, Holzgrabe U. Rational design of dualsteric GPCR ligands: quests and promise. *Br J Pharmacol*. 2010;159(5):997–1008.
235. Mohr K, Schmitz J, Schrage R, Tränkle C, Holzgrabe U. Molecular alliance-from orthosteric and allosteric ligands to dualsteric/bitopic agonists at G protein coupled receptors. *Angew Chem Int Ed Engl*. 2013;52(2):508–16.
236. Guo RF, Ward PA. Role of C5a in inflammatory responses. *Annu Rev Immunol*. 2005;23:821–52.
237. Griffin RS, Costigan M, Brenner GJ, Ma CH, Scholz J, Moss A, et al. Complement induction in spinal cord microglia results in anaphylatoxin C5a-mediated pain hypersensitivity. *J Neurosci*. 2007;27(32):8699–708.
238. Ricklin D, Lambris JD. Complement-targeted therapeutics. *Nat Biotechnol*. 2007;25(11):1265–75.
239. Ting E, Guerrero AT, Cunha TM, Verri WA Jr, Taylor SM, Woodruff TM, et al. Role of complement C5a in mechanical inflammatory hypernociception: potential use of C5a receptor antagonists to control inflammatory pain. *Br J Pharmacol*. 2008;153(5):1043–53.
240. Bertini R, Allegretti M, Bizzarri C, Moriconi A, Locati M, Zampella G, et al. Noncompetitive allosteric inhibitors of the inflammatory chemokine receptors CXCR1 and CXCR2: prevention of reperfusion injury. *Proc Natl Acad Sci U S A*. 2004;101(32):11791–6.
241. Tan Q, Zhu Y, Li J, Chen Z, Han GW, Kufareva I, et al. Structure of the CCR5 chemokine receptor-HIV entry inhibitor maraviroc complex. *Science*. 2013;341(6152):1387–90.
242. Dassault Systèmes BIOVIA. Discovery studio modeling environment. San Diego: Dassault Systèmes; 2016.
243. Beccari AR, Cavazzoni C, Beato C, Costantino G. LiGen: a high performance workflow for chemistry driven de novo design. *J Chem Inf Model*. 2013;53(6):1518–27.
244. Beato C, Beccari AR, Cavazzoni C, Lorenzi S, Costantino G. Use of experimental design to optimize docking performance: the case of LiGenDock, the docking module of LiGen, a new de novo design program. *J Chem Inf Model*. 2013;53(6):1503–17.
245. Yekkirala AS, Roberson DP, Bean BP, Woolf CJ. Breaking barriers to novel analgesic drug development. *Nat Rev Drug Discov*. 2017;16(8):545–64.
246. Ludwig MG, Vanek M, Guerini D, Gasser JA, Jones CE, Junker U, et al. Proton-sensing G-protein-coupled receptors. *Nature*. 2003;425(6953):93–8.
247. Huang CW, Tzeng JN, Chen YJ, Tsai WF, Chen CC, Sun WH. Nociceptors of dorsal root ganglion express proton-sensing G-protein-coupled receptors. *Mol Cell Neurosci*. 2007;36(2):195–210.
248. Sali A, Blundell TL. Comparative protein modelling by satisfaction of spatial restraints. *J Mol Biol*. 1993;234(3):779–815.
249. Wu B, Chien EY, Mol CD, Fenalti G, Liu W, Katritch V, et al. Structures of the CXCR4 chemokine GPCR with small-molecule and cyclic peptide antagonists. *Science*. 2010;330(6007):1066–71.
250. Yang Q, Sharp KA. Building alternate protein structures using the elastic network model. *Proteins*. 2009;74(3):682–700.
251. Mysinger MM, Shoichet BK. Rapid context-dependent ligand desolvation in molecular docking. *J Chem Inf Model*. 2010;50(9):1561–73.
252. Coleman RG, Carchia M, Sterling T, Irwin JJ, Shoichet BK. Ligand pose and orientational sampling in molecular docking. *PLoS One*. 2013;8(10):e75992.
253. Leach K, Sexton PM, Christopoulos A. Allosteric GPCR modulators: taking advantage of permissive receptor pharmacology. *Trends Pharmacol Sci*. 2007;28(8):382–9.
254. Keiser MJ, Roth BL, Armbruster BN, Ernsberger P, Irwin JJ, Shoichet BK. Relating protein pharmacology by ligand chemistry. *Nat Biotechnol*. 2007;25(2):197–206.
255. Girault JA, Greengard P. The neurobiology of dopamine signaling. *Arch Neurol*. 2004;61(5):641–4.
256. Joyce JN, Millan MJ. Dopamine D3 receptor agonists for protection and repair in Parkinson's disease. *Curr Opin Pharmacol*. 2007;7(1):100–5.
257. Gaulton A, Bellis LJ, Bento AP, Chambers J, Davies M, Hersey A, et al. ChEMBL: a large-scale bioactivity database for drug discovery. *Nucleic Acids Res*. 2012;40(Database issue):D1100–7.
258. Chien EY, Liu W, Zhao Q, Katritch V, Han GW, Hanson MA, et al. Structure of the human dopamine D3 receptor in complex with a D2/D3 selective antagonist. *Science*. 2010;330(6007):1091–5.
259. Lane JR, Chubukov P, Liu W, Canals M, Cherezov V, Abagyan R, et al. Structure-based ligand discovery targeting orthosteric and allosteric pockets of dopamine receptors. *Mol Pharmacol*. 2013;84(6):794–807.
260. Katritch V, Rueda M, Abagyan R. Ligand-guided receptor optimization. *Methods Mol Biol*. 2012;857:189–205.
261. Abagyan R, Totrov M, Kuznetsov D. ICM—a new method for protein modeling and design: applications to docking and structure prediction from the distorted native conformation. *J Comput Chem*. 1994;15(5):488–506.
262. Neves MA, Totrov M, Abagyan R. Docking and scoring with ICM: the benchmarking results and strategies for improvement. *J Comput Aided Mol Des*. 2012;26(6):675–86.

263. Fyfe TJ, Zarzycka B, Lim HD, Kellam B, Mistry SN, Katrich V, et al. A thieno[2,3-d]pyrimidine scaffold is a novel negative allosteric modulator of the dopamine D2 receptor. *J Med Chem.* 2019;62(1):174–206.
264. Wang S, Che T, Levit A, Shoichet BK, Wacker D, Roth BL. Structure of the D2 dopamine receptor bound to the atypical antipsychotic drug risperidone. *Nature.* 2018;555(7695):269–73.
265. Allen JA, Yost JM, Setola V, Chen X, Sassano MF, Chen M, et al. Discovery of β -arrestin-biased dopamine D2 ligands for probing signal transduction pathways essential for antipsychotic efficacy. *Proc Natl Acad Sci U S A.* 2011;108(45):18488–93.
266. Lane JR, Donthamsetti P, Shonberg J, Draper-Joyce CJ, Dentry S, Michino M, et al. A new mechanism of allostery in a G protein-coupled receptor dimer. *Nat Chem Biol.* 2014;10(9):745–52.
267. Shonberg J, Draper-Joyce C, Mistry SN, Christopoulos A, Scammells PJ, Lane JR, et al. Structure-activity study of N-((trans)4-(2-(7-cyano-3,4-dihydroisoquinolin-2(1H)-yl)ethyl)cyclohexyl)-1H-indole-2-carboxamide (SB269652), a bitopic ligand that acts as a negative allosteric modulator of the dopamine D2 receptor. *J Med Chem.* 2015;58(13):5287–307.
268. Fronik P, Gaiser BI, Bitopic Ligands SPD. Metastable binding sites: opportunities for G protein-coupled receptor (GPCR) medicinal chemistry. *J Med Chem.* 2017;60(10):4126–34.
269. Brubaker PL, Drucker DJ. Structure–function of the glucagon receptor family of G protein-coupled receptors: the glucagon, GIP, GLP-1, and GLP-2 receptors. *Recept Channels.* 2002;8(3–4):179–88.
270. Zhang H, Qiao A, Yang D, Yang L, Dai A, de Graaf C, et al. Structure of the full-length glucagon class B G-protein-coupled receptor. *Nature.* 2017;546(7657):259–64.
271. Verdonk ML, Cole JC, Hartshorn MJ, Murray CW, Taylor RD. Improved protein-ligand docking using GOLD. *Proteins.* 2003;52(4):609–23.
272. Dassault Systèmes BIOVIA. Pipeline Pilot. San Diego: Dassault Systèmes; 2020.
273. Rush TS, Grant JA, Mosyak L, Nicholls A. A shape-based 3-D scaffold hopping method and its application to a bacterial protein-protein interaction. *J Med Chem.* 2005;48(5):1489–95.
274. ROCS: OpenEye Scientific Software, Santa Fe, NM.
275. Marcou G, Rognan D. Optimizing fragment and scaffold docking by use of molecular interaction fingerprints. *J Chem Inf Model.* 2007;47(1):195–207.
276. Sheth S, Brito R, Mukherjee D, Rybak LP, Ramkumar V. Adenosine receptors: expression, function and regulation. *Int J Mol Sci.* 2014;15(2):2024–52.
277. von Kügelgen I, Hoffmann K. Pharmacology and structure of P2Y receptors. *Neuropharmacology.* 2016;104:50–61.
278. Deganutti G, Cuzzolin A, Ciancetta A, Moro S. Understanding allosteric interactions in G protein-coupled receptors using supervised molecular dynamics: a prototype study analysing the human A3 adenosine receptor positive allosteric modulator LUF6000. *Bioorg Med Chem.* 2015;23(14):4065–71.
279. Conroy S, Kindon N, Kellam B, Stocks MJ. Drug-like antagonists of P2Y receptors—from Lead identification to drug development. *J Med Chem.* 2016;59(22):9981–10005.
280. Brash AR. Lipoxygenases: occurrence, functions, catalysis, and acquisition of substrate. *J Biol Chem.* 1999;274(34):23679–82.
281. Mashima R, Okuyama T. The role of lipoxygenases in pathophysiology; new insights and future perspectives. *Redox Biol.* 2015;6:297–310.
282. Kelavkar UP, Badr KF. Effects of mutant p53 expression on human 15-lipoxygenase-promoter activity and murine 12/15-lipoxygenase gene expression: evidence that 15-lipoxygenase is a mutator gene. *Proc Natl Acad Sci U S A.* 1999;96(8):4378–83.
283. Meng H, McClendon CL, Dai Z, Li K, Zhang X, He S, et al. Discovery of novel 15-lipoxygenase activators to shift the human arachidonic acid metabolic network toward inflammation resolution. *J Med Chem.* 2016;59(9):4202–9.
284. Choi J, Chon JK, Kim S, Shin W. Conformational flexibility in mammalian 15S-lipoxygenase: reinterpretation of the crystallographic data. *Proteins.* 2008;70(3):1023–32.
285. Jacobson MP, Friesner RA, Xiang Z, Honig B. On the role of the crystal environment in determining protein side-chain conformations. *J Mol Biol.* 2002;320(3):597–608.
286. Jacobson MP, Pincus DL, Rapp CS, Day TJ, Honig B, Shaw DE, et al. A hierarchical approach to all-atom protein loop prediction. *Proteins.* 2004;55(2):351–67.
287. Schrödinger: Prime, Schrödinger, LLC, New York, NY.
288. Bowers KJ, Chow DE, Xu H, Dror RO, Eastwood MP, Gregersen BA, et al. Scalable algorithms for molecular dynamics simulations on commodity clusters. In: SC '06: proceedings of the 2006 ACM/IEEE conference on supercomputing: 11–17 November 2006; 2006.
289. Schrödinger: Desmond Molecular Dynamics System, D. E. Shaw Research, New York, NY. Maestro-Desmond Interoperability Tools, Schrödinger, New York, NY.
290. Jorgensen WL, Madura JD, Swenson CJ. Optimized intermolecular potential functions for liquid hydrocarbons. *J Am Chem Soc.* 1984;106(22):6638–46.
291. Jorgensen WL, Maxwell DS, Tirado-Rives J. Development and testing of the OPLS all-atom force field on conformational energetics and properties of organic liquids. *J Am Chem Soc.* 1996;118(45):11225–36.
292. Kaminski GA, Friesner RA, Tirado-Rives J, Jorgensen WL. Evaluation and Reparametrization of the OPLS-AA force field for proteins via comparison with accurate quantum chemical calculations on peptides. *J Phys Chem B.* 2001;105(28):6474–87.
293. Specs. Compound management services and research. <https://www.specs.net/>
294. Lang PT, Brozell SR, Mukherjee S, Pettersen EF, Meng EC, Thomas V, et al. DOCK 6: combining techniques to model RNA-small molecule complexes. *RNA.* 2009;15(6):1219–30.
295. Allen WJ, Balias TE, Mukherjee S, Brozell SR, Moustakas DT, Lang PT, et al. DOCK 6: impact of new features and current docking performance. *J Comput Chem.* 2015;36(15):1132–56.

296. Morris GM, Goodsell DS, Halliday RS, Huey R, Hart WE, Belew RK, et al. Automated docking using a Lamarckian genetic algorithm and an empirical binding free energy function. *J Comput Chem*. 1998;19(14):1639–62.
297. Morris GM, Huey R, Lindstrom W, Sanner MF, Belew RK, Goodsell DS, et al. AutoDock4 and AutoDockTools4: automated docking with selective receptor flexibility. *J Comput Chem*. 2009;30(16):2785–91.
298. Fajardo-Ortiz D, Lopez-Cervantes M, Duran L, Dumontier M, Lara M, Ochoa H, et al. The emergence and evolution of the research fronts in HIV/AIDS research. *PLoS One*. 2017;12(5):e0178293.
299. Goldgur Y, Craigie R, Cohen GH, Fujiwara T, Yoshinaga T, Fujishita T, et al. Structure of the HIV-1 integrase catalytic domain complexed with an inhibitor: a platform for antiviral drug design. *Proc Natl Acad Sci U S A*. 1999;96(23):13040–3.
300. Ni H, Sotriffer CA, McCammon JA. Ordered water and ligand mobility in the HIV-1 integrase-5CITEP complex: a molecular dynamics study. *J Med Chem*. 2001;44(19):3043–7.
301. Schames JR, Henchman RH, Siegel JS, Sotriffer CA, Ni H, McCammon JA. Discovery of a novel binding trench in HIV integrase. *J Med Chem*. 2004;47(8):1879–81.
302. Summa V, Petrocchi A, Bonelli F, Crescenzi B, Donghi M, Ferrara M, et al. Discovery of raltegravir, a potent, selective orally bioavailable HIV-integrase inhibitor for the treatment of HIV-AIDS infection. *J Med Chem*. 2008;51(18):5843–55.
303. Brik A, Wong CH. HIV-1 protease: mechanism and drug discovery. *Org Biomol Chem*. 2003;1(1):5–14.
304. Carlson HA, Masukawa KM, McCammon JA. Method for including the dynamic fluctuations of a protein in computer-aided drug design. *J Phys Chem A*. 1999;103(49):10213–9.
305. Carlson HA, Masukawa KM, Rubins K, Bushman FD, Jorgensen WL, Lins RD, et al. Developing a dynamic pharmacophore model for HIV-1 integrase. *J Med Chem*. 2000;43(11):2100–14.
306. Meagher KL, Carlson HA. Incorporating protein flexibility in structure-based drug discovery: using HIV-1 protease as a test case. *J Am Chem Soc*. 2004;126(41):13276–81.
307. Spinelli S, Liu QZ, Alzari PM, Hirel PH, Poljak RJ. The three-dimensional structure of the aspartyl protease from the HIV-1 isolate BRU. *Biochimie*. 1991;73(11):1391–6.
308. Wlodawer A, Miller M, Jaskolski M, Sathyanarayana BK, Baldwin E, Weber IT, et al. Conserved folding in retroviral proteases: crystal structure of a synthetic HIV-1 protease. *Science*. 1989;245(4918):616–21.
309. Lapatto R, Blundell T, Hemmings A, Overington J, Wilderspin A, Wood S, et al. X-ray analysis of HIV-1 proteinase at 2.7 Å resolution confirms structural homology among retroviral enzymes. *Nature*. 1989;342(6247):299–302.
310. Molecular Operating Environment. Chemical Computing Group Inc.: Montreal, Canada.
311. Damm KL, Ung PM, Quintero JJ, Gestwicki JE, Carlson HA. A poke in the eye: inhibiting HIV-1 protease through its flap-recognition pocket. *Biopolymers*. 2008;89(8):643–52.
312. Martin YC. 3D database searching in drug design. *J Med Chem*. 1992;35(12):2145–54.
313. Hurst T. Flexible 3D searching: the directed tweak technique. *J Chem Inf Model*. 1994;34(1):190–6.
314. Certara. SYBYL-X. St. Louis, MO.
315. EON: OpenEye Scientific Software, Santa Fe, NM.
316. Hu WS, Hughes SH. HIV-1 reverse transcription. *Cold Spring Harb Perspect Med*. 2012;2(10):a006882.
317. Spence RA, Kati WM, Anderson KS, Johnson KA. Mechanism of inhibition of HIV-1 reverse transcriptase by nonnucleoside inhibitors. *Science*. 1995;267(5200):988–93.
318. Schauer GD, Huber KD, Leuba SH, Sluis-Cremer N. Mechanism of allosteric inhibition of HIV-1 reverse transcriptase revealed by single-molecule and ensemble fluorescence. *Nucleic Acids Res*. 2014;42(18):11687–96.
319. Namasivayam V, Vanangamudi M, Kramer VG, Kurup S, Zhan P, Liu X, et al. The journey of HIV-1 non-nucleoside reverse transcriptase inhibitors (NNRTIs) from lab to clinic. *J Med Chem*. 2019;62(10):4851–83.
320. Zhuang C, Pannecouque C, De Clercq E, Chen F. Development of non-nucleoside reverse transcriptase inhibitors (NNRTIs): our past twenty years. *Acta Pharm Sin B*. 2020;10(6):961–78.
321. Jorgensen WL. Computer-aided discovery of anti-HIV agents. *Bioorg Med Chem*. 2016;24(20):4768–78.
322. Jorgensen WL. The many roles of computation in drug discovery. *Science*. 2004;303(5665):1813–8.
323. Jorgensen WL, Tirado-Rives J. Molecular modeling of organic and biomolecular systems using BOSS and MCPRO. *J Comput Chem*. 2005;26(16):1689–700.
324. Jorgensen WL. Efficient drug lead discovery and optimization. *Acc Chem Res*. 2009;42(6):724–33.
325. Lee WG, Chan AH, Spasov KA, Anderson KS, Jorgensen WL. Design, conformation, and crystallography of 2-naphthyl phenyl ethers as potent anti-HIV agents. *ACS Med Chem Lett*. 2016;7(12):1156–60.
326. Chan AH, Lee WG, Spasov KA, Cisneros JA, Kudalkar SN, Petrova ZO, et al. Covalent inhibitors for eradication of drug-resistant HIV-1 reverse transcriptase: from design to protein crystallography. *Proc Natl Acad Sci U S A*. 2017;114(36):9725–30.
327. Kudalkar SN, Beloor J, Quijano E, Spasov KA, Lee WG, Cisneros JA, et al. From in silico hit to long-acting late-stage preclinical candidate to combat HIV-1 infection. *Proc Natl Acad Sci U S A*. 2018;115(4):E802–e11.
328. Sasaki T, Gannam ZTK, Kudalkar SN, Frey KM, Lee WG, Spasov KA, et al. Molecular and cellular studies evaluating a potent 2-cyanoindolizine catechol diether NNRTI targeting wildtype and Y181C mutant HIV-1 reverse transcriptase. *Bioorg Med Chem Lett*. 2019;29(16):2182–8.
329. Dodda LS, Tirado-Rives J, Jorgensen WL. Unbinding dynamics of non-nucleoside inhibitors from HIV-1 reverse transcriptase. *J Phys Chem B*. 2019;123(8):1741–8.
330. Duong VN, Ippolito JA, Chan AH, Lee WG, Spasov KA, Jorgensen WL, et al. Structural investigation of 2-naphthyl phenyl ether inhibitors bound to WT and Y181C reverse

transcriptase highlights key features of the NNRTI binding site. *Protein Sci.* 2020;29(9):1902–10.

331. Frey KM, Puleo DE, Spasov KA, Bollini M, Jorgensen WL, Anderson KS. Structure-based evaluation of non-nucleoside inhibitors with improved potency and solubility that target HIV reverse transcriptase variants. *J Med Chem.* 2015;58(6):2737–45.

332. Lee WG, Frey KM, Gallardo-Macias R, Spasov KA, Bollini M, Anderson KS, et al. Picomolar inhibitors of HIV-1 reverse transcriptase: design and crystallography of naphthyl phenyl ethers. *ACS Med Chem Lett.* 2014;5(11):1259–62.

333. Nichols SE, Domaoal RA, Thakur VV, Tirado-Rives J, Anderson KS, Jorgensen WL. Discovery of wild-type and Y181C mutant non-nucleoside HIV-1 reverse transcriptase inhibitors using virtual screening with multiple protein structures. *J Chem Inf Model.* 2009;49(5):1272–9.

334. Chambers TJ, Nestorowicz A, Amberg SM, Rice CM. Mutagenesis of the yellow fever virus NS2B protein: effects on proteolytic processing, NS2B-NS3 complex formation, and viral replication. *J Virol.* 1993;67(11):6797–807.

335. Noble CG, Seh CC, Chao AT, Shi PY. Ligand-bound structures of the dengue virus protease reveal the active conformation. *J Virol.* 2012;86(1):438–46.

336. Erbel P, Schiering N, D'Arcy A, Renatus M, Kroemer M, Lim SP, et al. Structural basis for the activation of flaviviral NS3 proteases from dengue and West Nile virus. *Nat Struct Mol Biol.* 2006;13(4):372–3.

337. Brecher M, Li Z, Liu B, Zhang J, Koetzner CA, Alifarag A, et al. A conformational switch high-throughput screening assay and allosteric inhibition of the flavivirus NS2B-NS3 protease. *PLoS Pathog.* 2017;13(5):e1006411.

338. Trott O, Olson AJ. AutoDock Vina: improving the speed and accuracy of docking with a new scoring function, efficient optimization, and multithreading. *J Comput Chem.* 2010;31(2):455–61.

339. Brecher M, Zhang J, Li H. The flavivirus protease as a target for drug discovery. *Virol Sin.* 2013;28(6):326–36.

340. Rusyn I, Lemon SM. Mechanisms of HCV-induced liver cancer: what did we learn from in vitro and animal studies? *Cancer Lett.* 2014; 345(2):210–5.

341. Ansaldi F, Orsi A, Sticchi L, Bruzzone B, Icardi G. Hepatitis C virus in the new era: perspectives in epidemiology, prevention, diagnostics and predictors of response to therapy. *World J Gastroenterol.* 2014;20(29):9633–52.

342. GBD 2015 Disease and Injury Incidence and Prevalence Collaborators. Global, regional, and national incidence, prevalence, and years lived with disability for 310 diseases and injuries, 1990–2015: a systematic analysis for the Global Burden of Disease Study 2015. *Lancet.* 2016;388(10053):1545–602.

343. Talele TT. Multiple allosteric pockets of HCV NS5B polymerase and its inhibitors: a structure based insight. *Curr Bioactive Compd.* 2008;4(2):86–109.

344. Mahmoud AH, Abou El Ella DA, Ismail MA, Abouzid KA. A highly selective structure-based virtual screening model of Palm I allosteric inhibitors of HCV Ns5b polymerase enzyme and its

application in the discovery and optimization of new analogues. *Eur J Med Chem.* 2012;57:468–82.

345. Elhefnawi M, ElGamacy M, Fares M. Multiple virtual screening approaches for finding new Hepatitis c virus RNA-dependent RNA polymerase inhibitors: structure-based screens and molecular dynamics for the pursue of new poly pharmacological inhibitors. *BMC Bioinformatics.* 2012;13:S5.

346. Venkatesan A, Prabhu Dass JF. Review on chemogenomic approaches towards hepatitis C viral targets. *J Cell Biochem.* 2019;120(8):12167–81.

347. Walter S, Buchner J. Molecular chaperones – cellular machines for protein folding. *Angew Chem Int Ed Engl.* 2002;41(7):1098–113.

348. Borges JC, Ramos CH. Protein folding assisted by chaperones. *Protein Pept Lett.* 2005;12(3):257–61.

349. Li Z, Srivastava P. Heat-shock proteins. *Curr Protoc Immunol.* 2004;78(1):A.1T–T6.

350. Ali MM, Roe SM, Vaughan CK, Meyer P, Panaretou B, Piper PW, et al. Crystal structure of an Hsp90-nucleotide-p23/Sba1 closed chaperone complex. *Nature.* 2006;440(7087):1013–7.

351. Van Der Spoel D, Lindahl E, Hess B, Groenhof G, Mark AE, Berendsen HJ. GROMACS: fast, flexible, and free. *J Comput Chem.* 2005;26(16):1701–18.

352. Scott WRP, Hünenberger PH, Tironi IG, Mark AE, Billeter SR, Fennel J, et al. The GROMOS biomolecular simulation program package. *J Phys Chem A.* 1999;103(19):3596–607.

353. Morra G, Verkhivker G, Colombo G. Modeling signal propagation mechanisms and ligand-based conformational dynamics of the Hsp90 molecular chaperone full-length dimer. *PLoS Comput Biol.* 2009;5(3):e1000323.

354. Morra G, Neves MA, Plescia CJ, Tsutsumi S, Neckers L, Verkhivker G, et al. Dynamics-based discovery of allosteric inhibitors: selection of new ligands for the C-terminal domain of Hsp90. *J Chem Theory Comput.* 2010;6(9):2978–89.

355. Sattin S, Tao J, Vettoretti G, Moroni E, Pennati M, Lopercolo A, et al. Activation of Hsp90 enzymatic activity and conformational dynamics through rationally designed allosteric ligands. *Chemistry.* 2015;21(39):13598–608.

356. D'Annessa I, Sattin S, Tao J, Pennati M, Sánchez-Martín C, Moroni E, et al. Design of allosteric stimulators of the Hsp90 ATPase as new anticancer leads. *Chemistry.* 2017;23(22):5188–92.

357. Ferraro M, D'Annessa I, Moroni E, Morra G, Paladino A, Rinaldi S, et al. Allosteric modulators of HSP90 and HSP70: dynamics meets function through structure-based drug design. *J Med Chem.* 2018;62(1):60–87.

358. Sriram M, Osipiuk J, Freeman B, Morimoto R, Joachimiak A. Human Hsp70 molecular chaperone binds two calcium ions within the ATPase domain. *Structure.* 1997;5(3):403–14.

359. Bertelsen EB, Chang L, Gestwicki JE, Zuiderweg ER. Solution conformation of wild-type *E. coli* Hsp70 (DnaK) chaperone complexed with ADP and substrate. *Proc Natl Acad Sci U S A.* 2009;106(21):8471–6.

360. Worrall LJ, Walkinshaw MD. Crystal structure of the C-terminal three-helix bundle subdomain of *C. elegans* Hsp70. *Biochem Biophys Res Commun*. 2007;357(1):105–10.
361. Rodina A, Patel PD, Kang Y, Patel Y, Baaklini I, Wong MJ, et al. Identification of an allosteric pocket on human Hsp70 reveals a mode of inhibition of this therapeutically important protein. *Chem Biol*. 2013;20(12):1469–80.
362. Halgren T. New method for fast and accurate binding-site identification and analysis. *Chem Biol Drug Des*. 2007;69(2):146–8.
363. Halgren TA. Identifying and characterizing binding sites and assessing druggability. *J Chem Inf Model*. 2009;49(2):377–89.
364. Schrödinger: SiteMap, Schrödinger, LLC, New York, NY.
365. Kang Y, Taldone T, Patel HJ, Patel PD, Rodina A, Gozman A, et al. Heat shock protein 70 inhibitors. 1. 2,50 -thiodipyrimidine and 5-(phenylthio)pyrimidine acrylamides as irreversible binders to an allosteric site on heat shock protein 70. *J Med Chem*. 2014;57(4):1188–207.
366. Taldone T, Kang Y, Patel HJ, Patel MR, Patel PD, Rodina A, et al. Heat shock protein 70 inhibitors. 2. 2,50 -thiodipyrimidines, 5-(phenylthio)pyrimidines, 2-(pyridin-3-ylthio)pyrimidines, and 3-(phenylthio)pyridines as reversible binders to an allosteric site on heat shock protein 70. *J Med Chem*. 2014;57(4):1208–24.
367. Rodina A, Taldone T, Kang Y, Patel PD, Koren J 3rd, Yan P, et al. Affinity purification probes of potential use to investigate the endogenous Hsp70 interactome in cancer. *ACS Chem Biol*. 2014;9(8):1698–705.
368. Blume-Jensen P, Hunter T. Oncogenic kinase signalling. *Nature*. 2001;411(6835):355–65.
369. Fujikake N, Shin M, Shimizu S. Association between autophagy and neurodegenerative diseases. *Front Neurosci*. 2018;12:255.
370. Galdadas I, Gervasio FL, Cournia Z. Unravelling the effect of the E545K mutation on PI3K α kinase. *Chem Sci*. 2020;11(13):3511–5.
371. Biondi RM, Cheung PC, Casamayor A, Deak M, Currie RA, Alessi DR. Identification of a pocket in the PDK1 kinase domain that interacts with PIF and the C-terminal residues of PKA. *EMBO J*. 2000;19(5):979–88.
372. Zheng J, Trafny EA, Knighton DR, Xuong NH, Taylor SS, Ten Eyck LF, et al. 2.2 Å refined crystal structure of the catalytic subunit of cAMP-dependent protein kinase complexed with MnATP and a peptide inhibitor. *Acta Crystallogr D*. 1993;49(3):362–5.
373. Biondi RM, Komander D, Thomas CC, Lizcano JM, Deak M, Alessi DR, et al. High resolution crystal structure of the human PDK1 catalytic domain defines the regulatory phosphopeptide docking site. *EMBO J*. 2002;21(16):4219–28.
374. Rettenmaier TJ, Fan H, Karpiak J, Doak A, Sali A, Shoichet BK, et al. Small-molecule allosteric modulators of the protein kinase PDK1 from structure-based docking. *J Med Chem*. 2015;58(20):8285–91.
375. Hindie V, Stroba A, Zhang H, Lopez-Garcia LA, Idrissova L, Zeuzem S, et al. Structure and allosteric effects of low-molecular-weight activators on the protein kinase PDK1. *Nat Chem Biol*. 2009;5(10):758–64.
376. Irwin JJ, Shoichet BK. ZINC – a free database of commercially available compounds for virtual screening. *J Chem Inf Model*. 2005;45(1):177–82.
377. Irwin JJ, Sterling T, Mysinger MM, Bolstad ES, Coleman RG. ZINC: a free tool to discover chemistry for biology. *J Chem Inf Model*. 2012;52(7):1757–68.
378. Mysinger MM, Carchia M, Irwin JJ, Shoichet BK. Directory of useful decoys, enhanced (DUD-E): better ligands and decoys for better benchmarking. *J Med Chem*. 2012;55(14):6582–94.
379. Zhang H, Berezov A, Wang Q, Zhang G, Drebin J, Murali R, et al. ErbB receptors: from oncogenes to targeted cancer therapies. *J Clin Invest*. 2007;117(8):2051–8.
380. Zhao P, Yao MY, Zhu SJ, Chen JY, Yun CH. Crystal structure of EGFR T790M/C797S/V948R in complex with EAI045. *Biochem Biophys Res Commun*. 2018;502(3):332–7.
381. Hefti FF, Rosenthal A, Walicke PA, Wyatt S, Vergara G, Shelton DL, et al. Novel class of pain drugs based on antagonism of NGF. *Trends Pharmacol Sci*. 2006;27(2):85–91.
382. Skerratt SE, Andrews M, Bagal SK, Bilsland J, Brown D, Bungay PJ, et al. The discovery of a potent, selective, and peripherally restricted pan-Trk inhibitor (PF-06273340) for the treatment of pain. *J Med Chem*. 2016;59(22):10084–99.
383. Bagal SK, Omoto K, Blakemore DC, Bungay PJ, Bilsland JG, Clarke PJ, et al. Discovery of allosteric, potent, subtype selective, and peripherally restricted TrkA kinase inhibitors. *J Med Chem*. 2019;62(1):247–65.
384. Young T, Abel R, Kim B, Berne BJ, Friesner RA. Motifs for molecular recognition exploiting hydrophobic enclosure in protein–ligand binding. *Proc Natl Acad Sci U S A*. 2007;104(3):808–13.
385. Abel R, Young T, Farid R, Berne BJ, Friesner RA. Role of the active-site solvent in the thermodynamics of factor Xa ligand binding. *J Am Chem Soc*. 2008;130(9):2817–31.
386. Murphy RB, Repasky MP, Greenwood JR, Tubert-Brohman I, Jerome S, Annabhimoju R, et al. WScore: a flexible and accurate treatment of explicit water molecules in ligand-receptor docking. *J Med Chem*. 2016;59(9):4364–84.
387. Schrödinger: WaterMap, Schrödinger, LLC, New York, NY.
388. Schrödinger: LigPrep, Schrödinger, LLC, New York, NY.
389. Denu JM, Dixon JE. Protein tyrosine phosphatases: mechanisms of catalysis and regulation. *Curr Opin Chem Biol*. 1998;2(5):633–41.
390. Alonso A, Sasin J, Bottini N, Friedberg I, Friedberg I, Osterman A, et al. Protein tyrosine phosphatases in the human genome. *Cell*. 2004;117(6):699–711.
391. Tartaglia M, Mehler EL, Goldberg R, Zampino G, Brunner HG, Kremer H, et al. Mutations in PTPN11, encoding the protein tyrosine phosphatase SHP-2, cause Noonan syndrome. *Nat Genet*. 2001;29(4):465–8.
392. Tartaglia M, Niemeyer CM, Fragale A, Song X, Buechner J, Jung A, et al. Somatic mutations in PTPN11 in juvenile myelomonocytic leukemia, myelodysplastic syndromes and acute myeloid leukemia. *Nat Genet*. 2003;34(2):148–50.

393. Chen YN, LaMarche MJ, Chan HM, Fekkes P, Garcia-Foranet J, Acker MG, et al. Allosteric inhibition of SHP2 phosphatase inhibits cancers driven by receptor tyrosine kinases. *Nature*. 2016;535(7610):148–52.
394. Garcia Foranet J, Chen CH, Chen YN, Chen Z, Deng Z, Firestone B, et al. Allosteric inhibition of SHP2: identification of a potent, selective, and orally efficacious phosphatase inhibitor. *J Med Chem*. 2016;59(17):7773–82.
395. Fodor M, Price E, Wang P, Lu H, Argintaru A, Chen Z, et al. Dual allosteric inhibition of SHP2 phosphatase. *ACS Chem Biol*. 2018;13(3):647–56.
396. Bagdanoff JT, Chen Z, Acker M, Chen YN, Chan H, Dore M, et al. Optimization of fused bicyclic allosteric SHP2 inhibitors. *J Med Chem*. 2019;62(4):1781–92.
397. Sarver P, Acker M, Bagdanoff JT, Chen Z, Chen YN, Chan H, et al. 6-Amino-3-methylpyrimidinones as potent, selective, and orally efficacious SHP2 inhibitors. *J Med Chem*. 2019;62(4):1793–802.
398. Greenfield LJ Jr. Molecular mechanisms of antiseizure drug activity at GABAA receptors. *Seizure*. 2013;22(8):589–600.
399. Rogawski MA, Löscher W, Rho JM. Mechanisms of action of antiseizure drugs and the ketogenic diet. *Cold Spring Harb Perspect Med*. 2016;6(5):a022780.
400. Rarey M, Kramer B, Lengauer T, Klebe G. A fast flexible docking method using an incremental construction algorithm. *J Mol Biol*. 1996;261(3):470–89.
401. Claussen H, Buning C, Rarey M, Lengauer T. FlexE: efficient molecular docking considering protein structure variations. *J Mol Biol*. 2001;308(2):377–95.
402. Richter L, de Graaf C, Sieghart W, Varagic Z, Mörzinger M, de Esch IJ, et al. Diazepam-bound GABAA receptor models identify new benzodiazepine binding-site ligands. *Nat Chem Biol*. 2012;8(5):455–64.
403. Wolber G, Langer T. LigandScout: 3-D pharmacophores derived from protein-bound ligands and their use as virtual screening filters. *J Chem Inf Model*. 2005;45(1):160–9.
404. Korb O, Stützel T, Exner TE. Empirical scoring functions for advanced protein-ligand docking with PLANTS. *J Chem Inf Model*. 2009;49(1):84–96.
405. Heusser SA, Howard RJ, Borghese CM, Cullins MA, Broemstrup T, Lee US, et al. Functional validation of virtual screening for novel agents with general anesthetic action at ligand-gated ion channels. *Mol Pharmacol*. 2013;84(5):670–8.
406. Nury H, Van Renterghem C, Weng Y, Tran A, Baaden M, Dufresne V, et al. X-ray structures of general anaesthetics bound to a pentameric ligand-gated ion channel. *Nature*. 2011;469(7330):428–31.
407. Lynch JW. Native glycine receptor subtypes and their physiological roles. *Neuropharmacology*. 2009;56(1):303–9.
408. Mowrey DD, Cui T, Jia Y, Ma D, Makhov AM, Zhang P, et al. Open-channel structures of the human glycine receptor $\alpha 1$ fulllength transmembrane domain. *Structure*. 2013;21(10):1897–904.
409. Duan Y, Wu C, Chowdhury S, Lee MC, Xiong G, Zhang W, et al. A point-charge force field for molecular mechanics simulations of proteins based on condensed-phase quantum mechanical calculations. *J Comput Chem*. 2003;24(16):1999–2012.
410. Wells MM, Tillman TS, Mowrey DD, Sun T, Xu Y, Tang P. Ensemble-based virtual screening for cannabinoid-like potentiators of the human glycine receptor $\alpha 1$ for the treatment of pain. *J Med Chem*. 2015;58(7):2958–66.
411. Law V, Knox C, Djoumbou Y, Jewison T, Guo AC, Liu Y, et al. DrugBank 4.0: shedding new light on drug metabolism. *Nucleic Acids Res*. 2014;42(Database issue):D1091–7.
412. Bregman H, Simard JR, Andrews KL, Ayube S, Chen H, Gunaydin H, et al. The discovery and hit-to-lead optimization of tricyclic sulfonamides as potent and efficacious potentiators of glycine receptors. *J Med Chem*. 2017;60(3):1105–25.
413. Huang X, Shaffer PL, Ayube S, Bregman H, Chen H, Lehto SG, et al. Crystal structures of human glycine receptor $\alpha 3$ bound to a novel class of analgesic potentiators. *Nat Struct Mol Biol*. 2017;24(2):108–13.
414. Chakka N, Andrews KL, Berry LM, Bregman H, Gunaydin H, Huang L, et al. Applications of parallel synthetic lead hopping and pharmacophore-based virtual screening in the discovery of efficient glycine receptor potentiators. *Eur J Med Chem*. 2017;137:63–75.
415. Wemmie JA, Taugher RJ, Kreple CJ. Acid-sensing ion channels in pain and disease. *Nat Rev Neurosci*. 2013;14(7):461–71.
416. Callejo G, Pattison LA, Greenhalgh JC, Chakrabarti S, Andreopoulou E, Hockley JRF, et al. In silico screening of GMQ-like compounds reveals guanabenz and sephin1 as new allosteric modulators of acid-sensing ion channel 3. *Biochem Pharmacol*. 2020;174:113834.
417. Pihan E, Colliandre L, Guichou JF, Douguet D. e-Drug3D: 3D structure collections dedicated to drug repurposing and fragment-based drug design. *Bioinformatics*. 2012;28(11):1540–1.
418. Millar NS, Gotti C. Diversity of vertebrate nicotinic acetylcholine receptors. *Neuropharmacology*. 2009;56(1):237–46.
419. Newcombe J, Chatzidaki A, Sheppard TD, Topf M, Millar NS. Diversity of nicotinic acetylcholine receptor positive allosteric modulators revealed by mutagenesis and a revised structural model. *Mol Pharmacol*. 2018;93(2):128–40.
420. Smelt CLC, Sanders VR, Newcombe J, Burt RP, Sheppard TD, Topf M, et al. Identification by virtual screening and functional characterisation of novel positive and negative allosteric modulators of the $\alpha 7$ nicotinic acetylcholine receptor. *Neuropharmacology*. 2018;139:194–204.
421. Cereto-Massagué A, Guasch L, Valls C, Mulero M, Pujadas G, Garcia-Vallvé S. DecoyFinder: an easy-to-use python GUI application for building target-specific decoy sets. *Bioinformatics*. 2012;28(12):1661–2.
422. Elmore S. Apoptosis: a review of programmed cell death. *Toxicol Pathol*. 2007;35(4):495–516.
423. Taylor RC, Cullen SP, Martin SJ. Apoptosis: controlled demolition at the cellular level. *Nat Rev Mol Cell Biol*. 2008;9(3):231–41.

424. Lakhani SA, Masud A, Kuida K, Porter GA Jr, Booth CJ, Mehal WZ, et al. Caspases 3 and 7: key mediators of mitochondrial events of apoptosis. *Science*. 2006;311(5762):847–51.
425. Hardy JA, Lam J, Nguyen JT, O'Brien T, Wells JA. Discovery of an allosteric site in the caspases. *Proc Natl Acad Sci U S A*. 2004;101(34):12461–6.
426. Thornberry NA, Rano TA, Peterson EP, Rasper DM, Timkey T, Garcia-Calvo M, et al. A combinatorial approach defines specificities of members of the caspase family and granzyme B. Functional relationships established for key mediators of apoptosis. *J Biol Chem*. 1997;272(29):17907–11.
427. Chai J, Shiozaki E, Srinivasula SM, Wu Q, Datta P, Alnemri ES, et al. Structural basis of caspase-7 inhibition by XIAP. *Cell*. 2001;104(5):769–80.
428. Krishna Deepak RNV, Abdullah A, Talwar P, Fan H, Ravanani P. Identification of FDA-approved drugs as novel allosteric inhibitors of human executioner caspases. *Proteins*. 2018;86(11):1202–10.
429. Fan J, Teng X, Liu L, Mattaini KR, Looper RE, Vander Heiden MG, et al. Human phosphoglycerate dehydrogenase produces the oncometabolite D-2-hydroxyglutarate. *ACS Chem Biol*. 2015;10(2):510–6.
430. Okazaki K, Koga N, Takada S, Onuchic JN, Wolynes PG. Multiple-basin energy landscapes for large-amplitude conformational motions of proteins: structure-based molecular dynamics simulations. *Proc Natl Acad Sci U S A*. 2006;103(32):11844–9.
431. Qi Y, Wang Q, Tang B, Lai L. Identifying allosteric binding sites in proteins with a two-state Gō model for novel allosteric effector discovery. *J Chem Theory Comput*. 2012;8(8):2962–71.
432. Thompson JR, Bell JK, Bratt J, Grant GA, Banaszak LJ. Vmax regulation through domain and subunit changes. The active form of phosphoglycerate dehydrogenase. *Biochemistry*. 2005;44(15):5763–73.
433. Schuller DJ, Grant GA, Banaszak LJ. The allosteric ligand site in the Vmax-type cooperative enzyme phosphoglycerate dehydrogenase. *Nat Struct Biol*. 1995;2(1):69–76.
434. Kenzaki H, Koga N, Hori N, Kanada R, Li W, Okazaki K, et al. CafeMol: a coarse-grained biomolecular simulator for simulating proteins at work. *J Chem Theory Comput*. 2011;7(6):1979–89.
435. Wang Q, Qi Y, Yin N, Lai L. Discovery of novel allosteric effectors based on the predicted allosteric sites for *Escherichia coli* D3-phosphoglycerate dehydrogenase. *PLoS One*. 2014;9(4):e94829.
436. Dixon SL, Smondyrev AM, Knoll EH, Rao SN, Shaw DE, Friesner RA. PHASE: a new engine for pharmacophore perception, 3D QSAR model development, and 3D database screening: 1. Methodology and preliminary results. *J Comput Aided Mol Des*. 2006;20(10–11):647–71.
437. Yang WS, SriRamaratnam R, Welsch ME, Shimada K, Skouta R, Viswanathan VS, et al. Regulation of ferroptotic cancer cell death by GPX4. *Cell*. 2014;156(1–2):317–31.
438. Meng H, Liu Y, Lai L. Diverse ways of perturbing the human arachidonic acid metabolic network to control inflammation. *Acc Chem Res*. 2015;48(8):2242–50.
439. Scheerer P, Borchert A, Krauss N, Wessner H, Gerth C, Hohne W, et al. Structural basis for catalytic activity and enzyme polymerization of phospholipid hydroperoxide glutathione peroxidase-4 (GPx4). *Biochemistry*. 2007;46(31):9041–9.
440. Li C, Deng X, Zhang W, Xie X, Conrad M, Liu Y, et al. Novel allosteric activators for ferroptosis regulator glutathione peroxidase 4. *J Med Chem*. 2019;62(1):266–75.
441. Frye RA. Phylogenetic classification of prokaryotic and eukaryotic Sir2-like proteins. *Biochem Biophys Res Commun*. 2000;273(2):793–8.
442. Kugel S, Mostoslavsky R. Chromatin and beyond: the multitasking roles for SIRT6. *Trends Biochem Sci*. 2014;39(2):72–81.
443. Tasselli L, Zheng W, Chua KF. SIRT6: novel mechanisms and links to aging and disease. *Trends Endocrinol Metab*. 2017;28(3):168–85.
444. Jiang H, Khan S, Wang Y, Charron G, He B, Sebastian C, et al. SIRT6 regulates TNF- α secretion through hydrolysis of long-chain fatty acyl lysine. *Nature*. 2013;496(7443):110–3.
445. Huang Z, Zhao J, Deng W, Chen Y, Shang J, Song K, et al. Identification of a cellularly active SIRT6 allosteric activator. *Nat Chem Biol*. 2018;14(12):1118–26.
446. You W, Rotili D, Li TM, Kambach C, Meleshin M, Schutkowski M, et al. Structural basis of sirtuin 6 activation by synthetic small molecules. *Angew Chem Int Ed Engl*. 2017;56(4):1007–11.
447. Shang JL, Ning SB, Chen YY, Chen TX, Zhang J. MDL-800, an allosteric activator of SIRT6, suppresses proliferation and enhances EGFR-TKIs therapy in non-small cell lung cancer. *Acta Pharmacol Sin*. 2021;42(1):120–31.
448. Cover TL, Blanke SR. *Helicobacter pylori* VacA, a paradigm for toxin multifunctionality. *Nat Rev Microbiol*. 2005;3(4):320–32.
449. Ishijima N, Suzuki M, Ashida H, Ichikawa Y, Kanegae Y, Saito I, et al. BabA-mediated adherence is a potentiator of the *Helicobacter pylori* type IV secretion system activity. *J Biol Chem*. 2011;286(28):25256–64.
450. Alfarouk KO, Bashir AHH, Aljarbou AN, Ramadan AM, Muddathir AK, AlHoufie STS, et al. The possible role of *Helicobacter pylori* in gastric cancer and its management. *Front Oncol*. 2019;9:75.
451. Hoy B, Lower M, Weydig C, Carra G, Tegtmeyer N, Geppert T, et al. *Helicobacter pylori* HtrA is a new secreted virulence factor that cleaves E-cadherin to disrupt intercellular adhesion. *EMBO Rep*. 2010;11(10):798–804.
452. Altschul SF, Gish W, Miller W, Myers EW, Lipman DJ. Basic local alignment search tool. *J Mol Biol*. 1990;215(3):403–10.
453. Krojer T, Sawa J, Huber R, Clausen T. HtrA proteases have a conserved activation mechanism that can be triggered by distinct molecular cues. *Nat Struct Mol Biol*. 2010;17(7):844–52.
454. Larkin MA, Blackshields G, Brown NP, Chenna R, McGettigan PA, McWilliam H, et al. Clustal W and Clustal X version 2.0. *Bioinformatics*. 2007;23(21):2947–8.

455. Weisel M, Proschak E, Schneider G. PocketPicker: analysis of ligand binding-sites with shape descriptors. *Chem Cent J*. 2007;1:7.
456. Weisel M, Kriegl JM, Schneider G. Architectural repertoire of ligand-binding pockets on protein surfaces. *Chembiochem*. 2010;11(4):556–63.
457. Reisen F, Weisel M, Kriegl JM, Schneider G. Self-organizing fuzzy graphs for structure-based comparison of protein pockets. *J Proteome Res*. 2010;9(12):6498–510.
458. Geppert T, Reisen F, Pillong M, Hahnke V, Tanrikulu Y, Koch CP, et al. Virtual screening for compounds that mimic protein-protein interface epitopes. *J Comput Chem*. 2012;33(5):573–9.
459. Bush K, Jacoby GA. Updated functional classification of β -lactamases. *Antimicrob Agents Chemother*. 2010;54(3):969–76.
460. Wang X, Minasov G, Shoichet BK. Evolution of an antibiotic resistance enzyme constrained by stability and activity trade-offs. *J Mol Biol*. 2002;320(1):85–95.
461. Horn JR, Shoichet BK. Allosteric inhibition through core disruption. *J Mol Biol*. 2004;336(5):1283–91.
462. Beauchamp KA, Bowman GR, Lane TJ, Maibaum L, Haque IS, Pande VS. MSMBuilder2: modeling conformational dynamics at the picosecond to millisecond scale. *J Chem Theory Comput*. 2011;7(10):3412–9.
463. Hendlich M, Rippmann F, Barnickel G. LIGSITE: automatic and efficient detection of potential small molecule-binding sites in proteins. *J Mol Graph Model*. 1997;15(6):359–63. 89.
464. Jain AN. Surflex-Dock 2.1: robust performance from ligand energetic modeling, ring flexibility, and knowledge-based search. *J Comput Aided Mol Des*. 2007;21(5):281–306.
465. Hart KM, Moeder KE, Ho CMW, Zimmerman MI, Frederick TE, Bowman GR. Designing small molecules to target cryptic pockets yields both positive and negative allosteric modulators. *PLoS One*. 2017;12(6):e0178678.
466. Hart KM, Ho CM, Dutta S, Gross ML, Bowman GR. Modelling proteins' hidden conformations to predict antibiotic resistance. *Nat Commun*. 2016;7:12965.
467. Yu H, Pardoll D, Jove R. STATs in cancer inflammation and immunity: a leading role for STAT3. *Nat Rev Cancer*. 2009;9(11):798–809.
468. Harhous Z, Booz GW, Ovize M, Bidaux G, Kurdi M. An update on the multifaceted roles of STAT3 in the heart. *Front Cardiovasc Med*. 2019;6:150.
469. Ren Z, Mao X, Mertens C, Krishnaraj R, Qin J, Mandal PK, et al. Crystal structure of unphosphorylated STAT3 core fragment. *Biochem Biophys Res Commun*. 2008;374(1):1–5.
470. Costa AG, Cusano NE, Silva BC, Cremers S, Bilezikian JP. Cathepsin K: its skeletal actions and role as a therapeutic target in osteoporosis. *Nat Rev Rheumatol*. 2011;7(8):447–56.
471. Dai R, Wu Z, Chu HY, Lu J, Lyu A, Liu J, et al. Cathepsin K: the action in and beyond bone. *Front Cell Dev Biol*. 2020;8:433.
472. Novinec M, Korenč M, Caflisch A, Ranganathan R, Lenarčič B, Baici A. A novel allosteric mechanism in the cysteine peptidase cathepsin K discovered by computational methods. *Nat Commun*. 2014;5:3287.
473. Harris R, Olson AJ, Goodsell DS. Automated prediction of ligand-binding sites in proteins. *Proteins*. 2008;70(4):1506–17.
474. Zhao B, Janson CA, Amegadzie BY, D'Alessio K, Griffin C, Hanning CR, et al. Crystal structure of human osteoclast cathepsin K complex with E-64. *Nat Struct Biol*. 1997;4(2):109–11.
475. Karnoub AE, Weinberg RA. Ras oncogenes: split personalities. *Nat Rev Mol Cell Biol*. 2008;9(7):517–31.
476. Goodsell DS. The molecular perspective: the ras oncogene. *Stem Cells*. 1999;17(4):235–6.
477. Case D, Darden T, Cheatham T, Simmerling C, Wang J, Duke R, et al. AMBER 10. San Francisco: University of California; 2008.
478. Hornak V, Abel R, Okur A, Strockbine B, Roitberg A, Simmerling C. Comparison of multiple Amber force fields and development of improved protein backbone parameters. *Proteins*. 2006;65(3):712–25.
479. Grant BJ, Lukman S, Hocker HJ, Sayyah J, Brown JH, McCammon JA, et al. Novel allosteric sites on Ras for lead generation. *PLoS One*. 2011;6(10):e25711.
480. Grant BJ, Rodrigues AP, ElSawy KM, McCammon JA, Caves LS. Bio3d: an R package for the comparative analysis of protein structures. *Bioinformatics*. 2006;22(21):2695–6.
481. Lipinski CA, Lombardo F, Dominy BW, Feeney PJ. Experimental and computational approaches to estimate solubility and permeability in drug discovery and development settings. *Adv Drug Deliv Rev*. 2001;46(1–3):3–26.
482. Phillips JC, Braun R, Wang W, Gumbart J, Tajkhorshid E, Villa E, et al. Scalable molecular dynamics with NAMD. *J Comput Chem*. 2005;26(16):1781–802.
483. Prakash P, Sayyed-Ahmad A, Gorfe AA. The role of conserved waters in conformational transitions of Q61H K-ras. *PLoS Comput Biol*. 2012;8(2):e1002394.
484. Hocker HJ, Cho KJ, Chen CY, Rambahal N, Sagineedu SR, Shaari K, et al. Andrographolide derivatives inhibit guanine nucleotide exchange and abrogate oncogenic Ras function. *Proc Natl Acad Sci U S A*. 2013;110(25):10201–6.
485. Maurer T, Garrenton LS, Oh A, Pitts K, Anderson DJ, Skelton NJ, et al. Small-molecule ligands bind to a distinct pocket in Ras and inhibit SOS-mediated nucleotide exchange activity. *Proc Natl Acad Sci U S A*. 2012;109(14):5299–304.
486. McCarthy MJ, Pagba CV, Prakash P, Naji AK, van der Hoeven D, Liang H, et al. Discovery of high-affinity noncovalent allosteric KRAS inhibitors that disrupt effector binding. *ACS Omega*. 2019;4(2):2921–30.
487. Gupta AK, Wang X, Pagba CV, Prakash P, Sarkar-Banerjee S, Putkey J, et al. Multi-target, ensemble-based virtual screening yields novel allosteric KRAS inhibitors at high success rate. *Chem Biol Drug Des*. 2019;94(2):1441–56.
488. Schmidtke P, Bidon-Chanal A, Luque FJ, Barril X. MDpocket: open-source cavity detection and characterization on molecular dynamics trajectories. *Bioinformatics*. 2011;27(23):3276–85.
489. Sander T, Freyss J, von Korff M, Rufener C. DataWarrior: an open-source program for chemistry aware data visualization and analysis. *J Chem Inf Model*. 2015;55(2):460–73.

490. ChemDiv. Accelerate Your Discovery Chemistry. <http://www.chemdiv.com>
491. Xie C, Li Y, Li LL, Fan XX, Wang YW, Wei CL, et al. Identification of a new potent inhibitor targeting KRAS in non-small cell lung Cancer cells. *Front Pharmacol*. 2017;8:823.
492. Nussinov R, Tsai CJ. The design of covalent allosteric drugs. *Annu Rev Pharmacol Toxicol*. 2015;55:249–67.
493. Ostrem JM, Peters U, Sos ML, Wells JA, Shokat KM. K-Ras(G12C) inhibitors allosterically control GTP affinity and effector interactions. *Nature*. 2013;503(7477):548–51.
494. Patricelli MP, Janes MR, Li LS, Hansen R, Peters U, Kessler LV, et al. Selective inhibition of oncogenic KRAS output with small molecules targeting the inactive state. *Cancer Discov*. 2016;6(3):316–29.
495. Lito P, Solomon M, Li LS, Hansen R, Rosen N. Allele-specific inhibitors inactivate mutant KRAS G12C by a trapping mechanism. *Science*. 2016;351(6273):604–8.
496. Janes MR, Zhang J, Li LS, Hansen R, Peters U, Guo X, et al. Targeting KRAS mutant cancers with a covalent G12C-specific inhibitor. *Cell*. 2018;172(3):578–89.e17.
497. Gentile DR, Rathinaswamy MK, Jenkins ML, Moss SM, Siempelkamp BD, Renslo AR, et al. Ras binder induces a modified switch-II pocket in GTP and GDP states. *Cell Chem Biol*. 2017;24(12):1455–66.e14.
498. Canon J, Rex K, Saiki AY, Mohr C, Cooke K, Bagal D, et al. The clinical KRAS(G12C) inhibitor AMG 510 drives anti-tumour immunity. *Nature*. 2019;575(7781):217–23.
499. Lanman BA, Allen JR, Allen JG, Amegadzie AK, Ashton KS, Booker SK, et al. Discovery of a covalent inhibitor of KRASG12C (AMG 510) for the treatment of solid tumors. *J Med Chem*. 2020;63(1):52–65.
500. Weisner J, Gontla R, van der Westhuizen L, Oeck S, Ketzer J, Janning P, et al. Covalent-allosteric kinase inhibitors. *Angew Chem Int Ed Engl*. 2015;54(35):10313–6.
501. Weisner J, Landel I, Reintjes C, Uhlenbrock N, Trajkovic-Arsic M, Dienstbier N, et al. Preclinical efficacy of covalent-allosteric AKT inhibitor borussertib in combination with trametinib in KRAS-mutant pancreatic and colorectal cancer. *Cancer Res*. 2019;79(9): 2367–78.
502. Uhlenbrock N, Smith S, Weisner J, Landel I, Lindemann M, Le TA, et al. Structural and chemical insights into the covalent-allosteric inhibition of the protein kinase Akt. *Chem Sci*. 2019;10(12):3573–85.
503. Tang S, Liao JC, Dunn AR, Altman RB, Spudich JA, Schmidt JP. Predicting allosteric communication in myosin via a pathway of conserved residues. *J Mol Biol*. 2007;373(5):1361–73.
504. Ngan CH, Bohnuud T, Mottarella SE, Beglov D, Villar EA, Hall DR, et al. FTMAP: extended protein mapping with user-selected probe molecules. *Nucleic Acids Res*. 2012;40(Web Server issue):W271–5.
505. Preller M, Chinthalapudi K, Martin R, Knolker HJ, Manstein DJ. Inhibition of myosin ATPase activity by halogenated pseudilins: a structure–activity study. *J Med Chem*. 2011;54(11):3675–85.
506. Kharenko OA, Patel RG, Brown SD, Calosing C, White A, Lakshminarasimhan D, et al. Design and characterization of novel covalent bromodomain and extra-terminal domain (BET) inhibitors targeting a methionine. *J Med Chem*. 2018;61(18):8202–11.
507. Lv Z, Yuan L, Atkison JH, Williams KM, Vega R, Sessions EH, et al. Molecular mechanism of a covalent allosteric inhibitor of SUMO E1 activating enzyme. *Nat Commun*. 2018;9(1):5145.
508. Hassan AQ, Kirby CA, Zhou W, Schuhmann T, Kityk R, Kipp DR, et al. The novolactone natural product disrupts the allosteric regulation of Hsp70. *Chem Biol*. 2015;22(1):87–97.
509. Wang Y, Harrison CB, Schulten K, McCammon JA. Implementation of accelerated molecular dynamics in NAMD. *Comput Sci Discov*. 2011;4(1):015002.
510. Pronk S, Pall S, Schulz R, Larsson P, Bjelkmar P, Apostolov R, et al. GROMACS 4.5: a high-throughput and highly parallel open source molecular simulation toolkit. *Bioinformatics*. 2013;29(7):845–54.
511. Abraham MJ, Murtola T, Schulz R, Páll S, Smith JC, Hess B, et al. GROMACS: high performance molecular simulations through multi-level parallelism from laptops to supercomputers. *SoftwareX*. 2015;1-2:19–25.
512. Case DA, Belfon K, Ben-Shalom IY, Brozell SR, Cerutti DS, Cheatham ITE, et al. Amber 2020; 2020.
513. Beglov D, Hall DR, Wakefield AE, Luo L, Allen KN, Kozakov D, et al. Exploring the structural origins of cryptic sites on proteins. *Proc Natl Acad Sci U S A*. 2018;115(15):E3416–E25.
514. Wang Q, Zheng M, Huang Z, Liu X, Zhou H, Chen Y, et al. Toward understanding the molecular basis for chemical allosteric modulator design. *J Mol Graph Model*. 2012;38:324–33.
515. Campitelli P, Modi T, Kumar S, Ozkan SB. The role of conformational dynamics and allostery in modulating protein evolution. *Annu Rev Biophys*. 2020;49(1):267–88.
516. Zhang Y, Doruker P, Kaynak B, Zhang S, Krieger J, Li H, et al. Intrinsic dynamics is evolutionarily optimized to enable allosteric behavior. *Curr Opin Struct Biol*. 2020;62:14–21.